

AD-A043 065

GENERAL DYNAMICS/FORT WORTH TEX FORT WORTH DIV
WELDABILITY OF 10 NICKEL MODIFIED TYPE STEEL.(U)
MAY 77 P M MACHMEIER, J C COLLINS, R L JONES

F/G 11/6

F33615-75-C-5091

UNCLASSIFIED

AFML-TR-77-61

NL

1 OF 2
AD
A043 065



AD A 043065

AFML-TR-77-61

12

2

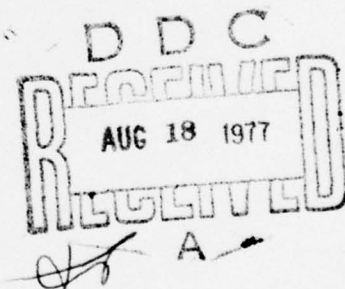
WELDABILITY OF 10 NICKEL MODIFIED TYPE STEEL

GENERAL DYNAMICS
FORT WORTH DIVISION
FORT WORTH, TEXAS 76101

MAY 1977

TECHNICAL REPORT AFML-TR-77-61
FINAL REPORT FOR PERIOD JANUARY 1975 - JULY 1976

Approved for public release; distribution unlimited



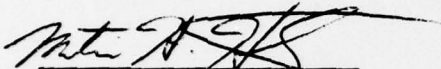
AU IVU.
DDC FILE COPY

AIR FORCE MATERIALS LABORATORY
AIR FORCE WRIGHT AERONAUTICAL LABORATORIES
AIR FORCE SYSTEMS COMMAND
WRIGHT-PATTERSON AIR FORCE BASE, OHIO 45433

NOTICES

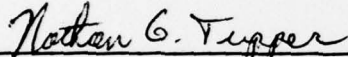
When Government drawings, specifications, or other data are used for any purpose other than in connection with a definitely related Government procurement operation, the United States Government thereby incurs no responsibility nor any obligation whatsoever; and the fact that the government may have formulated, furnished, or in any way supplied the said drawings, specifications, or other data, is not to be regarded by implication or otherwise as in any manner licensing the holder or any other person or corporation, or conveying any rights or permission to manufacture, use, or sell any patented invention that may in any way be related thereto.

This technical report has been reviewed and is approved for publication.



Martin H. Horowitz
Project Engineer

FOR THE COMMANDER



Nathan G. Tupper
Acting Chief, Structural Metals Branch
Metals and Ceramics Division
Air Force Materials Laboratory

Copies of this report should not be returned unless return is required by security considerations, contractual obligations, or notice on a specific document.

UNCLASSIFIED

SECURITY CLASSIFICATION OF THIS PAGE (When Data Entered)

REPORT DOCUMENTATION PAGE		READ INSTRUCTIONS BEFORE COMPLETING FORM
1. REPORT NUMBER AFM-TR-77-61	2. GOVT ACCESSION NO.	3. RECIPIENT'S CATALOG NUMBER
4. TITLE (and Subtitle) STABILITY OF 10 NICKEL MODIFIED TYPE STEEL	5. TYPE OF REPORT & PERIOD COVERED Final Report January 1975-July 1976	6. PERFORMING ORG. REPORT NUMBER
7. AUTHOR(s) P. M. Machmeier, J. C. Collins R. L. Jones	8. CONTRACT OR GRANT NUMBER(s) F33615-75C-5091	
9. PERFORMING ORGANIZATION NAME AND ADDRESS General Dynamics Fort Worth Division P.O. 748, Fort Worth, Texas 76101	10. PROGRAM ELEMENT, PROJECT, TASK AREA & WORK UNIT NUMBERS 62102F 73510230	
11. CONTROLLING OFFICE NAME AND ADDRESS Air Force Materials Laboratory (LLM) Air Force Wright Aeronautical Laboratories Air Force Systems Command, Wright-Patter- son Air Force Base Ohio, 45433	12. REPORT DATE May 1977	13. NUMBER OF PAGES 91
14. MONITORING AGENCY NAME & ADDRESS (if different from Controlling Office) 12/102P.	15. SECURITY CLASS. (of this report) Unclassified	15a. DECLASSIFICATION/DOWNGRADING SCHEDULE
16. DISTRIBUTION STATEMENT (of this Report) Approved for public release; distribution unlimited.		
17. DISTRIBUTION STATEMENT (of the abstract entered in Block 20, if different from Report)		
18. SUPPLEMENTARY NOTES		
19. KEY WORDS (Continue on reverse side if necessary and identify by block number) High Strength Steel, Arc Welding, Filler Metal Development, Lath Martensite, Secondary Hardening, Fracture Toughness, Stress Corrosion, Crack Growth Rates, AF 1410 Steel		
20. ABSTRACT (Continue on reverse side if necessary and identify by block number) Several filler metal heats, melted to a base composition of 14Co-10Ni-2Cr-1Mo-0.16C-bal Fe (AF 1410 steel) with controlled levels of impurity/deoxidizing elements, were evaluated by three arc welding processes. The CW-GTAW deposited weld metal exhibited the best balance between strength and toughness. Maximum fusion zone toughness was associated with low levels of Al, S, and O.		

DD FORM 1 JAN 73 1473

EDITION OF 1 NOV 65 IS OBSOLETE

UNCLASSIFIED

SECURITY CLASSIFICATION OF THIS PAGE (When Data Entered)

402 709

UNCLASSIFIED

SECURITY CLASSIFICATION OF THIS PAGE(When Data Entered)

20. A high purity filler metal composition deposited by the CW-GTAW process resulted in post weld aged mechanical properties of TYS-212 Ksi (1462 MPa), TUS-224 Ksi (1544 MPa), CVN absorbed energy - 43.5 ft-lbf (58.9J), and K_{ISCC} - 91 Ksi $\sqrt{\text{in}}$ (100 MPa $\sqrt{\text{m}}$). The post weld aged HAZ notch toughness exceeded 34 ft-lbf (46.1J) absorbed energy at equivalent FZ strength levels for all the arc weld processes evaluated.

The as-deposited (last pass) CW-GTAW fusion zone microstructure consisted of dislocated lath martensite, minor quantities of interlath retained austenite, and widmanstatten cementite. Post weld aging of multi-pass weld microstructures led to complete dissolution of cementite platelets in favor of alloy carbide precipitation and large amounts of reverted austenite at lath boundary and intralath sites.

91 KSI $\sqrt{\text{in}}$ (100 MPa $\sqrt{\text{m}}$)

UNCLASSIFIED

SECURITY CLASSIFICATION OF THIS PAGE(When Data Entered)

FOREWORD

The work reported in this final report, which is designated Report No. AFML-TR-77-61 was performed under Contract F33615-75-C-5091, Project No. 6210F, Task No. 735105. This contract with General Dynamics' Fort Worth Division (P.O. Box 748, Fort Worth, Texas 76101) was administered under the technical direction of the Air Force Materials Laboratory, Air Force Systems Command, United States Air Force. Mr. Martin H. Horowitz, AFML/LLS served as Project Engineer. All technical work was accomplished between January 1975 and July 1976. The report submittal date - January 1977.

The role and responsibilities of the Fort Worth Division personnel in the execution of this program are as follows: Dr. P. M. Machmeier, Program Manager and Principal Investigator; Mr. R. L. Jones, Mechanical Test, Mr. J. C. Collins, Welding and Mr. R. E. Johnson, general support. Mr. B. V. N. Rao, University of California at Berkeley, is credited with the thin foil microscopy in this investigation.

An acknowledgement is due Cannon-Muskegon Corporation and U. S. Welding Corporation for the VIM melting and reduction of redraw stock to weld wire, respectively.

ACCESSION NO.	
NTIS	Write Section <input checked="" type="checkbox"/>
DOC	Doc Section <input type="checkbox"/>
UNCLASSIFIED	<input type="checkbox"/>
CLASSIFICATION	
BY	
DISTRIBUTION AVAILABILITY CODES	
DEL.	MAIL ROOM
AL	AL

TABLE OF CONTENTS

<u>Section</u>	<u>Page</u>
I INTRODUCTION	1
II BACKGROUND	5
III EXPERIMENTAL PROGRAM	7
3.1 Filler Metal Selection and Processing	7
3.2 Arc Weld Processes and Parameters	10
3.3 Weld Thermal Analysis	13
3.4 Mechanical Testing	13
3.4.1 Tensile	13
3.4.2 Notch Toughness	13
3.4.3 Fracture Toughness	15
3.4.4 Compact Tension - K_{ISCC}	15
3.4.5 Fatigue	16
3.4.5.1 S/N Fatigue	16
3.4.5.2 Compact Tension, da/dN	16
3.5 Metallurgical Analysis	17
3.5.1 Microstructure	17
3.5.2 Microhardness	18
3.5.3 X-ray Diffraction	18
IV RESULTS AND DISCUSSION	19
4.1 Chemical Composition	19
4.2 Fusion Zone Properties	25
4.2.1 Fusion Zone Mechanical Properties (Heats VE 716-VE 717)	25
4.2.2 Effect of Welding Parameters and Fusion Zone Composition on Mech- anical Properties	29
4.2.3 Fusion Zone Mechanical Properties (Heats VE 799-800)	34
4.2.4 Fusion Zone Mechanical Character- ization Data (Heat VE 799)	37

TABLE OF CONTENTS

<u>Section</u>	<u>Page</u>
4.2.4.1 Strength and Toughness	37
4.2.4.2 Fatigue	40
4.2.4.3 Stress Corrosion	45
4.2.5 Fusion Zone Microstructural Properties	50
4.3 Heat Affected Zone Properties	63
4.3.1 Heat Affected Zone Microstructure	63
4.3.2 Heat Affected Zone Mechanical Properties	66
V CONCLUSIONS	75
VI RECOMMENDATIONS	77
Appendix 1 Chemical Analysis of Melt Stock	78
Appendix 2 Fusion Zone Chemical Analysis	79
Appendix 3 Ingot Aluminum Analyses	80
Appendix 4 AF 1410 Steel Weldment Mechanical Properties	81
Appendix 5 Low Temperature CVN Impact Properties of CW-GTAW Welded AF 1410 Steel Plate	83
Appendix 6 Axial Fatigue Properties of CW-GTA Welded AF 1410 Weldment	84
Appendix 7 Dry Air Fatigue Crack Growth Rate Data	85
Appendix 8 3.5% NaCl Fatigue Crack Growth Rate Data	86
Appendix 9 Transformation Temperatures	87
Appendix 10 Weldment Austenite Measurements	88
REFERENCES	89

L I S T O F I L L U S T R A T I O N S

<u>Figure</u>		<u>Page</u>
1	Investigation Outline	2
2	CW-GTA Pulse Arc Amperage and Voltage Response	14
3	Representative Multipass Arc Welds	26
4	Correlation Between Fusion Zone Mechanical Properties and Weld Process Utilizing Filler Metal Heats VE716 and VE717	27
5	Microstructural Refinement in Arc Weld Fusion Zones in the As-Welded Condition	28
6	Representative Center Line Cooling Rates	30
7	Effect of Post Weld Aging on Plasma Arc Fusion Zone Microstructure	31
8	Representative As-Deposited Solidification Microstructures in Gas Tungsten Arc and Plasma Arc Welds	32
9	Correlation Between CW-GTAW Fusion Zone Mechanical Properties and Filler Metal Composition	36
10	Effect of Test Temperature on Notch Toughness of AF 1410 Steel Weldments	38
11	Fracture Appearance of the Post Weld Aged CW-GTAW Fusion Zone As a Function of Temperature	39
12	Irregular Fatigue Crack Profile Evident in Post Weld Aged CW-GTAW Fusion Zone Fracture Toughness Specimens	43
13	S/N Fatigue Properties of AF 1410 Steel Weldment	44
14	Fatigue Crack Growth of AF 1410 Steel CW-GTA Weldment in Dry Air	46

LIST OF ILLUSTRATIONS
(Continued)

<u>Figure</u>		<u>Page</u>
15	Fatigue Crack Growth of AF 1410 Steel CW-GTA Weldment in 3.5% NaCl Solution	47
16	Stability of Solidification Structure in Arc Weld Fusion Zone	51
17	Decomposition on Heating and Cooling in the Fe-Ni System	52
18	Effect of Heating-Cooling Rate on Fusion Zone Transformation Temperatures	53
19	As-Deposited CW-GTAW Fusion Zone Microstructure	55
20	Autotempered Carbides in As-Deposited CW-GTAW Fusion Zone Microstructure	57
21	As-Deposited CW-PAW Fusion Zone Microstructure	58
22	Autotempered Carbides in As-Deposited CW-PAW Fusion Zone Microstructure	59
23	As-Deposited CW-GTAW Fusion Zone Microstructures Subject to Multiple Thermal Reversals	60
24	As-Deposited CW-GTAW Fusion Zone Microstructures Subject to Multiple Thermal Reversals	61
25	Post Weld Aged CW-GTAW Fusion Zone Microstructures Representative of Multiple Thermal Reversals	62
26	Post Weld Aged CW-GTAW Fusion Zone Microstructures Representative of Multiple Thermal Reversals	64

LIST OF ILLUSTRATIONS
(Concluded)

<u>Figure</u>		<u>Page</u>
27	Heat Affected Zone Cooling Rates	65
28	HW-GTAW Heat Affected Zone Microstructures of Unaged Base Plate	67
29	Cold Wire Gas Tungsten Arc Weld HAZ Properties	68
30	Hot Wire Gas Tungsten Arc Weld HAZ Properties	69
31	Cold Wire Plasma Arc Weld HAZ Properties	70
32	Cold Wire Plasma Arc Weld HAZ Properties	71
33	Microhardness Measurements in 1.25 inch (3.18 cm) thick CW-GTA Weldments	72

L I S T O F T A B L E S

<u>Table</u>		<u>Page</u>
1	Program Goals	3
2	Required Chemical Analyses for Initial Two Filler Metal Heats	8
3	Required Chemical Analyses for Final Six Filler Metal Heats	9
4	Welding Parameters (Heats VE 716-717)	11
5	Welding Parameters (Heats VE 798-800)	12
6	AF 1410 Rolled Plate Properties	20
7	Filler Metal Chemical Analyses (Hts. VE 716, VE 717)	21
8	Ingot Chemical Analyses (Hts. VE798-803)	23
9	Filler Metal Chemical Analyses (Hts. VE 798-800)	24
10	Comparison Between Fusion Zone Composition and Notch Toughness	33
11	Fusion Zone Mechanical Properties	35
12	Weldment Mechanical Properties	41
13	Fracture Toughness of CW-GTAW Welded AF 1410 Steel	42
14	Alternate Immersion Stress Corrosion Data	48
15	Stress Corrosion of CW-GTA Welded AF 1410 Steel	49

SECTION I

INTRODUCTION

A high strength steel alloy, possessing high fracture toughness and good stress corrosion resistance, was recently developed in a cooperative program by General Dynamics and U. S. Steel under the sponsorship of the Air Force Materials Laboratory, Reference 1. The nominal composition of the alloy steel resulting from the development program is 14Co-10Ni-2Cr-1Mo-0.16C-bal Fe. This 230-250 Ksi (1586-1724 MPa) TUS steel, designated AF 1410, is attractive for aerospace structural applications due to its superior fracture properties and stress corrosion resistance.

Preliminary welding investigations using a matching AF 1410 filler metal composition indicated good weldability with arc welding processes, References 1 and 2. However, some tensile ductility and/or notch toughness degradation was present in the heat affected zone and postweld aged fusion zone. These losses of toughness properties, while not serious enough to limit the welding of AF 1410 steel, indicated the need for additional study.

In this investigation the effect of (1) heat input and number of thermal reversals on HAZ properties (2) filler metal composition, e.g. level of deoxidizing and impurity elements on mechanical properties, and (3) deposition rate, cooling rate, and post weld aging on fusion zone mechanical-metallurgical properties were briefly evaluated. Another factor which proved to be of some concern in this investigation was the level of molten pool contamination possible when welding with the CW-GTAW, HW-GTAW, and CW-PAW arc weld processes. The evaluation of the heat affected zone was curtailed when it was judged the resultant mechanical properties were adequate for the arc weld processes investigated. Thus, the remainder of the study was directed towards improving the fusion zone mechanical properties. Due to the scope of the variables involved in this program a screening of weld processes, filler metal heats, etc. was necessary to reach program goals. An outline of the investigation screening process is illustrated in Figure 1. Using this approach the program goals of high strength-high toughness-high corrosion resistant weldments were for the most part met, Table 1.

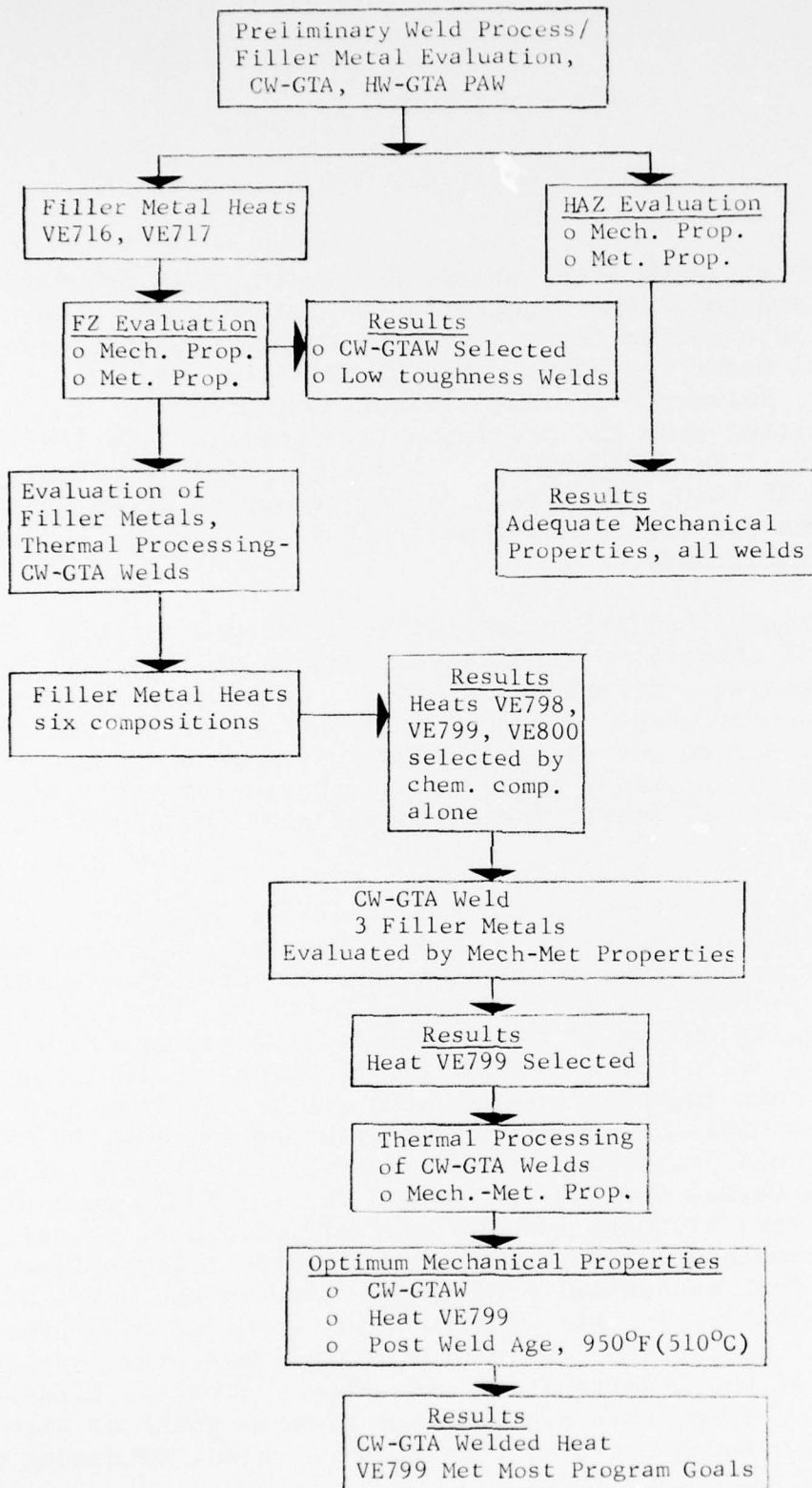


Figure 1 Investigation Outline

TABLE 1 PROGRAM GOALS

Property	Rolled Plate Goals (AF 1410 Steel)	Program Weldment Results (CW-GTAW, Heat VE799)	
TYS, Ksi (MPa)	210-230 (1448-1586)	212	(1462)
TUS, Ksi (MPa)	230-250 (1586-1724)	224	(1544)
K _{IC} , Ksi $\sqrt{\text{in}}$ (MPa $\sqrt{\text{m}}$)	≥ 115 (126.4)	139.5 ⁽²⁾	(153.3)
CVN equiv, ft-lbf (J)	≥ 35 (47.5)	43.5	(58.9)
K _{ISCC} , Ksi $\sqrt{\text{in}}$ (MPa $\sqrt{\text{m}}$)	≥ 100 (109.9)	91	(100)

Notes:

- (1) It was the intention of this investigation for post weld aged fusion zone mechanical properties to meet AF 1410 steel rolled plate goals.
- (2) K_Q value

It is not suggested that the resultant mechanical properties derived from the FZ or HAZ evaluations in this investigation cannot be improved upon with other weld processes, parameters, etc. Rather, improvements in filler metal composition and arc weld metal purity will further improve the fusion zone properties. In addition, metallurgical investigations of the effect of complex carbides, which are formed during multipass welding and/or post weld aging, on stress corrosion resistance also will result in meeting this goal. This feasibility investigation has demonstrated that the AF 1410 steel weld system is capable of achieving high toughness and high stress corrosion resistance concomitant with required strength levels in arc welds.

SECTION II

BACKGROUND

Matching filler metal compositions to the AF 1410 (14Co-10Ni-2Cr-1Mo-0.16C) alloy steel can be expected to demonstrate similar metallurgical behavior as the base plate composition. Maximum strengthening occurs during the precipitation of a fine dispersion of secondary hardening alloy carbides in a highly dislocated lath martensite matrix. Mo in conjunction with C forms dislocation nucleated M_2C alloy carbides, over a narrow range of aging temperatures, which are principally responsible for an abrupt increase in both strength and toughness. Cr in this composition is free to substitute to some extent in both the M_3C and M_2C carbide structures resulting in an accentuated hardening effect and shift in secondary hardening temperature. At optimum aging temperatures, the principal alloy carbide has been identified as $(Mo, Cr)_2C$ in a similar 10Ni-8Co-2Cr-1Mo-.11C steel, Reference 3, while in the 14Co-10Ni-2Cr-1Mo-0.16C composition, Fe_3C and complex alloy carbides (M_2C , M_xC) have been found, Reference 4. During higher aging temperatures an austenite reversion occurs which increases to a maximum at $1100^\circ - 1150^\circ F$ ($593 - 621^\circ C$), References 1 and 5. Weldment heat affected zones, subject to repeated thermal reversals in the austenite forming temperature ranges, may form up to 6.0 volume percent reverted austenite, Reference 1.

For optimum toughness in the base plate composition the deoxidation, (Mn, Si, Al, V, Ti) and impurity (S, P, O, N), elements were maintained at low levels. However, some deoxidation is required for arc weld deposited filler metals to alleviate porosity. A study to produce improved Ni-Co-Cr-Mo-C filler metals by eliminating porosity without affecting the weld metal mechanical properties, indicated additions of 0.10 to 0.20% Si, up to 0.02% Al, or up to 0.10%V were acceptable, Reference 6. When deoxidizing elements are used synergistically, adjustments in the levels should be made as over deoxidation is known to decrease weld metal toughness, Reference 7.

Numerous and complex variables interact in the fusion zone due to the diversity of weld parameters possible in different arc weld processes which control the resultant strength and toughness of the weld metal. The microstructure can be difficult

to interpret for each 14Co-10Ni-2Cr-1Mo-0.16C weldment due to the superimposing of the transformation structure on the solidification structure, the phase reversals, and continuous aging which occurs during multipass welding. In addition the deoxidation practice and as-deposited weld metal purity can vary with arc weld process.

In the heat affected zone, the documented toughness degradation (Reference 2) is expected to be a function of the number of thermal reversals and heat input. A large number of thermal reversals may result in up to 6.0 volume percent reverted austenite in the heat affected zone. Also, complex alloy carbide reactions are possible in Fe-Mo-C secondary hardening steels at higher than normal aging temperatures which could be responsible for this HAZ behavior. A study of the alloy carbide stability ranges in similar Fe-Mo-Cr-C secondary hardening steel systems disclosed that the M_2C , M_3C , and M_7C_3 type carbides would most likely occur during weld thermal cycling in the heat affected zone, Reference 8 and 9. A M_xC nonstoichiometric carbide has been identified in the AF 1410 steel. The M_6C equilibrium carbide is not expected to form under normal welding conditions.

SECTION III

EXPERIMENTAL PROGRAM

The scope of the experimental program was the melting, processing, and welding of selected filler metal compositions. Both the fusion and heat affected zones of the resultant multiple pass arc welds were evaluated for their mechanical and metallurgical properties.

3.1 FILLER METAL SELECTION AND PROCESSING

Based on data obtained from the Heat No. 7318-8091 weldments, References 1 and 2, the initial filler metal compositions were designed with a matching base plate composition, Table 2. Si, Al, and V were selected as deoxidizing elements. To obtain high fusion zone toughness the S, O, and N were limited to low levels in the wire composition and the as-deposited chemical composition. Following the fusion zone evaluation resulting from the subsequent weldments, six additional filler metal compositions were melted to the required chemistry as listed in Table 3. For these series of heats, the additions of Al and Mn as deoxidizing elements were limited. An attempt was made to closely control the levels of the deoxidizing and impurity elements by selection of high grade melt stock prior to VIM processing, Appendix 1. The resultant VIM ingot and finish wire chemistries are discussed in the next section.

The filler metal alloys were melted as 165 lb (74.8Kg) VIM heats. The ingot sizes were approximately 5.75 inch (14.6 cm) diameter tapering to 5.5 inch (14.0 cm) diameter with a length of 28 inches (71.1 cm). After hot rolling to 0.312 inch (7.9 mm) diameter rod, the redraw stock was Kalo turned to remove all external oxidation products. To keep the contaminants at low levels (1) annealing operations were conducted in a vacuum environment and (2) wire drawing was conducted without the use of contaminants. The finished product was 0.062 inch (1.6 mm) diameter weld wire which was subsequently given a complete chemical analysis.

Ingot heats 2, 3, and 4 were processed to 0.5 and 1.0 inch (1.3 and 2.5 cm) diameter redraw stock. Further processing of these heats was curtailed due to lack of compositional control.

TABLE 2 REQUIRED CHEMICAL ANALYSES FOR INITIAL TWO FILLER METAL HEATS

<u>ELEMENTS</u>	<u>NOMINAL CHEMISTRY</u>		<u>HEAT NO. VE717</u>	ALLOWABLE VARIATION OF <u>NOMINAL CHEMISTRY</u>
	<u>HEAT NO. VE716</u>			
C	0.15		0.15	± 0.01
Mo	1.0		1.0	± 0.1
Co	14.0		14.0	± 0.5
Cr	2.0		2.0	± 0.2
Ni	10.0		10.0	± 0.5
Si	0.10		0.10	± 0.02
Al	0.015		0.015	± 0.005
V	0.10		-	± 0.02
Mn			NA - .05 MAX	
Ti			NA - .01 MAX	
S			.005 MAX	
P			.006 MAX	
H			.0005 MAX	
O			.0030 MAX	
N			.0030 MAX	

Required Ingot Analysis in Weight Percent

TABLE 3 REQUIRED CHEMICAL ANALYSES FOR FINAL SIX FILLER METAL HEATS

Elements	Nominal Chemistry					Allowable Variation of	
	Heat No. 1	Heat No. 2	Heat No. 3	Heat No. 4	Heat No. 5	Heat No. 6	Nominal Chemistry
C	0.17	0.17	0.17	0.15	0.15	0.15	+0.01
Co	15.0	15.0	15.0	14.0	14.0	14.0	+0.5
Ni	10.5	10.5	10.5	10.0	10.0	10.0	+0.5
Cr	2.0	2.0	2.0	2.0	2.0	2.0	+0.2
Mo	1.0	1.0	1.0	1.0	1.0	1.0	+0.1
Si	0.1	0.1	0.1	0.1	0.1	NA	+0.02
Al	NA	NA	0.01	NA	NA	NA	+0.005
V	0.06	NA	NA	0.06	NA	NA	+0.02
Mn	NA	NA	NA	NA	NA	NA	
Ti			NA -0.01 MAX				
S			0.005 MAX				
P			0.006 MAX				
O			0.0030 MAX				
N			0.0030 MAX				
H			0.0005 MAX				

Deoxidation elements when designated NA (None added) are to be maintained below the following levels: Mn-0.05, Si-0.05, Al-0.005, V-0.02

Required Ingot Analyses in Weight Percent

3.2 ARC WELD PROCESSES AND PARAMETERS

Eleven-6 x 12-15 x 0.625 inch (15.2 x 30.5 - 38.1 x 1.6 cm) weldments using a 14Co-10Ni-2Cr-10Mo-0.16C steel base plate and matching filler metal were completed by the cold wire (pulse arc), hot wire (pulse arc) gas tungsten arc and cold wire plasma arc weld processes.

The base plate was in the double austenitized and water quenched(1650°F (898.9°C) - 1 hr/in WQ + 1500°F (815.6°C) - 1 hr/in WQ) heat treatment condition prior to welding. The object of using three arc weld processes was to increase the weld deposition rate appropriate levels for each process consistent with acceptable mechanical properties.

Since acceptable weld parameters had been previously established (Reference 1) for the CW and HW-GTAW welds, only minor adjustments were made. Additional effort was expended in determining the balance between heat input and deposition rate for CW-PAW welds by bead-on-plate and in-groove weld tests. These tests indicate that 3.5 lb/hr (1.58Kg/hr) is close to the maximum deposition rate for cold wire PAW welds. For higher deposition rates hot wire feed is recommended. The CW and HW-GTAW welds were deposited with low heat inputs while the CW-PAW weldments required a 2 to 3 fold increase, Table 4.

By developing a weld joint better suited for PAW welding a 2.0 lb/hr (0.9Kg/hr) deposition rate at 60-65 Kj/in (2.4-2.6Kj/mm) is possible and would result in improved weld metal cooling rates, Reference 10.

The non-keyhole mode was used for all multipass PAW welding in the investigation. (All welds except the CW-GTAW weldments were completed with a traveling gas shield to decrease gaseous contamination).

The CW-GTAW process was selected to continue the evaluation of filler metal compositions and to complete the weldments required for mechanical property characterization. Nine weldments were made in 0.5 inch (1.3 cm) and 1.125 inch (2.9 cm) thick rolled plate per the welding parameters listed in Table 5. All the weldments were made in 20 inch (50.8 cm) long plates as a 6 inch (15.2 cm) linear section was made available to AFML.

The weld plates were demagnetized to less than 1 gauss and preheated to 120°F (48.9°C) prior to welding. The weld groove configuration for the CW-GTA welds in 0.5 inch (1.3 cm) and

TABLE 4 WELDING PARAMETERS (HEATS VE 716-717)

PARAMETERS	CW-GTAW			WELD PROCESS					
	WELD A	WELD E	WELD F	WELD B	HM-GTAW		WELD C	WELD D	CW-PAW
					WELD G	WELD H			
Plate thickness, in.	0.5	0.5	0.5	0.5	0.5	0.5	0.5	0.5	0.5
Weld groove	40°J	40°J	40°J	60°J	60°J	60°J	60°J	60°J	60°J
Electrode diam., in.	0.125	0.125	0.125	0.156	0.156	0.156	0.125	0.125	.125
Electrode type	W-2Th	W-2Th	W-2Th	W-2Th	W-2Th	W-2Th	W-2Th	W-2Th	W-2Th
W distance from nozzle-setback, in.	0.625	0.5	0.5	0.625	0.625	0.625	1.343	1.343	1.343
Gas nozzle or orifice size	8	8	8	12	12	12	.125	.125	0.125
Wire diam., in.	0.062	0.062	0.062	0.062	0.062	0.062	0.062	0.062	0.062
Wire ht. No.	7318-8091	VE717	VE716	VE717	VE717	VE716	VE717	VE716	VE716
Passes to Complete	7	8	6	4	5	6	3	4	6
Total Weld Passes	9	11	8	6	8	7	4	7	7
Interpass Temp, °F	160	170	170	180	180	180	170	170	160
Center gas, A in cfm	-	-	-	-	-	-	2.0	2.0	2.0
Torch gas	75He-25A	50He-25A	50He-25A	50He-30A	50He-30A	50He-30A	A	A	A
Torch gas flow rate, cfm	100	75	75	80	80	80	22	22	22
Trailing shield, A in cfm	-	-	-	15	15	15	15	15	15
HM Torch gas, A in cfm	-	-	-	5	5	5	-	-	-
Arc current, amp	200-5	200-5	200-5	450-4	450-4	450-4	260	260	260
Arc Voltage, volt	160-15	160-15	160-15	300-4	300-4	300-4	30	32	31
Arc Travel Speed, ipm	13	13	13	18	18	18	5	6	5
Wire Feed, ipm	4	4	4	12	12	12	65	36	60
HM Amperage	22.8	22.0	22.0	-	-	-	-	-	-
HM Voltage	-	-	-	140	140	140	-	-	-
HM Wire Feed, ipm	-	-	-	5	5	5	-	-	-
Heat Input, Kj/in	33.2	33.2	33.2	104	108	108	93.6	83.2	96.7
Deposition rate, lbs/hr	1.2	1.1	1.1	5.4	5.6	5.6	3.4	1.9	3.1

in x 25.4 = mm
 °C = (°F-32)/1.8
 degrees x 0.01745 = rad
 Kj/in x 0.0394 = Kj/mm
 lbs/hr x 0.4536 = Kg/hr

TABLE 5 WELDING PARAMETERS (HEATS VE 798-800)

PARAMETERS	WELD 3A	WELD 3B	WELD 3C	WELD3D	WELD 3E	WELD 4A	WELD 4B	WELD 4C	WELD 4D
Plate thickness, in.		0.5				1.125	1.125	1.125	0.5
Weld groove		Double J - 40° included angle				40°	Double U		40°J
Electrode diam., in.		0.125					0.125		
Electrode type		W-2Th					W-2Th		
W distance from nozzle setback, in.		0.625, 0.500, 0.375					0.625, 0.500, 0.375		
Gas nozzle or orifice size		No. 8 (0.500 in. ID)					No. 8 (0.500 in. ID)		
Wire diam., in.		0.062					0.062		
Wire ht. No.		VE799		VE799	VE799		VE799		
Total weld passes		12		11	16		30		12
Interpass temp., °F		120-160		100-140	100-135		100-160		100-145
Back-Up gas, cfh		A-10		A-12	A-12		A-12		A-12
Torch gas		60		75He-25A			75He-25A		
Torch gas flow rate, cfh		200-5		200-15	200-15		60		
Arc current, amp		160-15		160-5	160-5		200-15		
Arc voltage, volt		14		14	13		160-5		
Arc travel speed, ipm		35.7		4	13		4		13
Wire feed, ipm							22		
Heat input, Kj/in.		35.7		37.1	37.1		37.1		37.1
Deposition rate, lbs/hr		1.1		1.1			1.1		

in x 25.4 = mm
 $^{\circ}\text{C} = (^{\circ}\text{F} - 32) / 1.8$
 degrees x 0.01745 = rad
 $\text{Kj/in} \times 0.0394 = \text{Kj/mm}$
 $\text{lbs/hr} \times 0.4536 = \text{Kg/hr}$

1.25 inch (2.9 cm) thick plate was Double J and Double U, respectively, both with 40° (0.70 rad) included angle. The HW-GTA and CW-PAW weld joints were Double J - 60° (1.05 rad) grooves. All the weld joints had 0.06 inch (1.5 mm) lands and a 0.125 inch (3.2 mm) groove radius.

The CW-GTA weldments (3A-4D) were accomplished with a Sciaky automatic welding control system capable of both pulse arc (amperage) and mechanical (transverse to weld direction) oscillation. The amperage was pulsed between two levels with the voltage being held near constant by the closed loop feed back system. Sample recordings were taken for all the above weldments per Figure 2. The rate of amperage response (overshoot) is less than a 40 amp swing which correlates to the correction factor of the solid state controls.

3.3 WELD THERMAL ANALYSIS

Weld center-line and HAZ cooling rates were monitored by W-3Re, W-25Re and chromel-alumel thermocouples, respectively. All fusion zone thermocouple insertions were made behind the traveling arc in the outer portions of the molten puddle. HAZ thermal measurements were made at the base plate center at varying distances from the weld centerline. A minimum of four thermocouples were spaced at approximately 0.5 inch (1.3 cm) intervals in the heat affected zones which were monitored.

3.4 MECHANICAL TESTING

The mechanical properties of the weldment fusion and heat affected zones were evaluated by tensile, notch toughness, fracture toughness, stress corrosion, S/N fatigue, and crack growth rate tests. The specimen configurations and detailed test procedures have previously been given in Reference 1.

3.4.1 Tensile

Tensile tests were conducted at room temperature in accordance with ASTM E8-68 and Federal Test Method Standard No. 151a. Tests were performed in both the longitudinal and transverse orientations with respect to the weld direction using a 120,000-pound-capacity BLH test machine. The yield point was determined with a strain rate of 0.003 inch/inch/min.

3.4.2 Notch Toughness

The notch toughness was determined by a standard-size Charpy V-Notch specimen in the T-L direction in both the FZ and HAZ with the notch oriented perpendicular to the weld plate surface. The

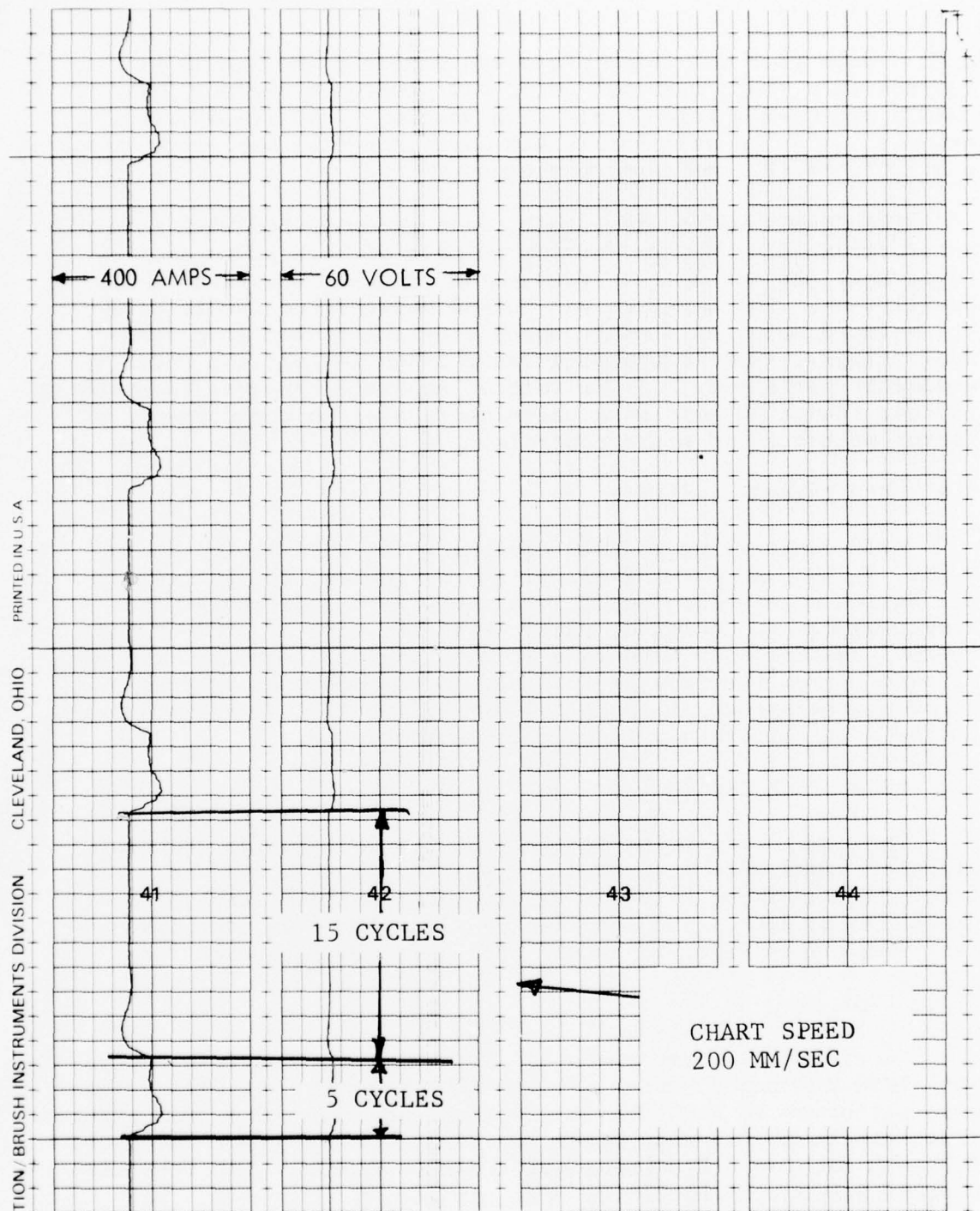


Figure 2 CW-GTA Pulse Arc Amperage and Voltage Response

location of charpy notches in the HAZ were measured from the weld centerline at the plate center. The testing was conducted in a Riehle Impact machine at ambient and cryogenic temperatures per ASTM 370A-1.

3.4.3 Fracture Toughness

Fracture toughness tests were conducted in the L-T plate orientation at room temperature using compact tension test specimens. The specimens, test fixtures, fatigue cracking, and test procedures met all the requirements of ASTM E399-72.

Fatigue precracking was accomplished in a BLH SF-1-U fatigue machine using decreasing fatigue loads to crack the specimens so that the final stress intensity was $\ll K_{IC}/2$ as required by ASTM E399-72. Difficulty was encountered in generating straight fronted fatigue cracks, and several specimens did not meet the requirements of paragraph 8.2.3 of ASTM E399-72. Therefore, those results could not be described as valid K_{IC} data.

Static testing was conducted at room temperature in a 60,000 pound (27,216 Kg) capacity AMTEK electrohydraulic test machine for $B=1.0$ inch (2.54 cm) specimens. A calibrated NASA-type compliance gauge was used to record crack opening displacement (COD).

The stress solution of the compact tension specimen ($H/W = 0.6$) is given by:

$$K_I = \left[P/B(W)^{\frac{1}{2}} \right] \left[\begin{array}{ccc} \frac{1}{2} & \frac{3}{2} & \frac{5}{2} \\ 29.6(a/w) & - 185.5(a/w) & + 655.7(a/w) \\ \frac{7}{2} & & \frac{9}{2} \\ - 1017(a/w) & + 638.9(a/w) & \end{array} \right]$$

3.4.4 Compact Tension- K_{Isc}

Stress corrosion tests were conducted in 3.5 percent NaCl solutions using the Novak-Rolfe Constant Displacement WOL environment test specimen.

The stress solution of the K_{Isc} constant displacement specimen is given by:

$$K_I = E V_o C_3(a/w) \text{ where} \\ \frac{C_6(a/w)}{\sqrt{a}}$$

$$C_3(a/w) = \frac{30.96(a/w) - 195.8(a/w)^2 + 730.6(a/w)^3}{-1186.3(a/w)^4 + 754.6(a/w)^5}$$

$$C_6(a/w) = \frac{1}{e} \left[4.495 - 16.130(a/w) + 63.838 (a/w)^2 - 89.125(a/w)^3 + 46.851(a/w)^4 \right]$$

E = Modulus of Elasticity

Vo = Crack Opening Displacement

a = Crack Length

No continuous crack propagation data was recorded as crack growth measurements were limited to visual inspection of specimens enduring 1000 hours without failure.

3.4.5 Fatigue

The fatigue properties of the fusion zone was determined by S/N fatigue and compact tension specimens.

3.4.5.1 S/N Fatigue

Axial tension-tension fatigue tests were run using a Sonntag SF-10-U fatigue machine with a 5:1 multiplying fixture. Smooth ($K_t=1$) were cyclic loaded at a stress ratio of 0.1.

3.4.5.2 Compact Tension, da/dN

The compact tension specimen used to measure crack growth had a thickness of 0.5 inch (1.3 cm). The specimen was fatigue precracked using decreasing load steps in a Baldwin SF-1-M Fatigue Test Machine. After precracking, the coupons were installed in a 60,000 lb. (27,216 kg) Electro-Servo Hydraulic Ametek Test Machine where the load range of 6,000 lbs. (2,722Kg) was used with measured accuracies of ± 30 lbs. (13.6 Kg) as read on a dial and ± 60 lbs. (27.2Kg) as observed with an oscilloscope during fatigue cycling.

The stress solution of the compact tension specimen ($H/W = 0.486$) is given by:

$$K = \frac{\Delta P}{B \sqrt{W}} f(a/w) \text{ where}$$

$$f(a/w) = 30.96(a/w)^{1/2} - 195.8(a/w)^{3/2} + 730.6(a/w)^{5/2} - 1186.3(a/w)^{7/2} + 754.6(a/w)^{9/2}$$

$$da/dN = C \Delta K^n$$

where a = actual half-crack length

N = number of cycles

ΔK = range of crack tip stress intensity parameter

A = proportionally constant

n = numerical exponent

In tests requiring a 3.5% NaCl aqueous solution, the environment was contained in a clear plexiglass chamber. Two chambers were used, one on either side of the coupon with a neoprene o-ring seal. The environment enters one chamber from a gallon plastic jug, flow through the crack into the other chamber and then into a reservoir. A submersible pump was used to pump the fluid to the upper container at the rate of two quarts/hour.

The cyclic rate for specimens tested in dry air and 3.5% NaCl was 360 cpm (6 Hertz) and 6, 60 cpm (0.1, 1.0 Hertz), respectively.

The results were calculated with a Hewlett-Packard 9100B calculator programmed to give da/dN and ΔK which is calculated as the average for each data point. A plot of da/dN versus average ΔK is drawn where constants fitting $da/dN = C(\Delta K)^n$ were found and tabulated.

3.5 METALLURGICAL ANALYSIS

Metallurgical analysis in this program was limited to a general phenomenological treatment of the effects of cooling rate, deposition rate, number of thermal reversals and post weld aging on fusion and heat affected zone properties.

3.5.1 Microstructure

Standard polishing and etching techniques were used in preparing metallographic specimens for optical microscopy analyses. A modification of a tint etchant (Reference 11) was used to reveal solidification structures. Transformation temperatures were measured on a high thermal response Dilatronic III Metallurgical Dilatometer.

The fracture topography of the test specimens were analyzed both at the macroscopic and microscopic level. High magnification fractographic analysis was performed on a JEOL JSM-2 Scanning Electron Microscope.

Thin foils for transmission electron microscopy were prepared from (0.09 in) (2.3 mm) diameter discs thinned to 2 mils thickness. After chemical thinning, the discs were electro-polished in a chromic-acetic acid solution (75 gm CrO_3 + 400 ml acetic acid + 20 ml distilled water) in a jet polishing apparatus. The polishing voltage varied from 16-19 volts and the polishing current between 65-90 milliamperes. Foils were examined in a Siemens Elmiskop IA microscope by bright and dark field techniques.

3.5.2 Microhardness

Microhardness readings were taken using a Knoop diamond indenter (500 gram load) for all the welds that were thermally analyzed. The indentations were made at the plate center from the fusion centerline into the heat affected zone for welds in the as-deposited and postweld aged condition. The FZ centerline and FZ/HAZ distances were measured for each HAZ microhardness reading to record hardness changes due to microstructural changes.

3.5.3 X-Ray Diffraction

X-Ray diffraction analyses were made with a General Electric XRD-5 diffractometer to determine the volume percent of retained and/or reverted austenite present in the fusion and heat affected zones, both in the as-deposited and postweld aged condition. Etching to reveal microstructure and microhardness readings were used to differentiate areas of interest prior to analysis. The volume percent austenite was determined on mechanically polished surfaces (6 μ diamond) by measurement of integrated diffraction intensities using the direct comparison method. In this method, the sample is irradiated with monochromatic Cr x-rays and the intensities of the resultant diffraction from the austenite and martensite (ferrite) planes are measured and recorded. Due to the possibility of preferred orientation in the samples, all sets of peaks were averaged in calculating the percentage of austenite present leading to improved accuracy.

SECTION IV

RESULTS AND DISCUSSION

Two filler metal compositions were deposited by three arc weld processes during the preliminary screening phase of the program. For the remainder of the evaluation the CW-GTAW was used in the welding of three additional filler metal heats. The scope of these investigations included the chemical, mechanical, and metallurgical analyses of the fusion and heat affected zones.

4.1 CHEMICAL COMPOSITION

Three rolled plate AF 1410 alloy steel compositions were used in various stages of the welding investigation, Table 6. The plate product was VIM/VAR processed, cross rolled, and double austenitized at 1650°F (898.8°C) and 1500°F (815.6°C) with water quenching at each interim. Aged mechanical properties indicated that a S level >0.005% will considerably degradate the notch toughness. The low toughness heats were used to establish fusion zone properties while the high toughness heat was used exclusively for evaluation of the heat affected zone properties.

The ingot and finished weld wire chemical analyses for Heats VE 716 and 717 indicated partial adherence to the specified filler metal chemistry (Table 2) with the exception of Al and S, Table 7. Deoxidizing (0.03-0.057% Al) and impurity (0.006-0.008% S) elements in excess of recommended levels (>0.02%Al and >0.005%S) can result in a decrease in weld metal notch toughness. Acceptable levels of O were present in the two heats of weld wire, Table 7.

Analyses of as-deposited fusion zone compositions, representing variations in weld process and/or filler metal composition, disclosed that Al, S, and in some cases, O and N, exceeded the levels required for adequate notch toughness, Appendix 2. The progressive increase in Al from 0.03-0.057% in the weld wire to 0.061-0.095% in the as-deposited weld metal represents a 3 to 6 fold increase over the nominal requirement. Since different laboratories are responsible for these analyses the variations may be due to technique. In either case Al at high levels, either present singly or combined with N, results in toughness degradation. It is also expected that toughness in the weld metal will be as sensitive to S in excess of 0.005% as has been reported in rolled plate, Reference 12.

Although all the HW-GTAW and CW-PAW weldments produced were shielded, oxygen and nitrogen contamination resulted in some

TABLE 6 AF 1410 ROLLED PLATE PROPERTIES

<u>Elements</u>	<u>HAZ Evaluation</u>	<u>Fusion Zone Evaluation</u>	
	<u>0.625 inch-t</u> <u>(1.58 cm)</u>	<u>0.625 inch-t</u> <u>(1.58 cm)</u>	<u>1.25 inch-t</u> <u>(3.18 cm)</u>
	(A)	(B)	(C)
C	0.16	0.14	0.14
Mo	0.98	0.95	0.97
Co	13.80	13.95	14.05
Cr	1.95	1.88	2.03
Ni	10.15	10.10	10.10
Si	0.04	0.031	0.041
Al	0.009	0.006	0.005
Mn	0.06	0.085	0.079
Ti	0.01	<0.01	<0.01
S	0.003	0.006	0.006
P	0.007	0.005	0.007
N	20 ppm	30 ppm	20 ppm
O	9 ppm	<10 ppm	<10 ppm

Mechanical Properties

TYS, Ksi (MPa)	230 (1585.8)	224 (1544.4)	230 (1585.8)
TUS, Ksi (MPa)	245 (1689.2)	235 (1620.3)	250 (1723.7)
CVN, ft-lbf (J)	51.3 (69.6)	31.3 (42.4)	29.3 (39.7)

Notes: chemical analyses expressed in weight percent

S > 0.005%, not to AF 1410 composition

VIM/VAR, rolled plate

Aged: 950°F (510°C) - 5 hrs/WQ

(A) Heat No. 9

(B) Heat No. 61690

(C) Heat No. 61689

TABLE 7 FILLER METAL CHEMICAL ANALYSES (HTS. VE 716, VE 717)

	<u>Ingot</u>	<u>WEIGHT PERCENT</u>				<u>Ingot</u>	<u>VE 717</u> <u>Check 1</u>	<u>Check 2</u>	<u>VE 717</u> <u>Check 1</u>	<u>Check 2</u>
		<u>VE 716</u> <u>Check 1</u>	<u>Check 1</u>	<u>Check 2</u>	<u>Check 2</u>					
C	0.151	0.15	0.15	0.15	0.15	0.155	0.15	0.15	0.15	0.15
Mo	0.93	1.06	1.06	0.95	0.95	0.93	1.02	0.95	1.02	0.95
Co	15.10	14.04	14.04	14.60	14.60	15.13	14.30	14.40	14.30	14.40
Cr	1.95	2.18	2.18	2.08	2.08	2.05	2.13	2.18	2.13	2.18
Ni	10.65	9.97	9.97	9.86	9.86	10.77	9.94	9.95	9.94	9.95
Si	0.113	0.14	0.14	0.12	0.12	0.106	0.13	0.12	0.13	0.12
Al	0.027	0.057	0.057	.03	.03	0.028	0.055	0.03	0.055	0.03
V	0.128	-	-	-	-	-	.02	.01	.02	.01
Mn	0.032	<0.01	<0.01	<0.03	<0.03	<0.032	<0.01	<0.03	<0.01	<0.03
Ti	<0.01	<0.01	<0.01	<0.01	<0.01	<0.01	<0.01	<0.01	<0.01	<0.01
S	<0.005	0.007	0.007	0.006	0.006	0.005	0.006	0.008	0.006	0.008
P	0.006	0.006	0.006	0.006	0.006	0.006	0.006	0.006	0.006	0.006
H	2*	3*	3*	-	-	1*	1*	-	1*	-
O	62*	14*	14*	40*	40*	28*	10*	-	10*	-
N	3*	2*	2*	5*	5*	4*	3*	5*	3*	5*

0.062 inch (1.57 mm) diameter weld wire

*ppm

welds, Appendix 2. Fortunately, this condition is not indigenous to the weld metal system or weld processes as high purity welds have been produced in other studies using identical weld conditions, Reference 10. It was the apparent infusion of air into the plasma arc weld metal pool that eliminated this weld process from further consideration. Another unexpected problem was the decreased arc-transfer efficiency for alloying elements, e.g., Ni and Co through the plasma arc, Appendix 2. Normally, these elements are not very volatile and would not present a problem. Additional chemical analyses of the as-deposited plasma arc weld metal will be required to adjust the filler metal compositions intended for plasma arc welding.

In the second phase of filler metal alloy development, an attempt was made to control the Al and S level in the heats by careful selection of melt materials, Appendix 1. Besides the Al addition, V and Si were the only deoxidizing elements selectively added to these series of heats. Mn was not added. The ingot chemistry for Heats VE 798-803 presented in Table 8 indicates S met the chemistry requirements while Al again was not controlled within desirable limits. Three separate Al analyses were conducted by different laboratories on each ingot heat to provide a suitable check, Appendix 3. Heat VE 798 was the only ingot with an acceptable Al analysis, but the finished wire analysis in Table 9 indicated the S content was in excess of the desired level. On the basis of the reported ingot compositions given in Table 8, three heats with the lowest combined levels of Al and S were selected for further processing to finished weld wire. The final selection of the filler metal compositions in Table 9 concomitant with high toughness welds was dependent on the mechanical properties of the CW-GTAW fusion zone. Heat VE 799 was selected as the best high toughness filler metal composition in this investigation.

The ultimate approach to determine the optimum selection and level of deoxidizing elements, e.g., Al, Mn, Si, V, etc., consistent with balanced weldability and good toughness, is to use a factorial experiment for the sorting procedure. However, the difficulty in controlling the impurity and deoxidizing elements to prescribed levels in this investigation precluded the application of these techniques.

TABLE 8 INGOT CHEMICAL ANALYSES (HTS. VE 798-803)
Heats 1-6 Required Chemical Composition, Heats VE 798-803 Ingot Chemistry

NOMINAL CHEMISTRY													
Elements	No. 1	VE-798	No. 2	VE-803	No. 3	VE-802	No. 4	VE-801	No. 5	VE-800	No. 6	VE-799	Allowable Variation of Nominal Chemistry
C	0.17	0.16	0.17	0.17	0.17	0.17	0.15	0.15	0.15	0.15	0.15	0.14	+0.01
Co	15.0	14.85	15.0	14.62	15.0	14.96	14.0	14.44	14.0	14.44	14.0	14.05	+0.5
Ni	10.5	10.35	10.5	10.12	10.5	10.35	10.0	9.94	10.0	9.93	10.0	9.71	+0.5
Cr	2.0	2.18	2.0	2.12	2.0	2.07	2.0	2.01	2.0	2.02	2.0	2.10	+0.2
Mo	1.0	0.98	1.0	0.90	1.0	0.97	1.0	0.96	1.0	1.02	1.0	1.09	+0.1
Si	0.10	0.08	0.10	0.11	0.10	0.08	0.10	0.08	0.10	0.10	NA	0.03	+0.02
Al	NA	0.011*	NA	0.052*	0.01	0.049*	NA	0.044*	NA	0.044*	NA	0.019*	+0.005
V	0.06	0.08	NA	0.02	NA	0.02	0.06	0.08	NA	0.02	NA	0.02	+0.02
Mn	NA	0.01	NA	0.01	NA	0.01	NA	0.01	NA	0.02	NA	0.01	-
Ti		0.005		0.005		0.005		0.005		0.005		0.005	0.01 MAX
S		0.004		0.004		0.004		0.004		0.003		0.004	0.005 MAX
P		0.002		0.003		0.002		0.004		0.004		0.005	0.006 MAX
O	-	-	-	-	-	-	-	-	-	23 ppm	-	-	0.030 MAX
N	-	-	-	-	-	-	-	-	-	3 ppm	-	-	0.0030 MAX
H	-	-	-	-	-	-	-	-	-	1 ppm	-	-	0.0005 MAX

* out of specification

NA - none added

* out of specification

NA - none added

TABLE 9 FILLER METAL CHEMICAL ANALYSES (HTS, VE 798-800)

Element	Heat 798		Heat 799		Heat 800	
	Ingot	Filler Wire	Ingot	Filler Wire	Ingot	Filler Wire
C	0.16	0.18	0.14	0.15	0.15	0.16
Co	14.85	14.34	14.05	13.76	14.44	14.06
Ni	10.35	10.36	9.71	9.82	9.93	9.99
Cr	2.18	1.92	2.10	1.90	2.20	1.94
Mo	0.98	1.04	1.09	1.00	1.02	1.06
Si	0.08	0.16	0.03	<0.01	0.10	0.16
Al	0.011	0.015	0.019	0.025	0.044	0.031
V	0.08	0.029	0.02	<0.01	0.02	<0.01
Mn	0.01	<0.05	0.01	<0.05	0.02	<0.05
Ti	0.005	<0.01	0.005	<0.01	0.005	<0.01
S	0.004	0.007	0.004	0.005	0.003	0.005
P	0.002	<0.001	0.005	<0.001	0.004	<0.001
O	-	37 ppm	-	52 ppm	23 ppm	74 ppm
N	-	3 ppm	-	4 ppm	3 ppm	2 ppm
H	-	1 ppm	-	1 ppm	1 ppm	2 ppm

0.062 inch (1.57 mm) diameter weld wire

4.2 FUSION ZONE PROPERTIES

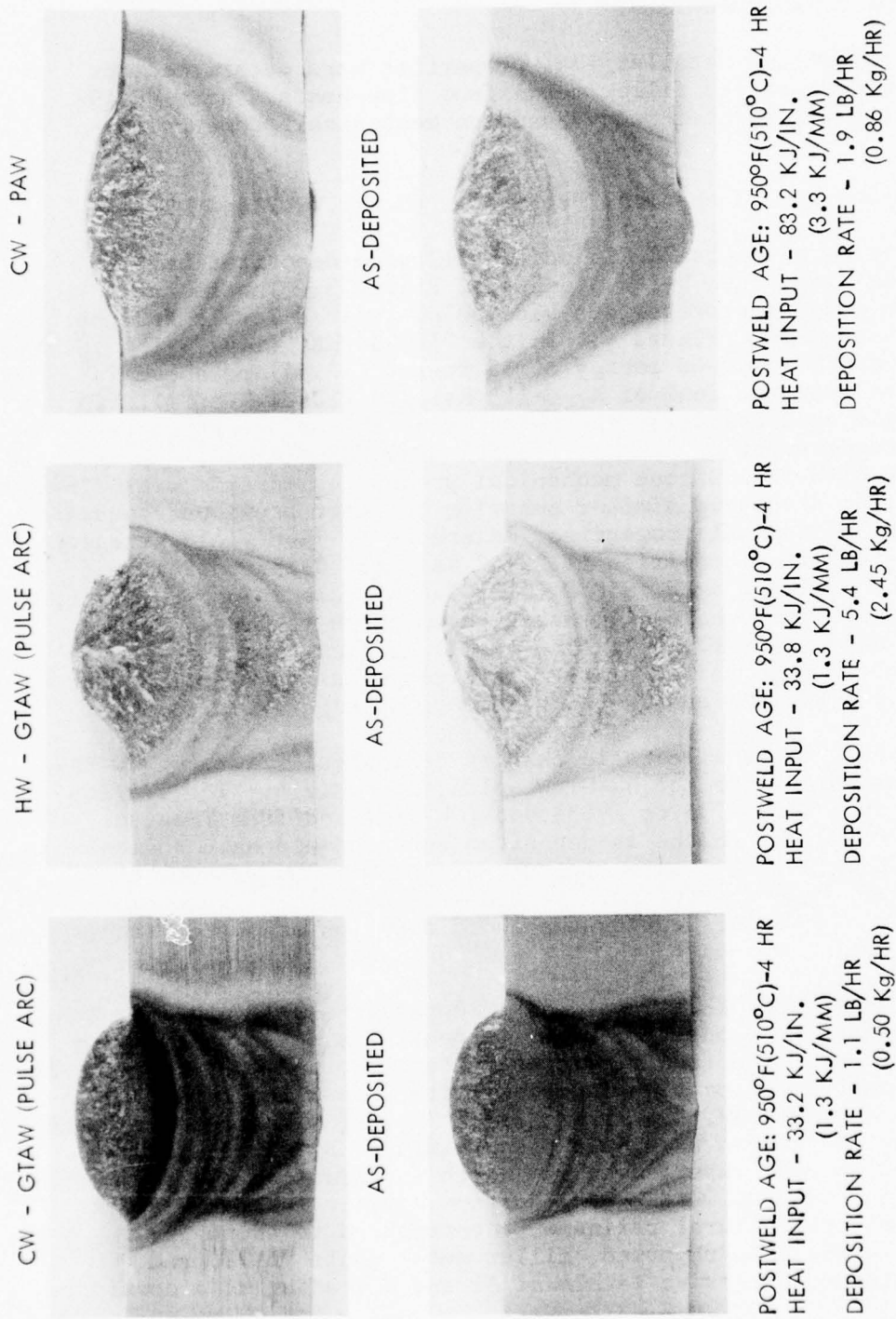
Mechanical and metallurgical properties were determined for the arc weld deposited filler metal from five heats. Heat VE 799 was selected for further study based on mechanical property performance.

4.2.1 Fusion Zone Mechanical Properties (Heats VE 716 - VE 717)

Filler metal heats VE 716 and VE 717 were deposited by the CW-GTAW, HW-GTAW, and CW-PAW processes, Figure 3. The fusion zone notch toughness properties were below desired levels for the multipass arc welds, Figure 4. In the 210-230 Ksi (1447.9-1585.8 MPa) TYS range a CVN absorbed energy of 35 ft-lbf (47.5J) or above is required to meet the goal of $K_{Ic} \geq 115 \text{ Ksi} \sqrt{\text{in}}$ ($126.4 \text{ MPa} \sqrt{\text{m}}$). In the postweld aged condition the majority of the weldments met the strength requirement of 230 Ksi (1585.8 MPa) TUS minimum, Appendix 4. The CW-GTAW fusion zone mechanical properties in this preliminary investigation displayed similar behavior to other previous reported fusion zone mechanical properties, Reference 1. The yield strength in the as-deposited condition is 23-42 Ksi (158.6-289.6 MPa) less than in the postweld aged, 950°F (510°C)-4 hr, condition. However, during the secondary hardening reaction, a notch toughness degradation is evident, 4-11 ft-lb (5.4-14.9J), rather than a toughness increase as in aged rolled plate. This toughness degradation also occurs in the HW-GTAW and CW-PAW weldments upon postweld aging.

The yield to tensile ratio changes dramatically for the CW-PAW welds as compared with the HW-GTAW welds, Appendix 4. The TYS/TUS increases from .699-.733 to .943-.948 (CW-PAW) and from .834 to .924-.927 (HW-GTAW) in the as-deposited and postweld aged fusion zones, respectively. Apparently, the plasma arc super heats the filler metal, thus resulting in some C loss and almost complete solutioning of carbides during the short duration at austenizing temperatures.

The CW-PAW and HW-GTAW weldments represent a 2-3 fold and 5 fold increase in deposition rate, respectively, over that of the CW-GTAW process. The lack of microstructural refinement occurring in the as-deposited fusion zone increases with deposition rate, Figure 5. The HW-GTAW, 5.0 lb/hr (2.3 Kg/hr), fusion zone displayed the minimum refinement with multipass welding. Both weld groups, HW-GTAW and CW-PAW, experienced low notch toughness in the as-deposited and/or post weld aged condition. Other factors besides decreased microstructural refinement contributed to these low toughness levels. As reported, filler metal heats VE 716 and VE 717 contained excessive levels of Al and S leading to a consider-



MAGNIFICATION - 3.5X

Figure 3 Representative Multipass Arc Welds

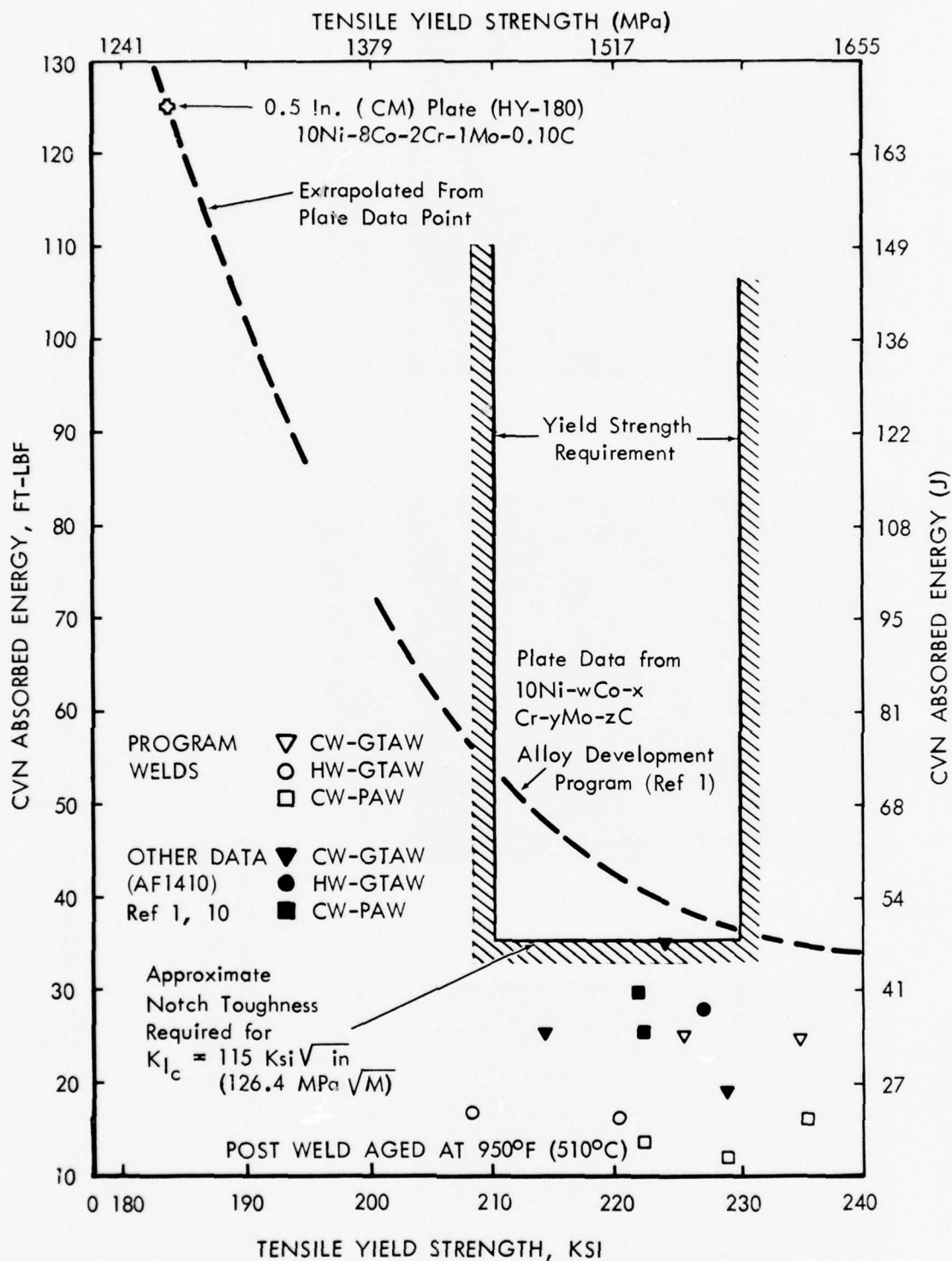
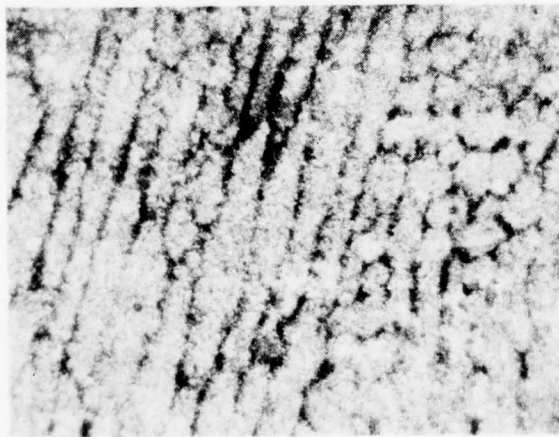


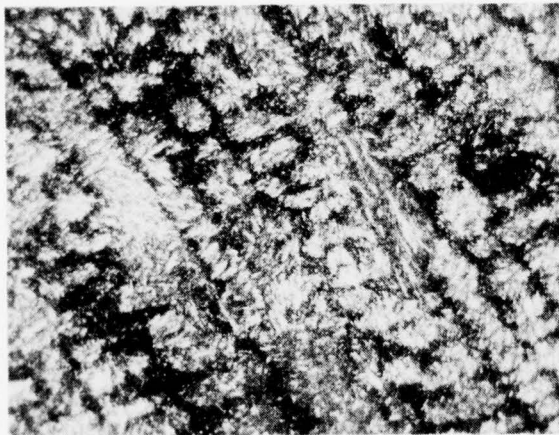
Figure 4 Correlation Between Fusion Zone Mechanical Properties and Weld Process Utilizing Filler Metal Heats VE 716 and VE 717

CW - GTAW (PULSE ARC)



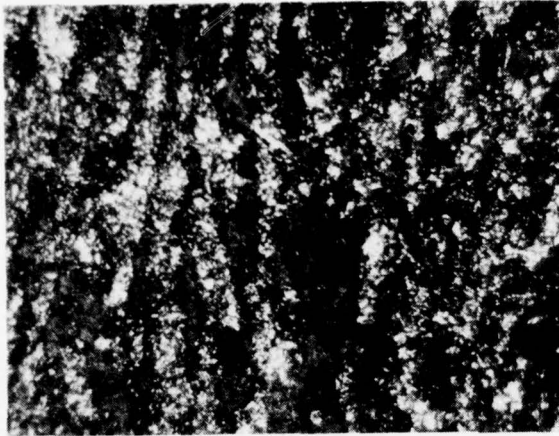
HI - 33.2 KJ/IN. (1.3 KJ/MM)
DR - 1.1 LB/HR (0.50 Kg/HR)

HW - GTAW (PULSE ARC)



HI - 33.8 KJ/IN. (1.3 KJ/MM)
DR - 5.4 LB/HR (2.45 Kg/HR)

CW - PAW



HI - 83.2 KJ/IN. (3.3 KJ/MM)
DR - 1.9 LB/HR (0.86 Kg/HR)

- LOCATION - FUSION ZONE CENTER
> 3 THERMAL REVERSALS

- MAGNIFICATION - 1000X

Figure 5 Microstructural Refinement in Arc Weld Fusion Zones in the As-Welded Condition

able toughness degradation, Table 7. Improvements in fusion zone toughness for high deposition rate weldments will be possible as follows: (1) HW-GTAW - high purity filler metal composition and improved weld parameters and (2) CW-PAW - high purity filler metal composition, decreased gaseous contamination during welding, and improved weld parameters.

4.2.2 Effect of Welding Parameters and Fusion Zone Composition on Mechanical Properties

Center-line cooling rates of representative weldments indicated that heat inputs greater than 70 Kj/in (2.8 Kj/mm) are not desirable, Figure 6. A comparison of the cooling rates of the CW and HW-GTAW processes revealed this parameter to be more sensitive to heat input than deposition rate. The plasma arc welds required excessive heat inputs to successfully deposit weld metal at greater than a deposition rate of 3 lbs/hr (1.4 Kg/hr). It was noticed in the root passes that the excessive cold wire feed shielded the lower portion of the molten weld puddle from the plasma arc so a tendency toward lack of fusion developed. Several techniques, e.g., increased angle of V or J-groove, oscillation, etc. can be used, but hot wire techniques should be more successful for deposition rates in excess of 3 lb/hr (1.4 Kg/hr). The high heat input of the majority of the plasma arc welds allowed some fusion zone refinement regardless of the increased bead size (Figure 7), but it can be expected that the slower cooling rates will result in excessive autotempered products and/or transformation products (carbides).

Excessive heat inputs can influence the solidification mode and the coarseness and segregation of the solidification microstructure. A cellular dendritic solidification mode was apparent for the wide range of welding conditions in this investigation, Figure 8. The cell size differential between the CW-GTAW, and CW-PAW weld metal microstructures indicates that the coarseness of the cellular dendrites are partially sensitive to heat input.

Overall the fusion zone notch toughness did not attain previous levels, Figure 4, or the levels believed to be obtainable with high purity as-deposited 14Co-10Ni-2Cr-1Mo-0.16C steel weld metal.

The attendant fusion zone toughness is dependent on the level of minor elements and the resultant as-welded and/or post weld microstructure, Table 10. A comparison of the fusion zone chemistry

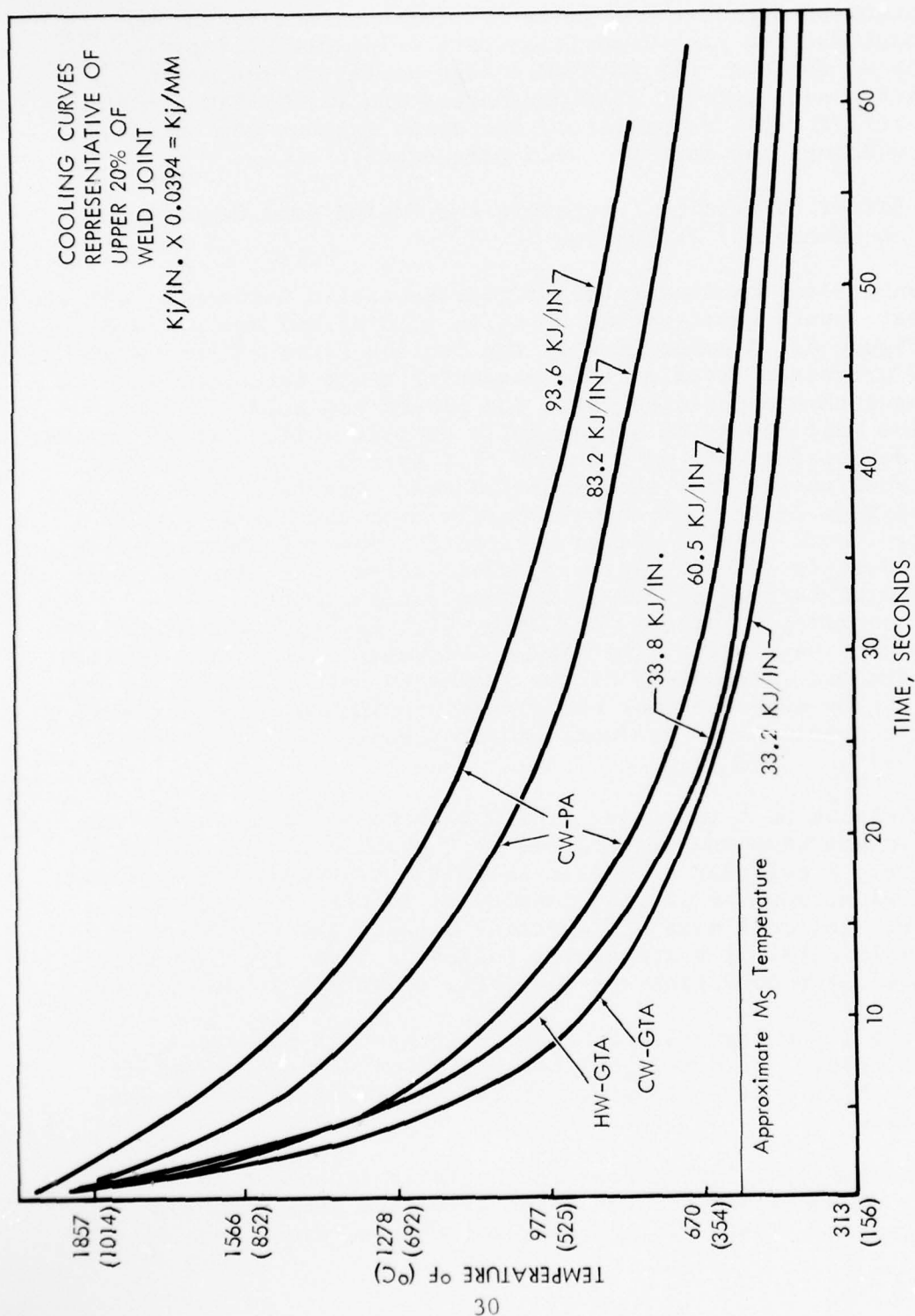
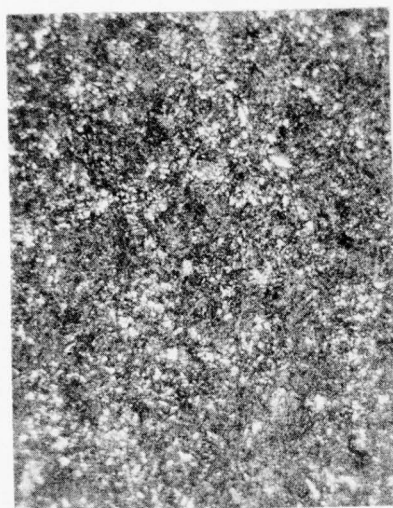
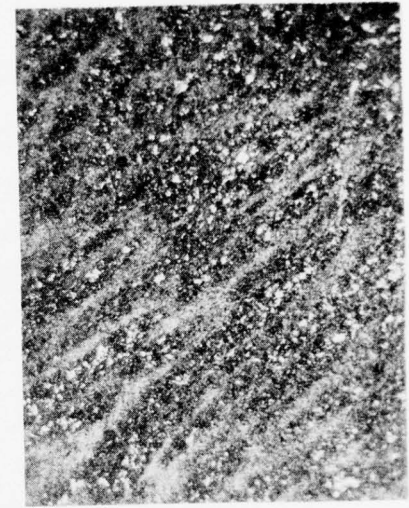


Figure 6 Representative Center Line Cooling Rates



AS-DEPOSITED 1000X



AGE - 950°F(510°C)-4 HR 1000X
● FUSION ZONE CENTER

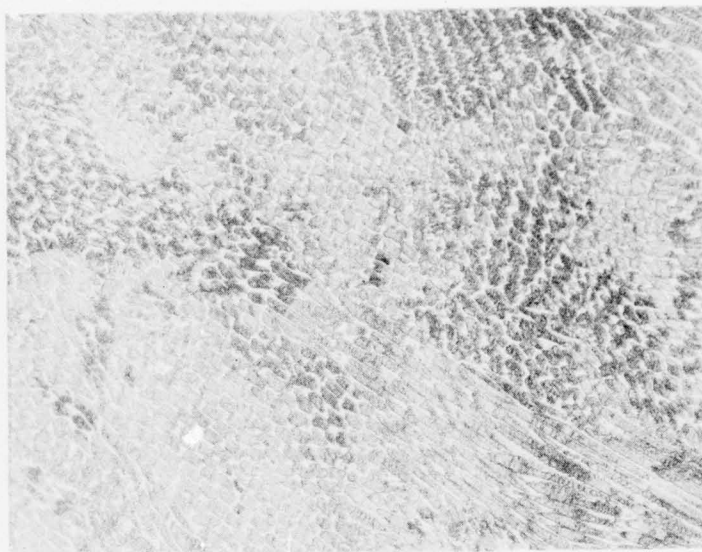


AS-DEPOSITED 1000X



AGE - 950°F(510°C)-4 HR 1000X
● LAST WELD PASS

Figure 7 Effect of Post Weld Aging on Plasma Arc Fusion Zone Microstructure



CW-GTA 100X
 HI-33.2 KJ/IN. (1.3 KJ/MM) DR-1.1 LB/HR (0.5 Kg/HR)



CW-PAW 100X
 HI-83.2 KJ/IN. (3.3 KJ/MM) DR-1.9 LB/HR (0.87 Kg/HR)

Figure 8 Representative As-Deposited Solidification Microstructures in Gas Tungsten Arc and Plasma Arc Welds

TABLE 10 COMPARISON BETWEEN FUSION ZONE COMPOSITION AND NOTCH TOUGHNESS

14Co-10Ni-2Cr-1Mo-0.16C Steel Filler Metals

Weld Process	Filler Metal	Heat Input Kj/in(Kj/mm)	Deposition Rate Lbs/hr(Kg/hr)	Deoxidation and/or Impurity Elements				CVN Absorbed Energy ft-lbs (J)	
				Al	Si	S	P	As-Deposited	Aged
CW-GTA	VE 717	33.2 (1.3)	1.1 (0.5)	0.086	0.21	0.007*	0.006	35.4 (48.0)	24.4 (33.1)
	7318-8091 (1)	33.1 (1.3)	1.1 (0.5)	0.042	0.13	0.003	0.001	45.4 (61.6)	34.5 (46.8)
	VE 799*	37.1 (1.5)	1.1 (0.5)	0.025	<0.01	0.005	0.001	40.4 (54.8)	47.8 (64.8)
HW-GTA	VE 717	33.8 (1.3)	5.6 (2.5)	0.061*	0.20	0.003	0.006	15.7-23.8 (21.3-32.3)	14.6-17.8 (19.8-24.1)
	7318-8091(1)	26.3 (1.1)	5.0 (2.3)	0.034	0.13	0.003	0.001	26.0 (35.3)	24.0 (32.5)
CW-PA	VE 717	93.6 (3.7)	3.4 (1.5)	0.095	0.22	0.006	0.007	23.1 (31.3)	13.3 (18.0)
	VE 717(2)	98.3 (3.9)	3.3 (1.5)	-	0.20	0.007	-	24.3 (32.9)	25.5 (34.6)
CW-PA	VE 717(2)	59.6 (2.3)	1.6 (0.7)	-	0.16	0.006	-	32.8 (44.5)	31.8 (43.1)

Acceptable Levels of Deoxidation and/or Impurity Levels

Al - 0.015 \pm 0.005, Si - 0.10 \pm 0.02

S - 0.005 MAX, P - 0.006 MAX

O - 0.0030 MAX, N - 0.0030 MAX

NOTES: Gas Analysis in ppm

(1) Data (Reference 1)

(2) Data (Reference 10)

* Finish Wire Analysis

with the accompanying notch toughness for each weld process demonstrates the detrimental effect excessive impurity and/or deoxidizing elements can have on mechanical properties, Table 10. For instance, previous CW-GTA weldments with a Heat 7318-8091 filler metal revealed higher notch toughness than obtainable with Heat VE 717 by virtue of reduced levels of Al, S, and O in the fusion zone. Basically, two sources are responsible for the high levels of the impurity elements: (1) filler metal composition (Al, S) and (2) gaseous contamination (O, N) during welding. At similar weld parameters for individual arc weld processes, excessive levels of deoxidation and/or impurity elements resulted in degradation of fusion zone notch toughness, Table 10. Deoxidation/impurity elements e.g., Al, S, O, N, etc., form inclusions or second phase particles and by changes in fracture sensitive parameters, e.g., volume percent, critical size, shape, location, etc., can substantially decrease the energy for ductile rupture in weld metal, Reference 13 and 14.

4.2.3 Fusion Zone Mechanical Properties (Heats VE 798-800)

The CW-GTAW process was selected for the continued evaluation of additional filler metal heats based on its ability to consistently obtain higher toughness weldments. The periodic contamination of the deposited CW-PAW weldments limited the use of this process to determine the effect of filler metal chemistry on mechanical properties.

After selection (refer to paragraph 4.1) of three filler metal heats with the best potential for improved fusion zone toughness, the CW-GTAW deposited weld metal was evaluated on the basis of tensile and notch toughness properties, Table 11. The fusion zone mechanical properties of Heats VE 798, 799, and 800 were determined in the as-deposited and 900°F (482°C) and 950°F (510°C) post weld heat treatment condition. Although the ability of Heat VE 799 to meet the TYS program goal, 210 Ksi (1447.9 MPa), was only marginal, the CVN/TYS ratio was the highest of the three heats, Figure 9. While the 900°F (482°C) post weld age was the only thermal treatment resulting in a TYS exceeding program goals, it is speculated that if the carbon content were increased to a nominal value (0.16%) the 950°F (510°C) aged properties could easily reach the 210 Ksi (1447.9 MPa) TYS level, Table 8. The combined low levels of Al and S in Heat VE 799 are credited with the 48 ft-lbf (65.1 J) absorbed energy obtained at 950°F (510°C)-4 hr post weld age. Since the Al and S were both at low levels in Heat 798, it was possible to evaluate the effect of 0.08%V on the fusion zone mechanical properties. The V addition increased the TYS and TUS to 230 Ksi (1585.8 MPa) and 241 Ksi (1661.6 MPa),

TABLE 11 FUSION ZONE MECHANICAL PROPERTIES

Cold Wire Gas Tungsten Arc Welds
0.625 Inch (1.59 cm) Thick Plate

Post Weld Age	Yield Strength Ksi (MPa)	Ultimate Strength, Ksi (MPa)	Elongation 1 inch, %	Reduction of Area, %	Charpy V-Notch Absorbed Energy, ft-lbf (J)
<u>Filler Metal Heat VE 798</u>					
As-Deposited	199.6 (1376)	241.6 (1666)	15.5	57.7	*29.5, 31.9 (39.9)(43.3)
900 [°] F-4 hrs/WQ (482°C)	-	-	-	-	*22.2, 22.5 (30.1)(30.5)
950 [°] F-4 hrs/WQ (510°C)	299.9 (1585)	241.4 (1664)	14.0	51.2	*23.0, 23.1 (31.2)(31.3)
<u>Filler Metal Heat VE 799</u>					
As-Deposited	202.4 (1395)	223.3 (1540)	16.0	57.1	*40.1, 40.7 (54.4)(55.2)
900 [°] F-2 hrs/WQ (482°C)	211.7 (1460)	223.7 (1542)	16.0	63.0	42.9, 44.1 (58.2)(59.8)
900 [°] F-4 hrs/WQ (482°C)	211.5 (1458)	221.5 (1527)	16.0	62.5	*34.1, 36.2 (46.2)(49.1)
900 [°] F-8 hrs/WQ	214.9 (1481)	219.9 (1516)	15.0	64.9	40.9, 42.9 (55.5)(58.2)
900 [°] F-12 hrs/WQ (482°C)	213.3 (1471)	220.3 (1519)	14.0	60.5	44.6, 45.8 (60.5)(62.1)
950 [°] F-2 hrs/WQ (510°C)	207.7 (1432)	215.1 (1483)	14.0	62.0	46.0, 48.2 (62.4)(65.4)
950 [°] F-4 hrs/WQ (510°C)	*207.2 (1429)	219.2 (1511)	16.5	65.2	*36.2, 37.2 (49.1)(50.4)
950 [°] F-4 hrs/WQ (510°C)	-	-	-	-	47.5, 48.0 (64.4)(65.1)
950 [°] F-8 hrs/WQ (510°C)	202.8 (1398)	210.7 (1455)	15.0	63.0	48.3, 48.8 (65.5)(66.2)
950 [°] F-12 hrs/WQ (510°C)	203.4 (1402)	208.4 (1437)	15.0	62.2	50.5, 52.8 (68.5)(71.6)
<u>Filler Metal Heat VE 800</u>					
As-Deposited	187.3 (1291)	223.3 (1540)	15.5	60.9	*38.4, 39.9 (52.1)(54.1)
900 [°] F-4 hrs/WQ (482°C)	-	-	-	-	*28.6, 28.9 (38.8)(39.2)
950 [°] F-4 hrs/WQ (510°C)	213.9 (1475)	222.9 (1537)	15.5	65.0	*32.9, 33.1 (44.6)(44.9)

longitudinal tensile orientation
Transverse CVN orientation
* First Weld Series

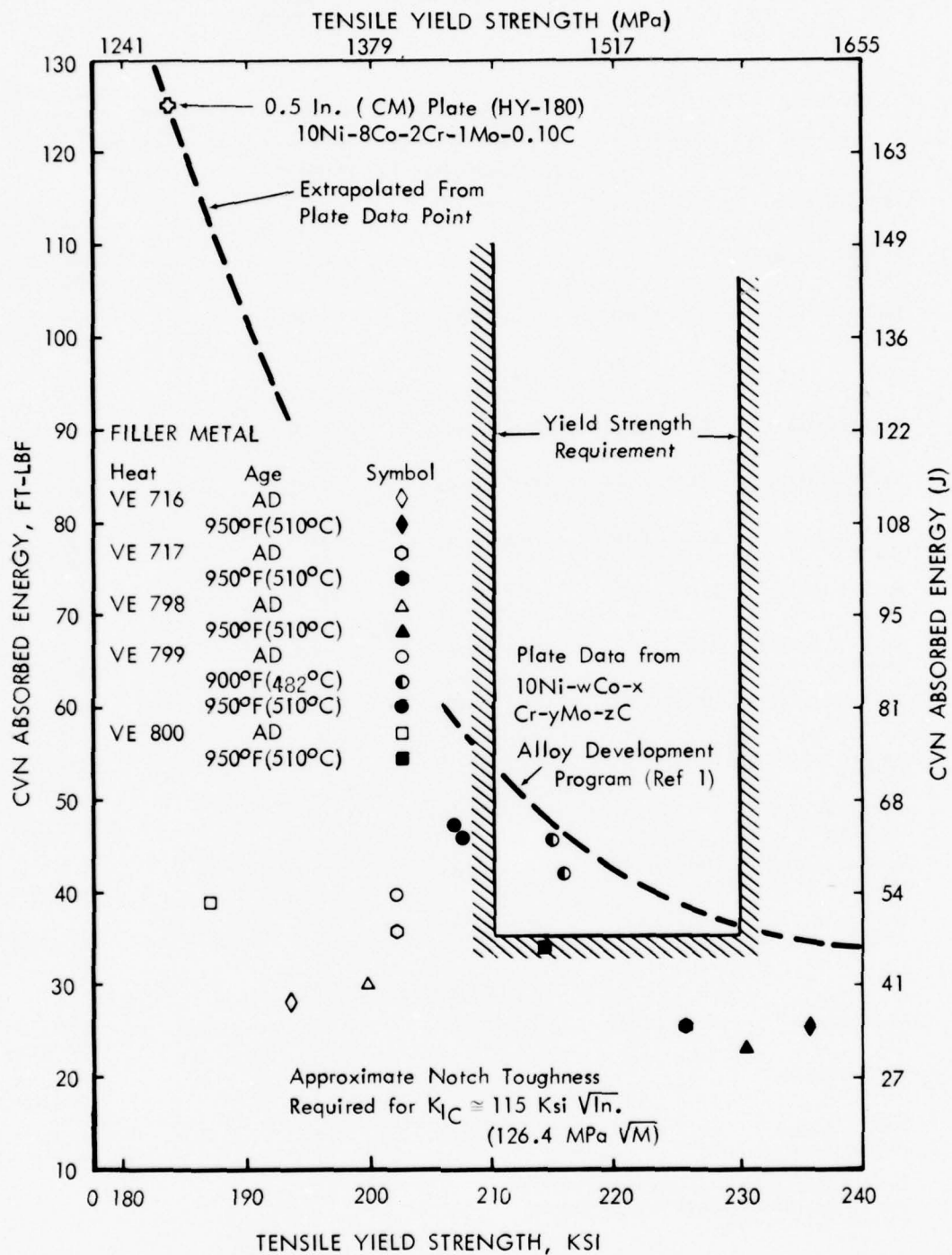


Figure 9 Correlation Between CW-GTAW Fusion Zone Mechanical Properties and Filler Metal Composition

respectively, with an accompanying reduction in absorbed energy to 23 ft-lbf (31.2J).

It should be noted that the notch toughness decrease accompanying (paragraph 4.2.1) the post weld aging of the as-welded fusion zone did not occur with Heat VE 799.

The effect of test temperature on the notch toughness of the Heat VE 799 filler metal in the post weld aged condition is shown in Figure 10 and Appendix 5. The CW-GTA welds in 0.625 inch (15.9 mm) thick plate were comparable to AF 1410 rolled plate properties. As expected in these alloys no pronounced ductile-brittle transition occurred, rather fracture occurred with progressively less energy required for ductile rupture. In room temperature fractures, small ductile dimples indicated failure by void coalescence, Figure 11. At cryogenic temperatures, -320°F (195.5°C), the low energy fractures also disclosed failure by a predominantly dimpled rupture mode.

Since the thermal reversals imposed by consecutive passes during multipass welding affect the as-deposited fusion zone microstructure and corresponding mechanical properties, it is recognized that the properties of FZ post weld aging and rolled plate aging possibly will differ on a direct comparison basis. Using this premise the 900°F (482°C) post weld age, which met mechanical property goals, may be microstructurally equivalent of a 950°F (510°C) aging treatment in rolled plate. However, sufficient fine structural analysis was not available to make this judgment. Thus, the 950°F (510°C) post weld aging treatment was selected for the continued mechanical characterization of Heat VE 799 based on the improved stress corrosion cracking previously documented for this aging temperature in rolled plate, References 1 and 4.

4.2.4 Fusion Zone Mechanical Characterization Data (Heat VE 799)

The mechanical property data was obtained from CW-GTAW deposited Heat VE 799 weld metal per the welding parameters listed in Table 5. All mechanical properties with the exception of S/N fatigue are representative of weldments made in 1.25 inch (3.18 cm) thick rolled plate. S/N fatigue specimens were machined from weldments made in 0.625 inch (1.58 cm) thick plate.

4.2.4.1 Strength and Toughness

The properties of the all-weld metal (longitudinal direction) tensile specimens, which were centrally located in the 1.25 inch

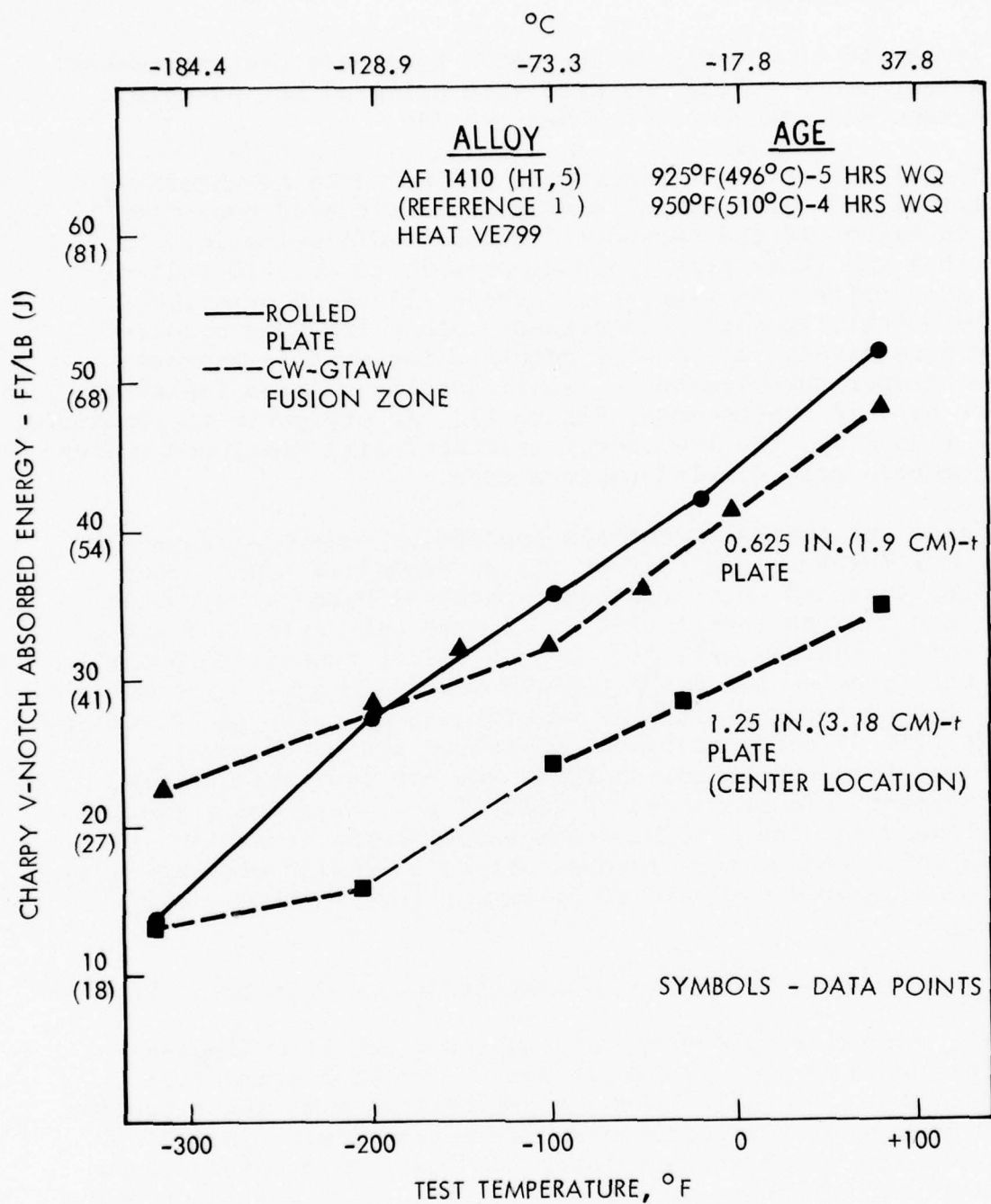
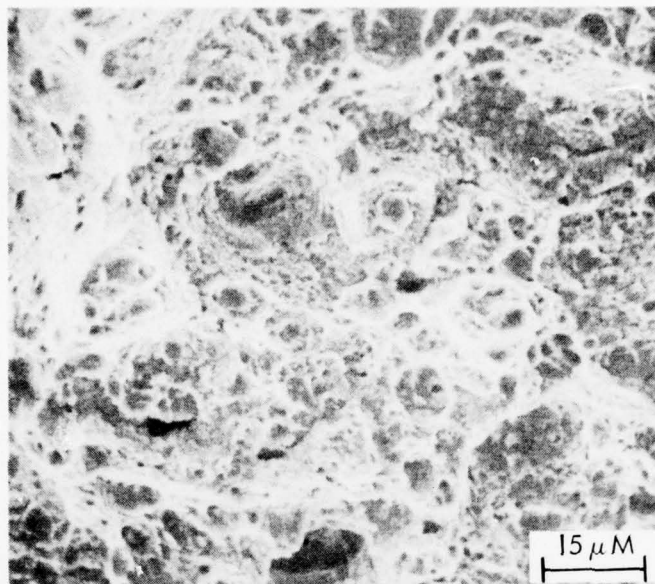
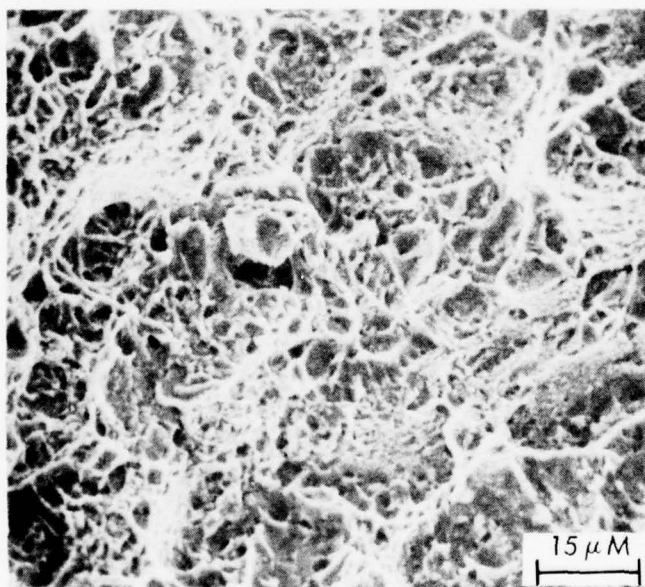


Figure 10 Effect of Test Temperature on Notch Toughness of AF1410 Steel Weldments



DUCTILE RUPTURE, RT, CVN-48 FT/LBF (65.0 J)



PREDOMINANTLY DUCTILE RUPTURE, -320°F(-195.5°C)
CVN - 24 FT/LBF (32.5 J)

Figure 11 Fracture Appearance of the Postweld Aged CW-GTAW
Fusion Zone as a Function of Temperature

(3.18 cm) thick welded plate, were comparable with those observed in 0.625 inch (1.59 cm) thick plate with the exception of the reduction of area, Tables 11 and 12. The loss in reduction of area proved to be indicative of a reduction in notch toughness. A comparison of notch toughness with location indicates that the CVN absorbed energy increased from 34 ft-lbf (46.1J) in the FZ center to 41 ft-lbf (55.6J) in the FZ top, Table 12, for the post weld aged weld metal. Apparently the number of thermal reversals imposed previous to post weld aging can control the resultant notch toughness. The selection of post weld aging schedule may need to be correlated with the previous thermal cycling history to prevent overaging. It was not possible to evaluate the effect of increased weld cycles on the HAZ notch toughness as the absorbed energy of 26-31 ft-lbf (35.3-42.0J) was comparable to the aged parent metal properties. Unfortunately, a low toughness heat of AF 1410 steel was the only 1.25 inch (3.18 cm) rolled plate available for these weldments, Table 6. However, all other HAZ investigations were accomplished with a high toughness heat.

Fracture toughness specimens were tested at ambient temperature with the crack extension occurring in the weld direction. Plane strain fracture toughness values (K_{IC}) were not determined due to: (a) crack front deviations greater than 5% - ASTM E399-72 and (b) P_{max}/P_Q greater than 1.1. The K_Q values ranged from 96.8 Ksi \sqrt{in} (106.3 MPa \sqrt{m}) to 139.3 Ksi \sqrt{in} (152.9 MPa \sqrt{m}), Table 13. There is evidence the crack front irregularity shown in Figure 12 was responsible for the low fracture toughness. As the crack growth retardation increased, the fracture toughness progressively declined, Figure 12. The location of the fatigue crack growth retardation approximates that of the fusion zone center. Comparison of shear lips with previously fractured high toughness plate specimens indicated the K_{IC} should be greater than 125 Ksi \sqrt{in} (137.4 MPa \sqrt{m}) for the specimens exhibiting the greatest crack front deviations. Although the fracture toughness goal of $K_{IC} \geq 115$ Ksi \sqrt{in} (126.4 MPa \sqrt{m}) was not technically met in the 1.25 inch (3.18 cm) weldments, there is evidence that this value could be exceeded since the average fusion zone notch toughness exceeds 35 ft-lbf (47.5J) absorbed energy at the 210 Ksi (1447.9 MPa) TYS level. The 0.625 inch (1.59 cm) thick weldments, with an absorbed energy of 43.5 ft-lbf (58.9 J), also meet this goal using the K_{IC} -CVN relationship established in Reference 1 as a criterion.

4.2.4.2 Fatigue

Preliminary S/N fatigue data indicates that at a $K_t = 1.0$, the AF 1410 steel (Heat VE 799) weld metal exhibited reduced fatigue performance compared with rolled plate data, Figure 13. As the endurance limit stress levels are approached, it becomes difficult to evaluate the fusion zone fatigue performance as

TABLE 12 WELDMET MECHANICAL PROPERTIES

Cold Wire Gas Tungsten Arc Welds
 1.25 inch (3.18 cm) thick Plate
 Filler Metal Heat VE 799
 Post Weld Age: 950°F(510°C) -4 hrs/WQ

Specimen Location	Yield Strength Ksi (MPa)	Ultimate Strength, Ksi (MPa)	Elongation 1 inch, %	Reduction of Area, %	Charpy V-Notch Absorbed Energy, ft-lbf (J)
FZ (center)	204.1 (1407) 211.5 (1458)	219.7 (1515) 225.1 (1552)	15 13	44.7 45.3	33.3 (45.1) 34.5 (46.8)
FZ (top)					38.1, 43.0 (51.7)(58.3)
HAZ (center)					31.2, 30.9 (42.3)(41.9) 30.2, 26.0 (40.9)(35.3)
FZ (center) transverse orient	214.0 (1475) 212.7 (1467)	224.1 (1545) 222.7 (1535)	14.5 13	63.6 58.5	

longitudinal tensile and transverse CVN orientations except as noted

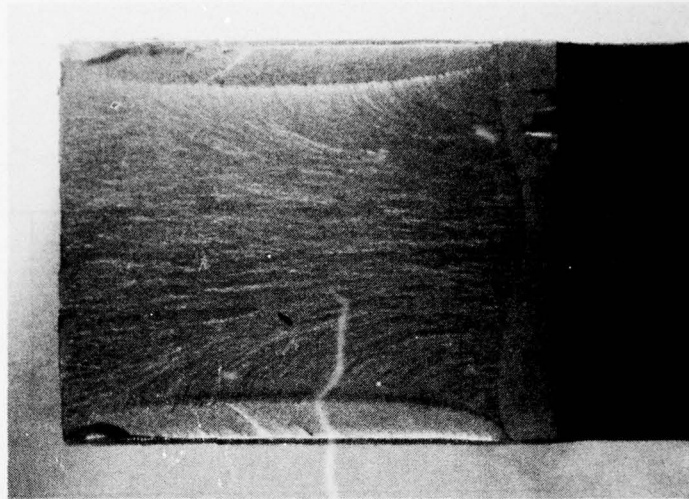
TABLE 13 FRACTURE TOUGHNESS OF CW-GTAW WELDED AF 1410 STEEL

Double J Groove, Fusion Zone Data
 Filler Metal Heat VE 799
 Compact Tension Specimens
 Post Weld Aged at 950°F (510°C) - 4 hrs/WQ

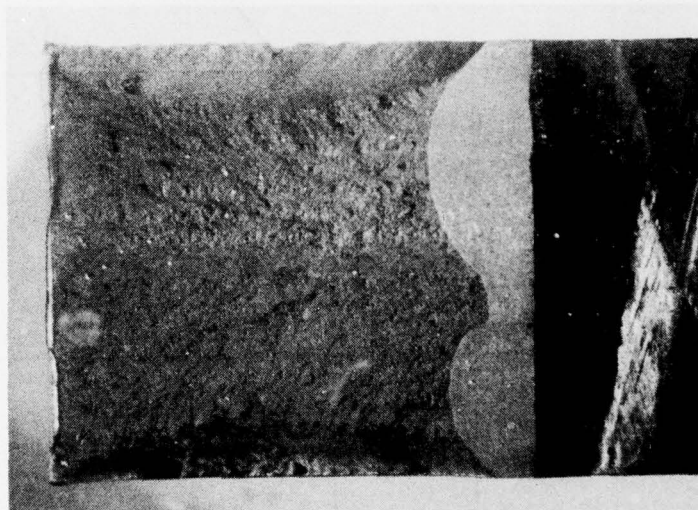
Specimen Number	B inch (cm)	W inch (cm)	a inch (cm)	P _Q lb (Kg) x 10 ³	P _{max} lb (Kg) x 10 ³	PM/PQ	K _Q Ksi \ in (MPa \ in)
4B9	1.000 (2.54)	2.006 (5.095)	1.022 (2.596)	17.70 (8.03)	21.7 (9.84)	1.23	99.3 (109.0)
4B10	1.000 (2.54)	2.004 (5.090)	1.020 (2.591)	17.24 (7.82)	21.55 (9.77)	1.25	96.8 (106.3)
4C1	1.000 (2.54)	2.001 (5.083)	1.080 (2.743)	18.00 (8.16)	20.80 (9.43)	1.16	139.3 (152.9)

(1) Crack front shape invalid per ASTM E399-72 requirement, all tests.

(2) $P_{\max}/P_Q > 1.1$, all tests.



ROLLED PLATE - 2X
 $K_{IC} = 130.7 \text{ Ksi}\sqrt{\text{INCH}} \quad (143.6 \text{ MPa}\sqrt{\text{M}})$



CW-GRAW FUSION ZONE - 2.5X
 DOUBLE J GROOVE
 $K_Q = 139.3 \text{ Ksi}\sqrt{\text{INCH}} \quad (153.1 \text{ MPa}\sqrt{\text{M}})$

Figure 12 Irregular Fatigue Crack Profile Evident in Postweld Aged CW-GTAW Fusion Zone Fracture Toughness Specimens

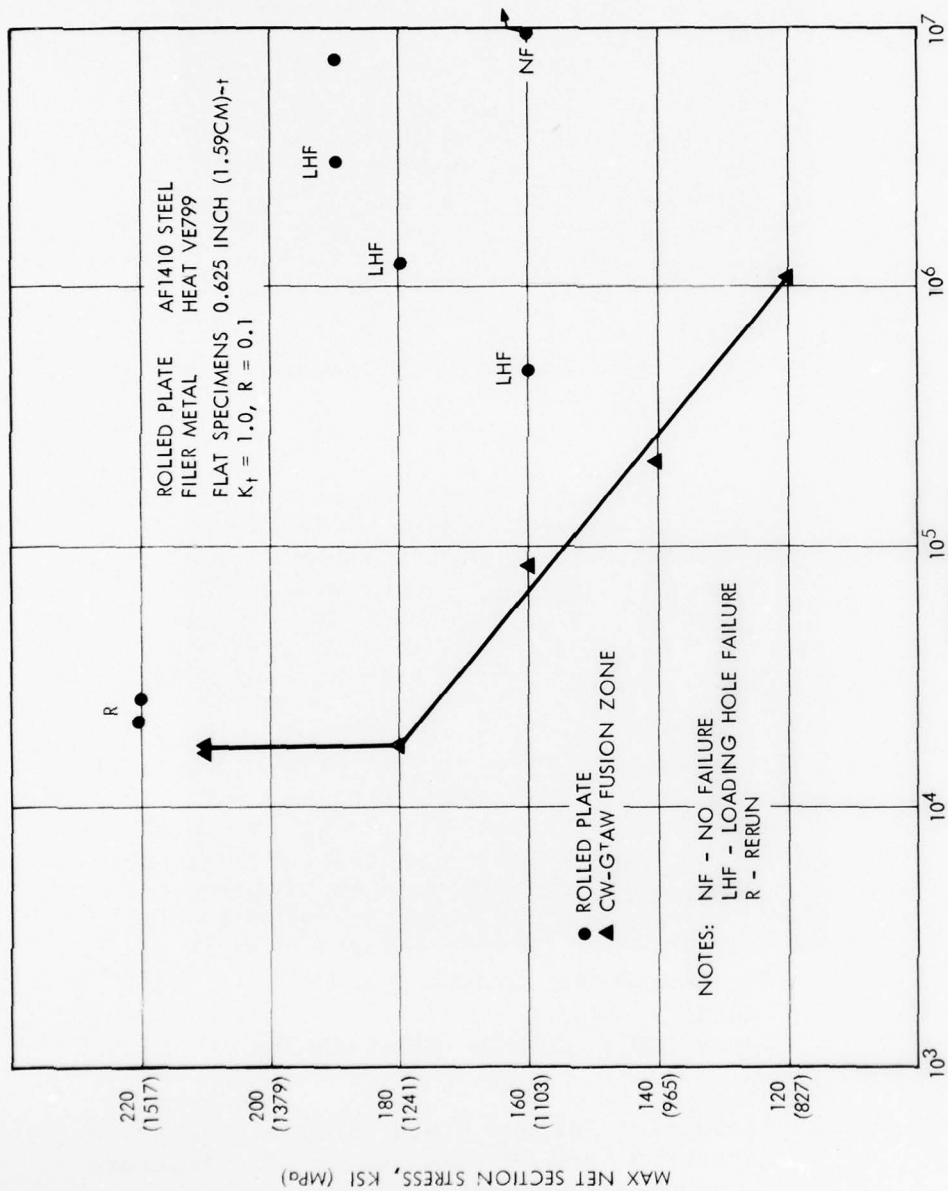


Figure 13 S/N Fatigue Properties of AF1410 Steel Weldment

internal cracking degraded the cyclic life, Appendix 6. In contrast, the crack growth rate in dry air (6 Hz) and 3.5% NaCl solution (at both 0.1 and 1 Hz) is considerably improved for fusion zone specimens as compared to rolled plate data, Figures 14 and 15. The fusion zone crack growth rate in 3.5% NaCl solution ($da/dN = 6.265 \times 10^{-11} \Delta K^{3.206}$ at 1 Hz) shows substantial improvement over the rolled plate crack growth rate in dry air ($da/dN = 7.010 \times 10^{-9} \Delta K^{2.136}$ at 6 Hz). It has not been determined if the microstructure and/or residual stresses are responsible for the difference in the rate of crack propagation. The fusion zone crack growth rates in dry air and 3.5% NaCl environments proved to be quite similar. Detailed crack growth data is included in Appendices 7 and 8.

4.2.4.3 Stress Corrosion

Alternate immersion stress corrosion testing performed on a CW-GTAW weldment indicated a tendency for early failure in the heat affected zone. The tensile loaded SCC specimens were sectioned in the transverse orientation from 1.25 inch (3.18 cm) thick weldments so all weld associated microstructures were subject to test. It is difficult to evaluate the level of SCC resistance in the HAZ as low toughness AF 1410 steel plate was used for the thick weldments. Regardless it is expected that susceptible HAZ microstructure will render a lower SCC limit than the FZ microstructures, on a comparable basis, Table 14.

The stress corrosion cracking properties of the fusion zone were determined by the Novak-Rolfe modified WOL K_{ISCC} specimen. Crack extension occurred at K_{Ii} greater than 85.4-93.0 Ksi $\sqrt{\text{in}}$ (93.8-102.2 MPa $\sqrt{\text{m}}$) in the upstream direction, Table 15. When crack extension occurred, the crack morphology was Type 1, e.g., a single crack extended from the tip of the fatigue precrack. Premature crack growth was thought to occur at K_{Ii} levels where crack arrest normally would be expected since an irregular fatigue pre-crack contour probably also exists for these specimens. This could have resulted in SC crack extension at lower than normal K_{Ii} levels. The K_{ISCC} values reported for the CW-GTAW weldment, 80.4 and 91.3 Ksi $\sqrt{\text{in}}$ (88.3 and 100.3 MPa $\sqrt{\text{m}}$) did not meet the program goal of 100 Ksi $\sqrt{\text{in}}$ (109.9 MPa $\sqrt{\text{m}}$). Additional investigations in the refinement of weld process and post weld age parameters, which can influence SCC properties, are expected to yield an improved K_{ISCC} in the fusion zone.

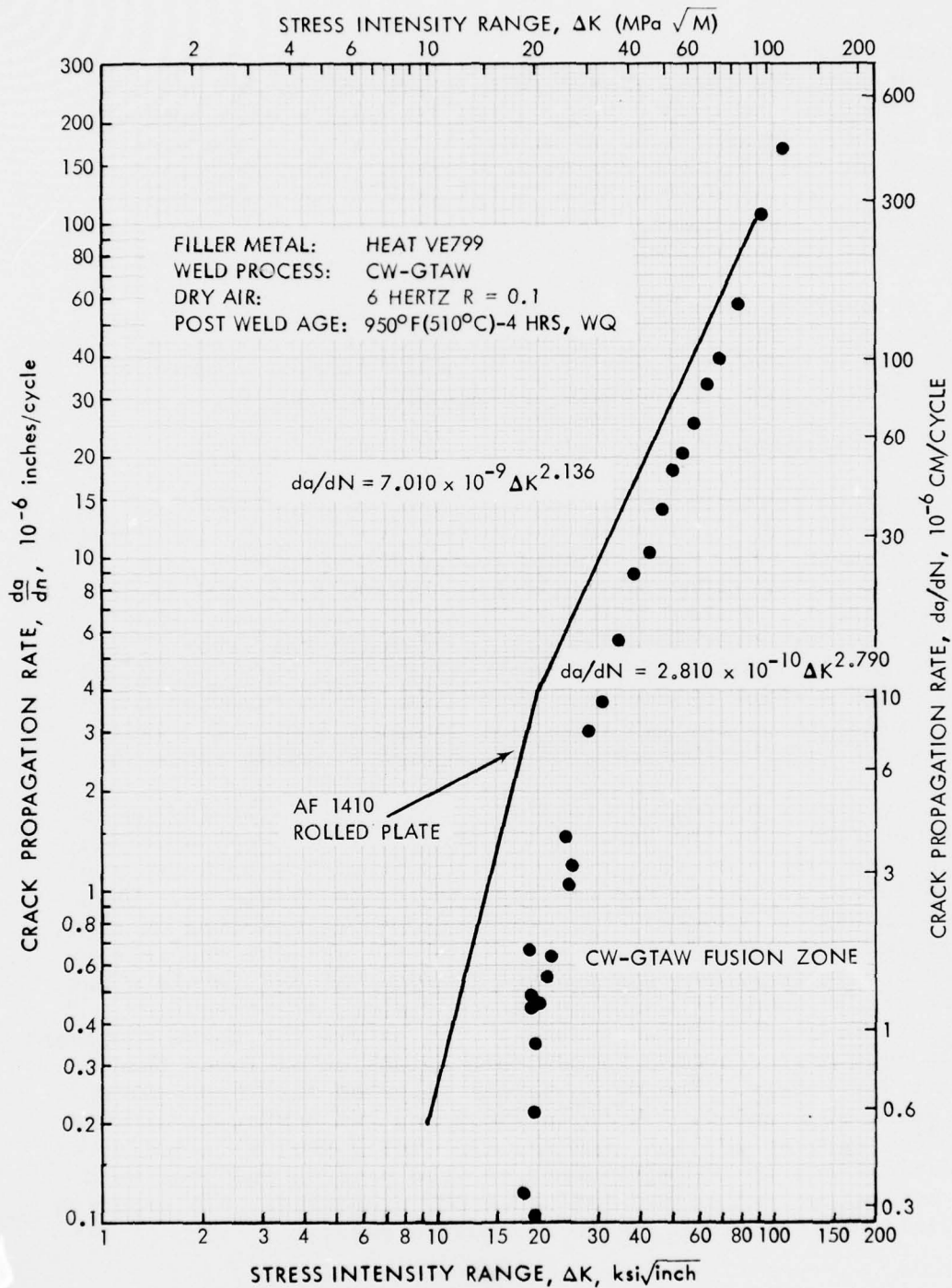


Figure 14 Fatigue Crack Growth of AF1410 Steel CW-GTA Weldment in Dry Air

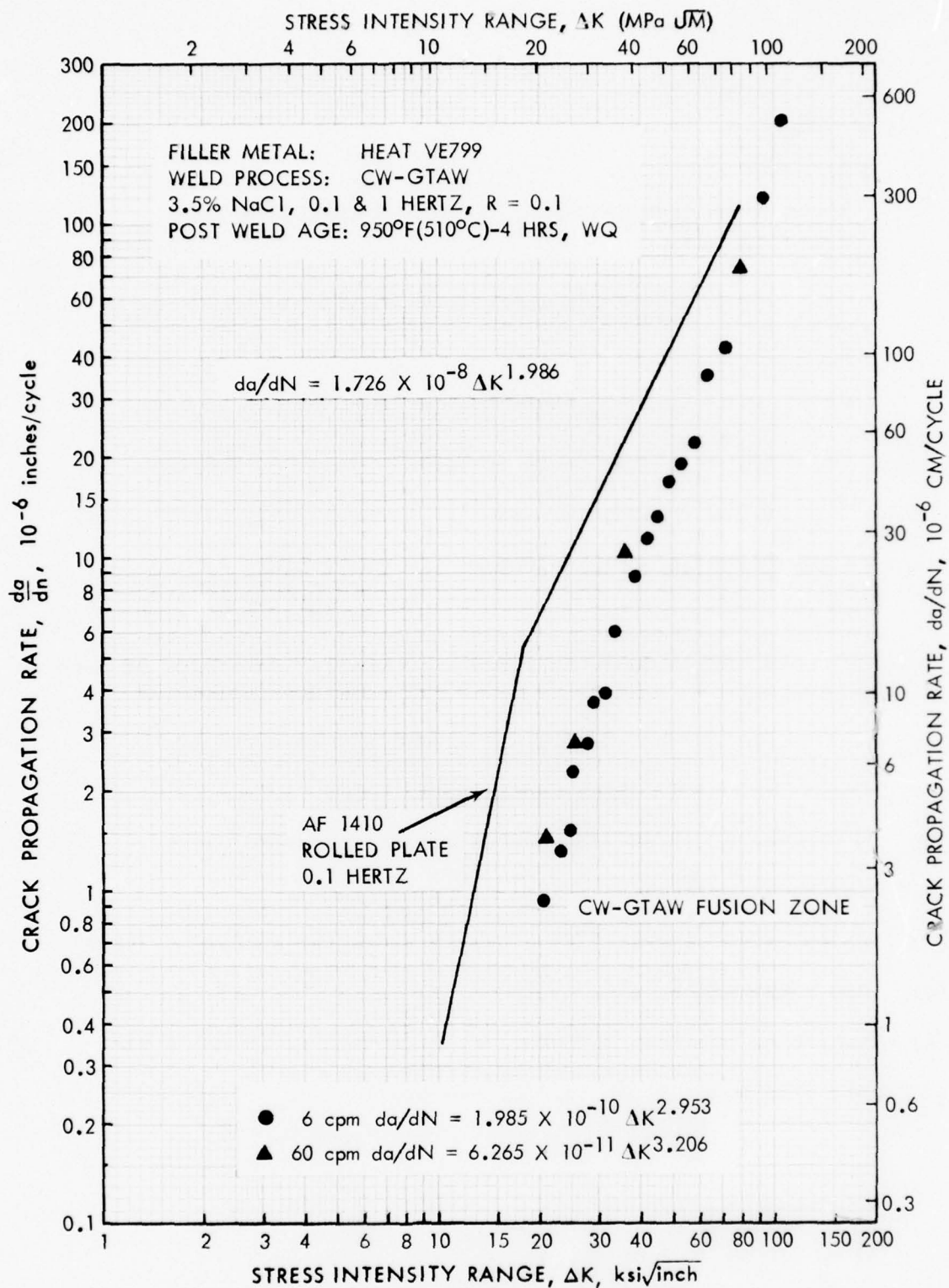


Figure 15 Fatigue Crack Growth of AF 1410 Steel CW-GTA Weldment in 3.5% NaCl Solution

TABLE 14 ALTERNATE IMMERSION STRESS CORROSION DATA

AF 1410 Steel CW-GTA Weldment
Filler Metal - Heat VE 799

<u>Results</u>			
<u>Specimen No.</u>	<u>Diameter Inch (cm)</u>	<u>Hours to Fail</u>	<u>Remarks</u>
4C4	0.200 (0.508)	488	Crack originated in HAZ
4C5	0.200 (0.508)	>1000	No failure - 226.6 KSI (1562.3 MPa) Residual Stress
4C6	0.200 (0.508)	198.9	Failed in radius at machine damaged tool marks

Test Conditions

- (a) 10 minutes immersed, 50 minutes air dry repeated cycle.
- (b) 3.5% NaCl corrodant
- (c) 165 KSI (1137.6 MPa) (75% ultimate strength) sustained stress
- (d) 1000 hours exposure
- (e) Transverse specimen orientation, 1.25 inch (3.18 cm)-t plate
- (f) Post weld aged: 950°F (510°C) - 4 hrs/WQ

TABLE 15 STRESS CORROSION OF CW-GTA WELDED AF 1410 STEEL

Double J Groove Fusion Zone Data,
Filler Metal Heat VE 799

Constant Deflection WOL Specimens

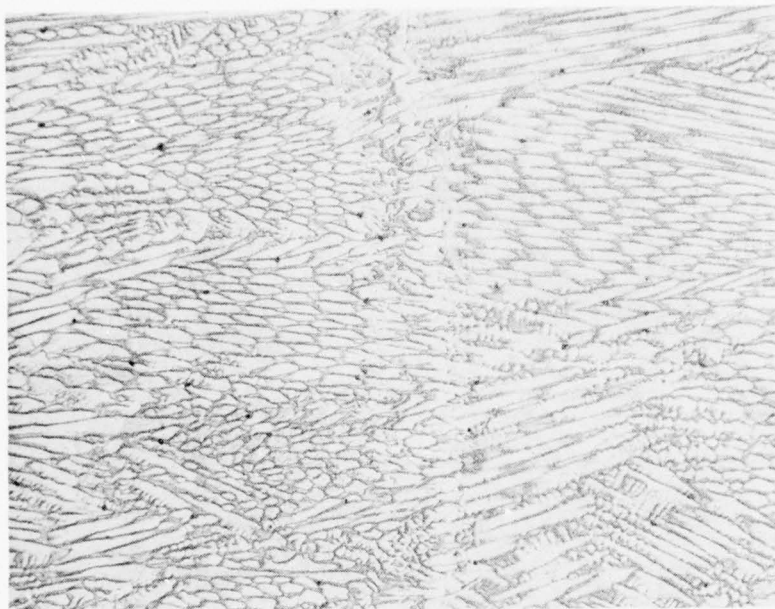
3.5% NaCl, 1000 Hour Exposure

Postweld Heat Treat	Specimen Number	B Inch (cm)	W Inch (cm)	Avg. Crack Length, Inches (cm)		Vo Inch (cm)	Stress Corrosion Resistance	
				Ai	Ascc		Ksi - $\sqrt{\text{inch}}$ (MPa $\sqrt{\text{m}}$)	K _{ISI}
950 ⁰ F (510 ⁰ C) 4 Hr	4B1	1.000 (2.54)	2.553 (6.485)	1.028 (2.611)	1.107 (2.811)	0.026 (0.066)	85.4 (93.8)	80.4 (88.3)
950 ⁰ F (510 ⁰ C) 4 Hr	4B8	1.000 (2.54)	2.547 (6.469)	1.013 (2.573)	1.037 (2.634)	0.028 (0.071)	93.0 (102.2)	91.3 (100.3)

4.2.5 Fusion Zone Microstructural Properties

The as-deposited fusion zone microstructure was coarse grained with lath martensite as the principal decomposition product. An inspection of microstructures representative of increasing thermal reversals, reveals the advantages of low deposition rate weld processes in refining the as-deposited microstructure. The refinement in high deposition rate weldments is dependent on two factors: (1) The bulk of the adjacent larger weld bead generally is not heated into a temperature range suitable for refinement and (2) the number of thermal reversals are decreased. The thermal cycling proves to be most important as the level of retained solidification microstructure and amount of reverted austenite depends on the number of reversals. The solidification microstructure of the 14Co-10Ni-2Cr-1Mo-0.16C weld metal remains quite stable during 1-2 consecutive thermal reversals, Figure 16.

Upon heating, the portion of the weld bead reaching the temperature for the start of the $\alpha \rightarrow \gamma$ transformation will result in decomposition of the martensite to austenite and ferrite compositions, Figure 17. The rate of this reversion depends on the temperature and diffusion rate of the solute elements. In Fe-Ni alloys, at high heating rates 64.8°F ($18.2^{\circ}\text{C}/\text{min}$), a reverse transformation ($\alpha_M \rightarrow \gamma$ At $A_s < A_f$) which is reported to be diffusionless occurs, References 17 and 18. At slower heating rates it is probably aided by a simultaneous diffusion controlled process as the A_s is defined over a range of temperatures. Upon thermal cycling the reverted austenite proved to be sufficiently distorted to exhibit marked differences in mechanical properties and to undergo recovery and recrystallization upon further heating. Austenite and martensite were both strengthened in the Fe-Ni alloys by reverse martensitic reactions with the major effect occurring in the first cycle. The effect of heating and cooling rates on transformation was briefly investigated for the AF 1410 steel composition. Heating rates comparable to those encountered in CW-GTA welding were used to determine the effect on the A_s and A_f temperatures, Appendix 9. At progressively higher heating rates the A_s increased, the A_f remained relatively unaffected, Figure 18. Comparable results were obtained in Gleeble-HAZ studies of a Fe-Co-Ni-Cr-Mo-C steel alloy in which the higher heating rates consistently increased the A_s temperatures, Reference 19. Alternating the magnitude of the heating rate increased the A_f temperature at a faster rate. A variance of the cooling rate between 41.7°F (5.4°C)/sec - 233.6°F (112.0°C)/sec had little effect on the M_s temperature. The M_s varied between 590°F (310°C) - 608°F (320°C) for numerous determinations.



CW - PAW
HI - 83.2 KJ/IN.
(3.3 KJ/MM)

AS-DEPOSITED
DR - 1.9 LB/HR
(0.87 Kg/HR)

100X

PHOTOMICROGRAPH REVEALING LACK OF
REFINEMENT FOR 1 THERMAL REVERSAL
IN 14Co-10Ni-2Cr-1Mo-0.16C
ALLOY STEEL MULTIPASS WELDMENTS

Figure 16 Stability of Solidification Structure in
Arc Weld Fusion Zone

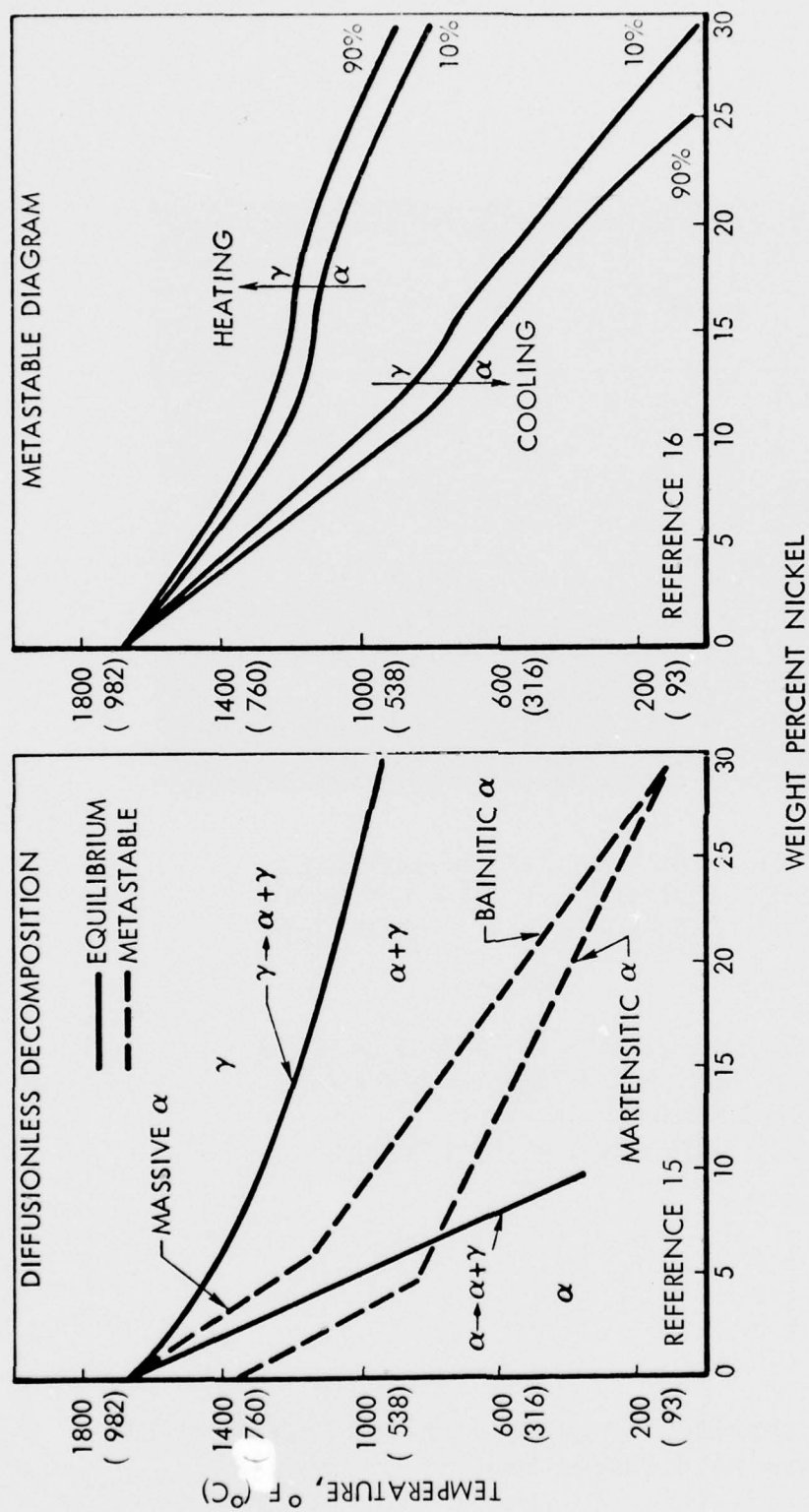


Figure 17 Decomposition on Heating and Cooling in the Fe-Ni System

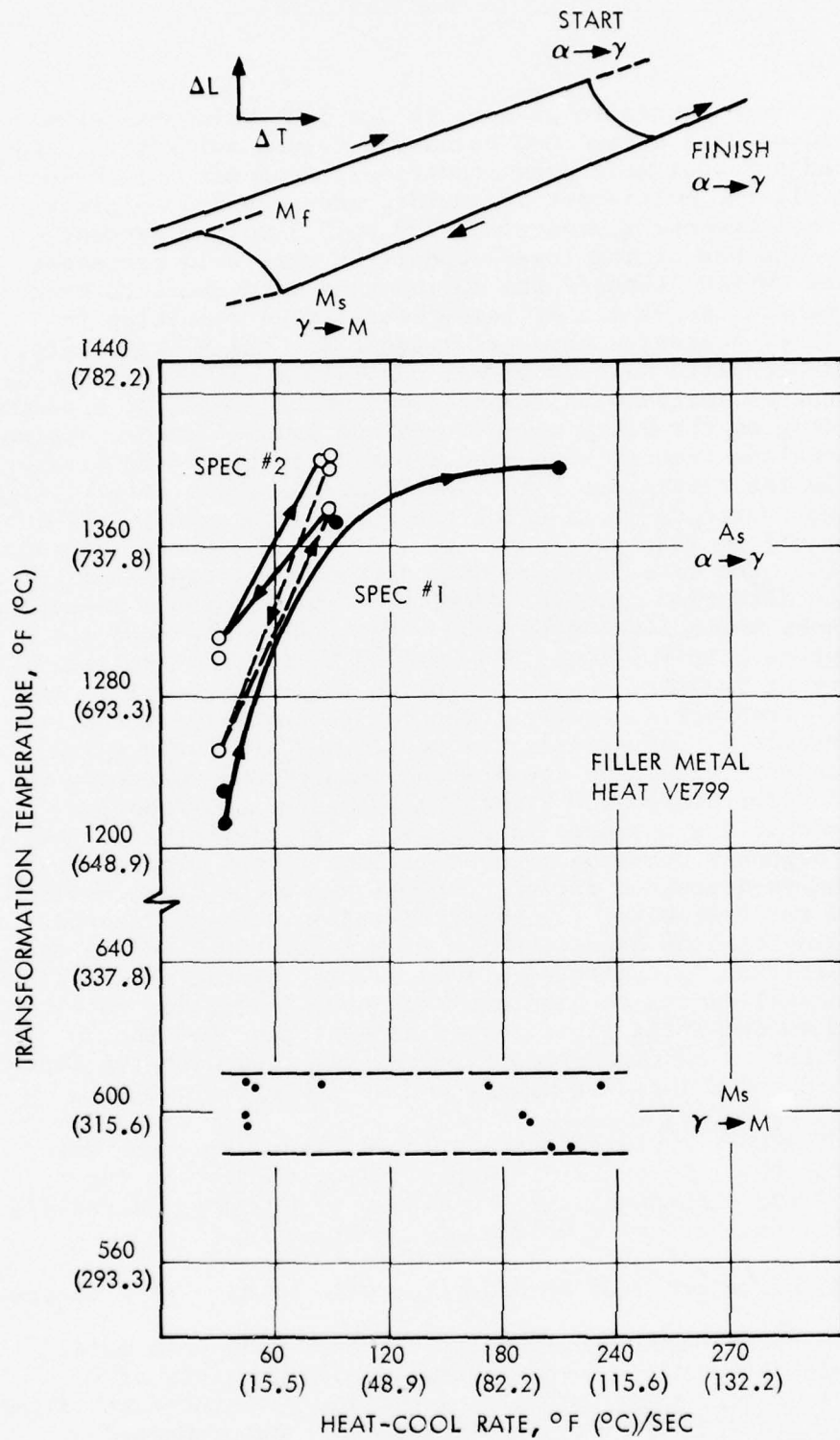


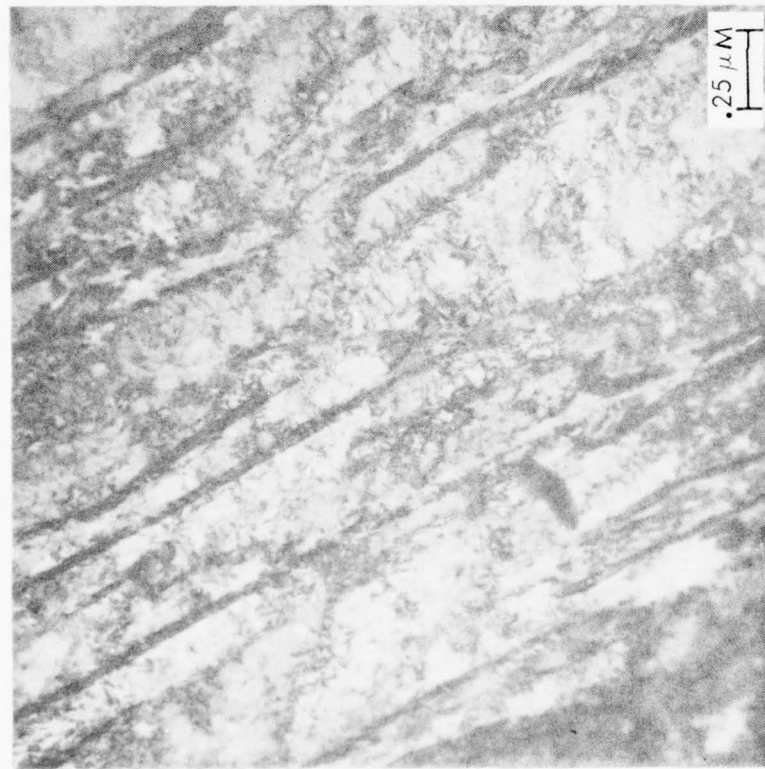
Figure 18 Effect of Heating-Cooling Rate On Fusion Zone Transformation Temperature

The retained austenite present in the last weld pass of all the arc weld processes remained below 2.0 volume percent for the as-deposited and post weld aged conditions, Appendix 10. Weld metal from all the multi-pass arc welds, when exposed to greater than 3 thermal reversals, contained 2.3 to 3.3 volume percent austenite. The use of the lower deposition rate weld processes (CW-GTAW and CW-PAW) exposed the fusion zone weld metal to more thermal reversals above the A₁ temperature, thus resulting in more stabilized austenite than was evident for the HW-GTAW weld. When the as-deposited weld metal was postweld aged, 950°F (510°C) - 4 hrs, a general increase in reverted austenite occurred, Appendix 10. Depending on the alloy composition and volume percent austenite present anomalous results have been reported in regard to fracture toughness in the literature. An investigation of the effect of increasing retained austenite in as-deposited steel weld metal (18Ni-8Co-4.5Mo maraging steel) on fracture toughness indicated a general degradation, Reference 20. The fracture toughness decrease was explained as initial void formation in interdendritic austenite pools resulting in microcracks which link up to reduce the energy required for ductile rupture. In the 14Co-10Ni-2Cr-1Mo-0.16C steel rolled plate, the quantity of reverted austenite formed is proportional to the cumulative exposure at temperatures in the austenite formation range, Reference 1. Apparently the additional post weld aging demonstrates this effect as considerable additional austenite was formed at a temperature, 950°F (510°C), where the $\alpha \rightarrow \gamma$ reaction should be stable for a longer time period. It is suggested that the notch toughness decrease evident in some of the program weld metal in the as-deposited and/or post weld aged condition could result from the following: (1) reverted austenite-easy fracture path (2) alloy carbide precipitation from retained austenite at fracture sensitive interlath locations and (3) overaging of alloy carbides and (4) excessive aluminum and other impurities which may precipitate second phase particles at non-optimum locations. Additional work is required to correlate toughness with the above factors which could interact singly and/or synergistically.

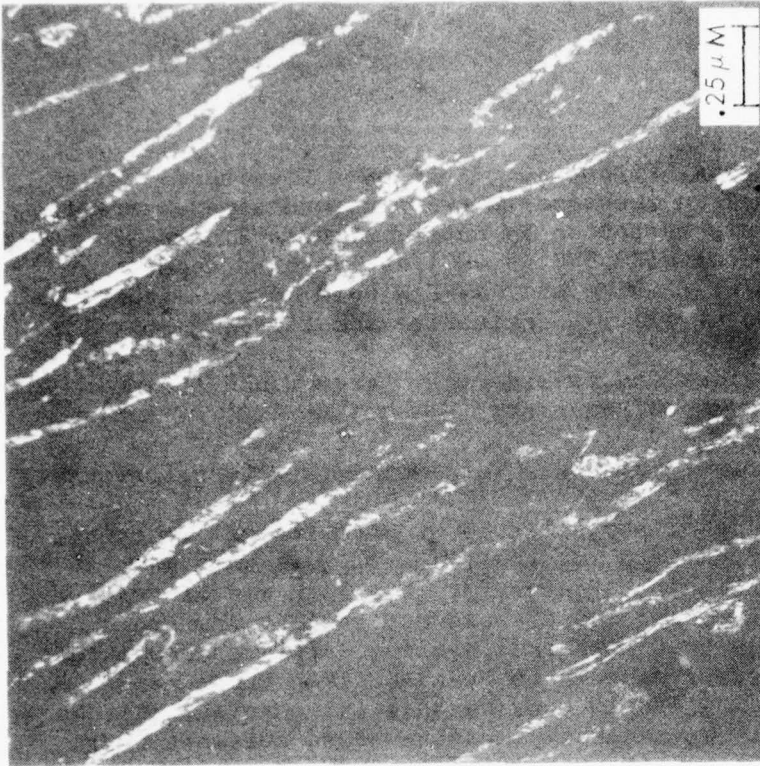
A brief microstructural examination of fine structure was completed for CW-GTAW and CW-PAW deposited weld metal in the (1) as-deposited (top pass), (2) multipass (3 or more reversals), and (4) multi-pass and post weld aged conditions.

(1) Microstructure of as-deposited weld metal - (1-2 reversals)

In the as-deposited condition the CW-GTAW weld metal microstructure of the last weld pass consists of dislocated parallel lath martensite with interlath films of stabilized austenite, Figure 19. Autotempered carbides, e.g., widmanstatten cementite platelets and spheroidized cementite particles, etc., are present



PARALLEL LATH MARTENSITE WITH
INTERLATH FILMS OF γ



~ 1.3 VOL % STABILIZED γ -DF

HEAT INPUT 33.2 KJ/IN. (1.3 KJ/MM)
DEPOSITION RATE: 1.1 LB/HR (0.5 Kg/HR)

Figure 19 As-Deposited CW-GTAW Fusion Zone Microstructure

within the laths, Figure 20. At slower cooling rates (CW-PAW welds) an increase in twinning, retained austenite and carbide precipitation is noted, Figures 21 and 22. At cooling rates of 9.8°F (5.4°C)/sec in high deposition rate, 3.3 lb/hr (1.5 Kg/hr), CW-PAW weld metal, extensive precipitation of $(110)_{\alpha}$ cementite and $(100)_{\alpha}$ ϵ -carbide platelets was noted, Reference 10. The size of the auto-tempered carbides was considerably larger than those formed at rapid cooling rates.

(2) Microstructure of Multipass Weld Metal (3 or more reversals)

CW-GTAW weld metal subject to 3 or more thermal reversals had a dislocated lath martensitic structure with no evidence of twinning, Figure 23. The lath widths were very narrow (0.1μ average) and seemed to reflect the grain refinement due to the thermal cycling. This is consistent with observations made in an Fe-Ni-C alloy where rapid re-austenitizing led to considerable martensitic refinement, Reference 21. Considerably more reverted austenite was present in the multipass weld microstructures, Figure 23. The stabilized austenite had an interlath film morphology thus indicating the preference for lath boundary sites. As before, the Kurdjumov-Sachs orientation relationship is obeyed between the martensite and austenite.

Due to the thermal reversals, the carbides which are present are complex and quite diverse. Complex carbides of the type M_2C and M_3C , where $\text{M} = \text{Fe}, \text{Mo}, \text{Cr}$, have been identified, Figure 24. The Widmanstätten $(110)_{\alpha}$ platelets of M_2C are about 1000\AA long and 100\AA in width. The M_2C carbides, tentatively identified as Mo_2C , are very small in size and precipitate predominantly at intralath sites. Another carbide with a spherical morphology (275\AA dia.) was present at lath interior and lath boundary sites. It is suggested that these carbides may be of the M_7C_3 type where $\text{M} = \text{Cr}, \text{Mo}$.

(3) Microstructure of post weld aged multipass weld metal - (3 or more reversals)

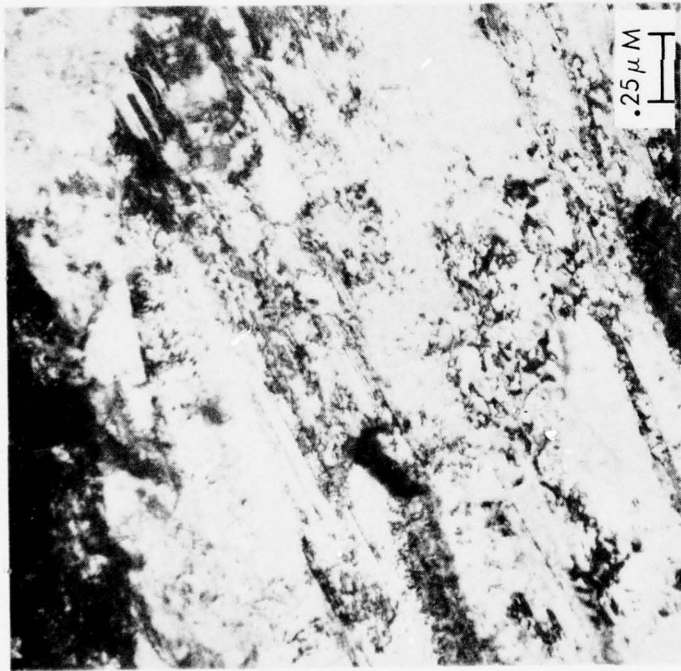
The microstructure from the multicycled fusion zone weld metal did not change significantly when post weld aged at 950°F (510°C). The dislocated lath martensite structure was not significantly affected by this aging treatment as recovery in the substructure was minor as evidenced by the fairly high dislocation densities, Figure 25. However, the amount of reverted austenite nucleated at the interlath boundary and intralath sites proved to be quite extensive, Figure 25. The estimated volume fraction of the reverted austenite from the EM micrographs corres-



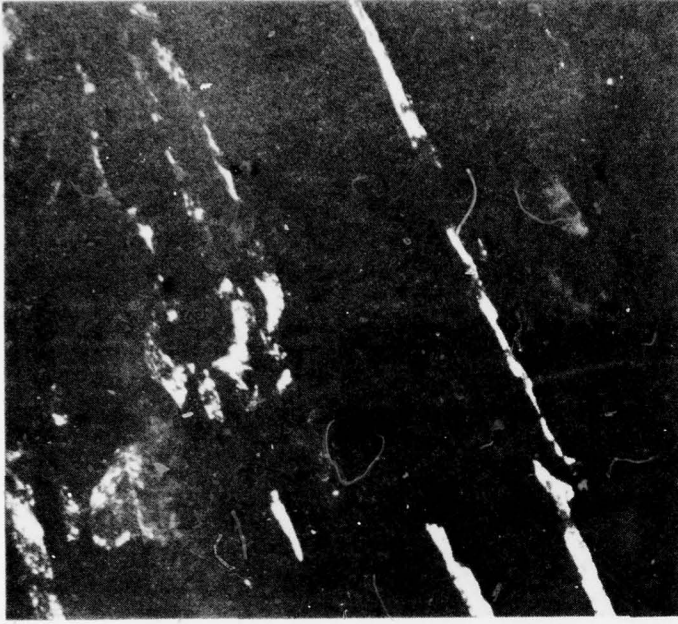
INTERLATH CEMENTITE PLATELETS AND SPHERIODIZED PARTICLES

HEAT INPUT: 33.2 KJ/IN. (1.3 KJ/MM)
DEPOSITION RATE: 1.1 LBS/HR (0.5 Kg/HR)

Figure 20 Autotempered Carbides in As-Deposited CW-GTAW Fusion Zone Microstructure



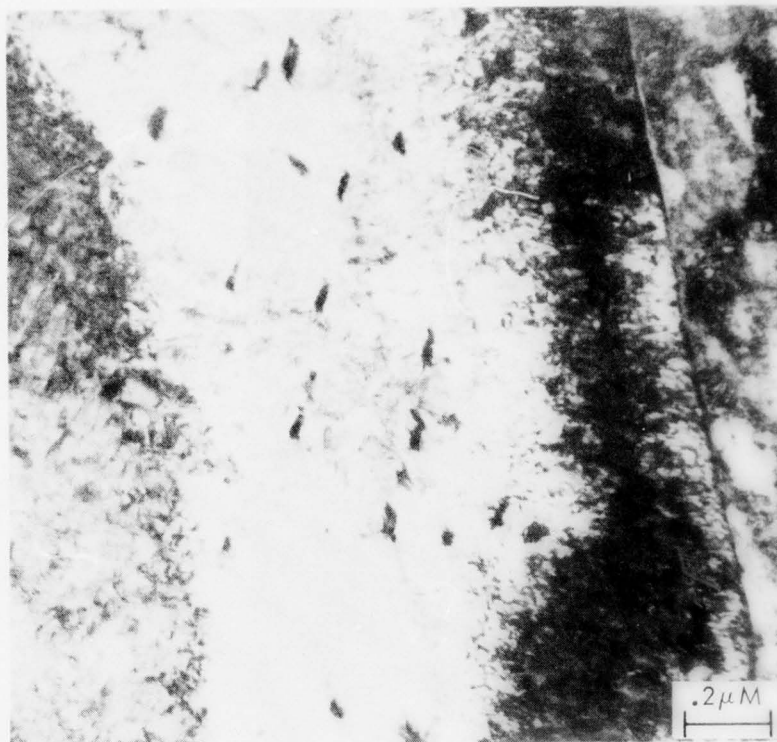
PRIMARILY DISLOCATED LATH MARTENSITE,
 SOME TWINNING PRESENT



CONTINUOUS FILM OF RETAINED
 AUSTENITE - DF
 (002) γ REFLECTION

HEAT INPUT: 100 KJ/IN. (3.9 KJ/MM)
 DEPOSITION RATE: 1.6 LBS/HR (0.7 Kg/HR)

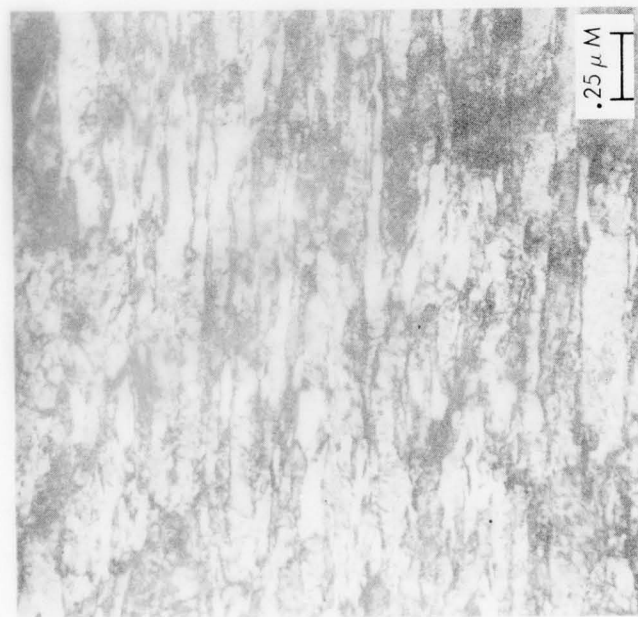
Figure 21 As-Deposited CW-PAW Fusion Zone Microstructure



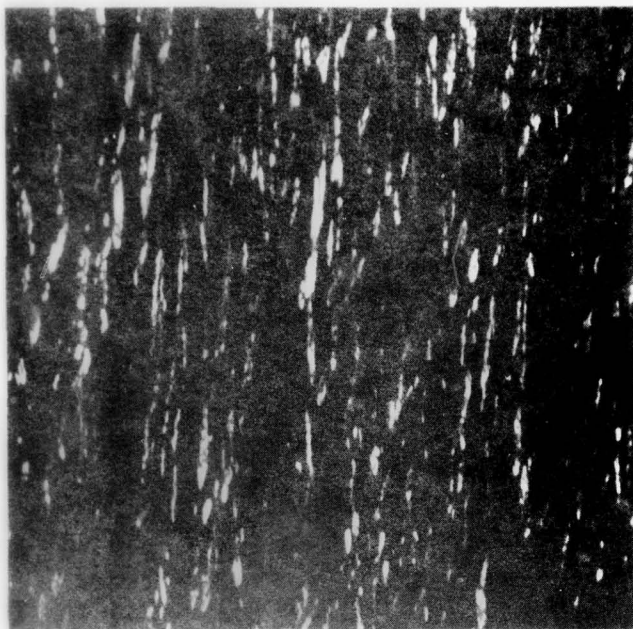
WIDMANSTATTEN CEMENTITE PLATELETS

HEAT INPUT: 100 KJ/IN. (3.9 KJ/MM)
DEPOSITION RATE: 1.6 LBS/HR (0.7 LBS/HR)

Figure 22 Autotempered Carbides in As-Deposited CW-PAW Fusion Zone Microstructure



SMALL PACKETS OF MARTENSITE LATHS
ASSOCIATED WITH GRAIN REFINEMENT
AVERAGE LATH WIDTH 0.2μ



~ 3.1 VOL % STABILIZED γ -DF

HEAT INPUT: 33.2 KJ/IN. (1.3 KJ/MM)
DEPOSITION RATE: 1.1 LBS/HR (0.5 Kg/HR)

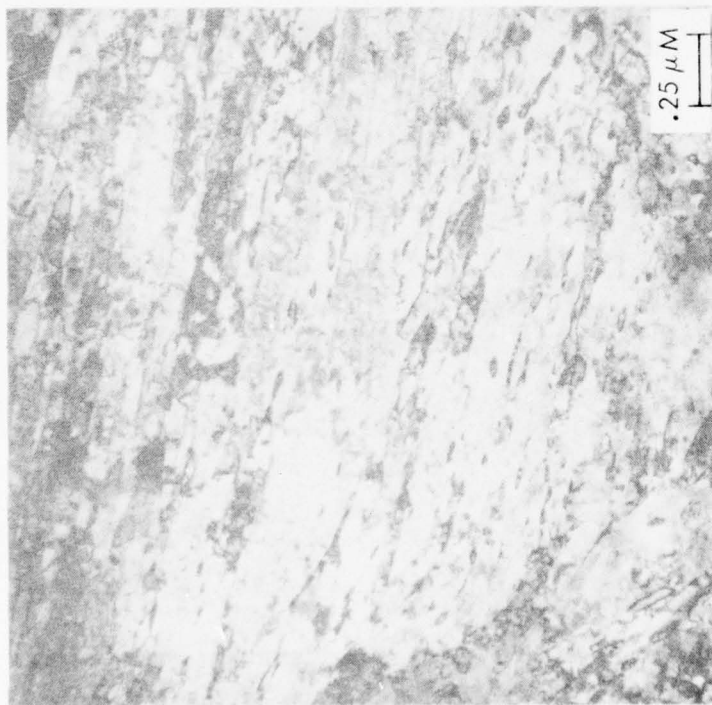
Figure 23 As-Deposited CW-GTAW Fusion Zone Microstructure Subject
To Multiple Thermal Reversals



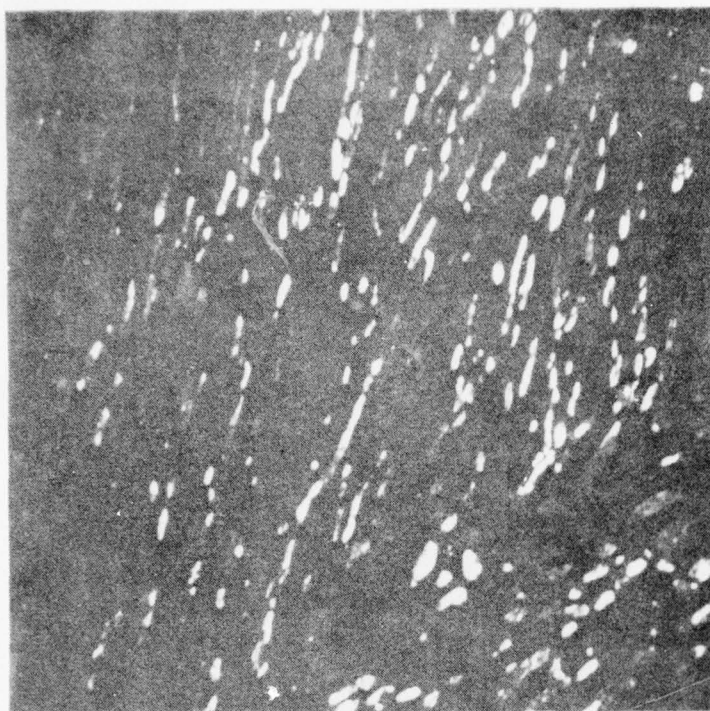
MULTIPLE THERMAL REVERSALS PRODUCE COMPLEX CARBIDES OF
THE TYPE: M_2C , M_3C , M_7C_3 WHERE (M = Fe, Mo, Cr)

HEAT INPUT: 33.2 KJ/IN. (1.3 KJ/MM)
DEPOSITION RATE: 1.1 LBS/HR (0.5 Kg/HR)

Figure 24 As-Deposited CW-GTAW Fusion Zone Microstructures Subject
To Multiple Thermal Reversals



DISLOCATED LATH MARTENSITE
AVERAGE LATH WIDTH 0.2μ



~ 6.5 VOL % STABILIZED γ -DF

HEAT INPUT 33.2 KJ/IN. (1.3 KJ/MM)
DEPOSITION RATE: 1.1 LBS/HR (0.5 Kg/HR)
POSTWELD AGE: 950°F(510°C)-4 HRS/WQ

Figure 25 Poseweld Aged CW-GTAW Fusion Zone Microstructures Representative of Multiple Thermal Reversals

ponded closely with the determined values by x-ray diffraction, e.g., ~ 6.5 vol. %. The interlath γ films were rather discontinuous while the intralath γ had a globular morphology.

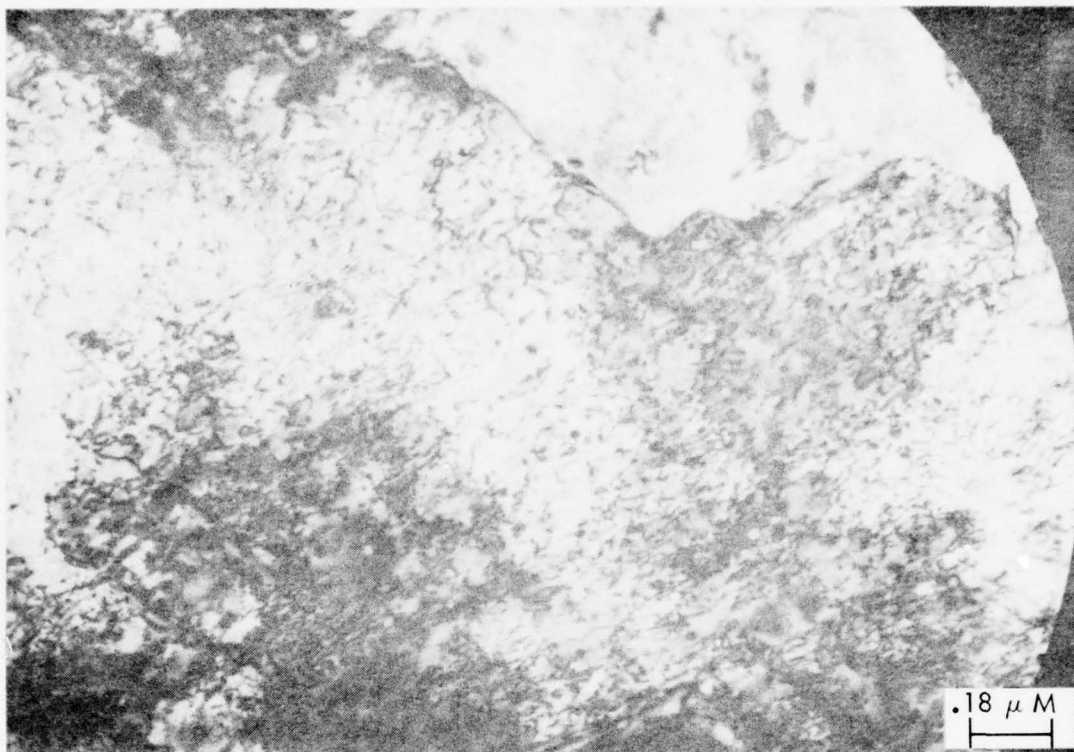
The complexity of the precipitated carbides is less than reported for the unaged condition as the $(110)\alpha$ cementite platelets have completely gone into solution. This indicates that the post weld aging at 950°F (510°C) of CW-GTAW weldments possibly results in a slightly overaged microstructure when the additive effects of thermal cycling and aging are considered. Rolled plate microstructures, aged at a similar temperature for increased time, show the presence of $(110)\alpha$ cementite platelets, albeit they are in a transitory state of dissolution, References 1 and 2. Alloy carbides tentatively identified as M_2C were present at martensite lath boundaries and intralath dislocation sites, Figure 26. The growth of these M_2C carbides was still in the early stages as there was only a small increase in average size from the unaged condition. Meanwhile the globular M_7C_3 precipitates appear to be decreasing in size. This follows the behavior of many investigators (Reference 9) reporting on the Fe-Mo-Cr-C system as the M_7C_3 carbide appears to be a metastable phase. There is general agreement that if Cr is present in a Fe-Mo-C steel, Cr_7C_3 occurs accompanied by a M_2C carbide. As overaging occurs, Cr_7C_3 redissolves as M_2C becomes richer in Mo, thus approaching Mo_2C .

4.3 HEAT AFFECTED ZONE PROPERTIES

The heat affected zone was investigated briefly in terms of resultant microstructure and mechanical properties.

4.3.1 Heat Affected Zone Microstructure

All microstructural HAZ investigations were conducted on double austenitized and water quenched 14Co-10Ni-2Cr-1Mo-0.16C (Heat No. 9) alloy steel rolled plate, Table 4. The microstructure was found to be dependent on the number, temperature-time profile, and effective position of each thermal reversal accompanying the weld pass. At approximately equivalent distances, 0.095-0.126 inch (2.41 - 3.20 mm), from the FZ/HAZ interface, an increasing heat input (HI) is shown to decrease the resulting cooling rate, Figure 27. The time at austenite forming temperatures is increased for each high heat input weld pass, Figure 17. However, the higher deposition rates associated with high heat input welds result in fewer thermal reversals and different "eye brow" locations which should have a limiting effect on the austenite reversion. Representative low HI - high thermal cycle CW-GTAW and high HI - medium thermal cycle CW-PAW heat affected zones contain 8.5 to 8.8 volume percent γ compared to considerably lower γ contents in the low HI - low thermal cycle HW-GTAW HAZ, Appendix 10 and Reference 1.



POSTWELD AGING RESULTED IN DISSOLUTION OF M_3C RESULTING
IN LESS COMPLEX CARBIDES OF THE M_2C AND M_7C_3 TYPE

HEAT INPUT:	33.2 KJ/IN. (1.3 KJ/MM)
DEPOSITION RATE:	1.1 LBS/HR (0.5 Kg/HR)
POSTWELD AGE:	950°F(510°C)-4 HRS/WQ

Figure 26 Postweld Aged CW-GTAW Fusion Zone Microstructures
Representative of Multiple Thermal Reversals

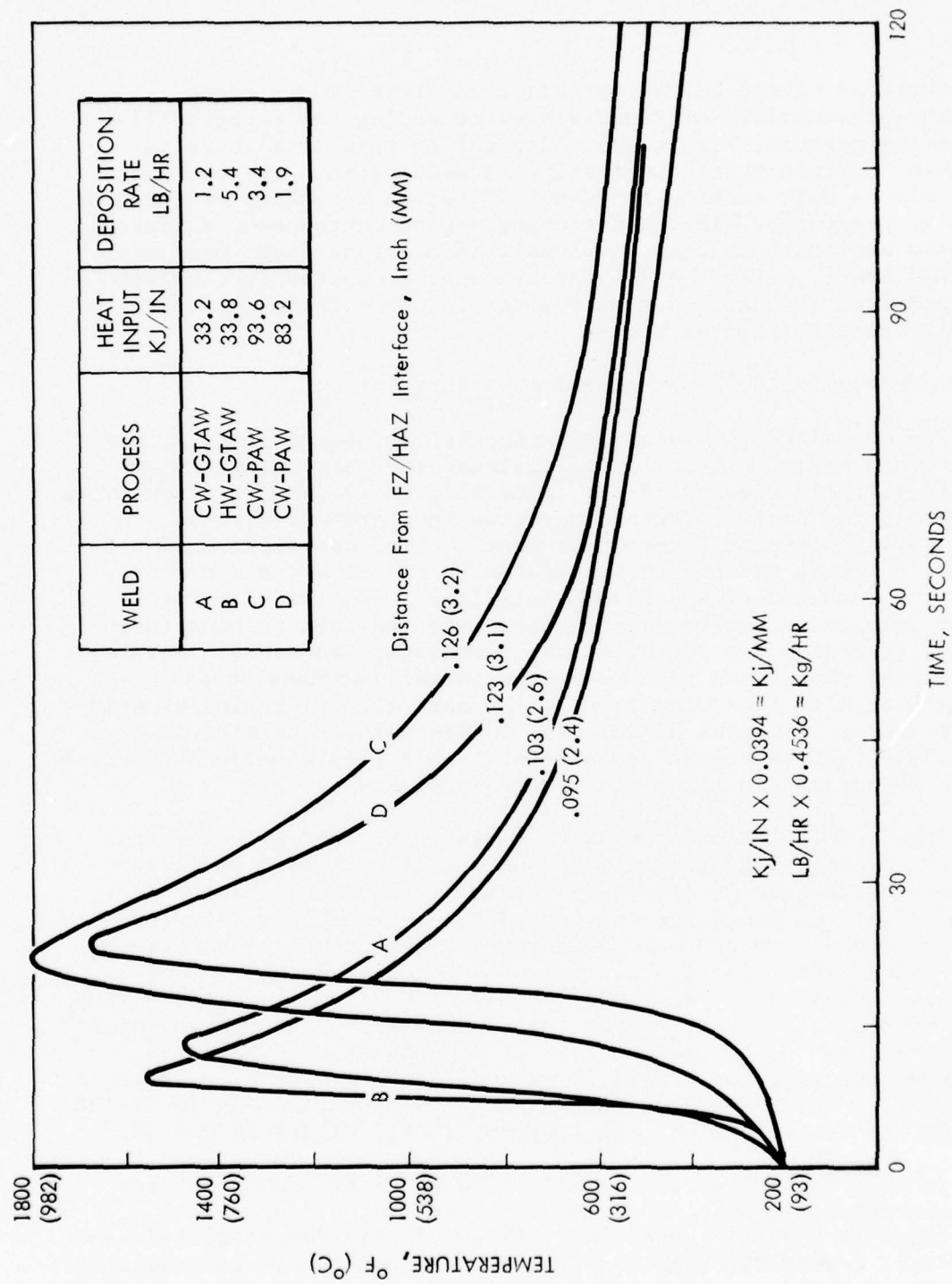


Figure 27 Heat Affected Zone Cooling Rates

Outboard of the FZ/HAZ interface exists a fine grained region representative of temperatures exceeding the recrystallization temperature, Figure 28. Adjacent to this area there is evidence of grain growth indicative of heating into the two phase field with a dark etching or "eyebrow" region occurring at somewhat lower temperatures. The dark etching region contained considerable reverted austenite as seen previously in maraging steel weld heat affected zones, Reference 22. An overaged microstructure exists outboard from the dark etching regions in which the majority of the HAZ tensile failures occur.

4.3.2 Heat Affected Zone Mechanical Properties,

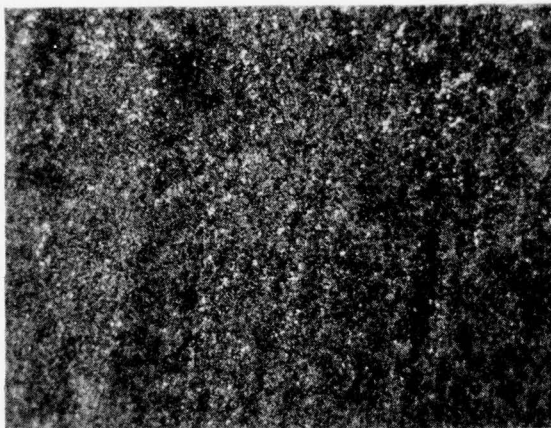
The correlation between peak temperature, microhardness, and notch toughness as a function of distance from the FZ/HAZ interface is given in Figures 29-33. Generally in all the representative arc welds, the postweld aging increased the hardness with an accompanying decrease in notch toughness. The combination of the highest hardness and toughness existed in the fine grain microstructure outboard of the FZ/HAZ interface. The lowest hardness and in some cases toughness coincides with the dark etching (high austenite) region and overaged area immediately adjacent. Several of the high deposition rate weldments reveal hardness drops concomitant with the relocation of the dark etching region as welding progresses, Figures 30-32. The CW-GTA welding results in a localized "eyebrow region" consistent with a single hardness decrease, Figure 29, except in thick plate weldments, Figure 33.

Previous investigations of weld simulated heat affected zone thermal response behavior in maraging steels indicated similar behavior, Reference 23 and 24. The amount of reverted austenite, extent of microsegregation and degradation of hardness increases with an increase in the number of thermal cycles and a decrease in the heating rate. Additional work on a Fe-Co-Ni-Cr-Mo-C steel approximating the composition of AF 1410 indicated that at CW-GTAW heat inputs, $T_p < A_f$, resulted in the minimum loss of strength while $T_p > A_f$, results in the minimum loss of toughness, Reference 19. At higher energy inputs there is an additional decrease in strength for $T_p > A_f$. The HAZ CVN absorbed energy is approximately 10 ft-lbf (13.6J) higher for the weldments where $T_p > A_f$, Figure 29 and 32.

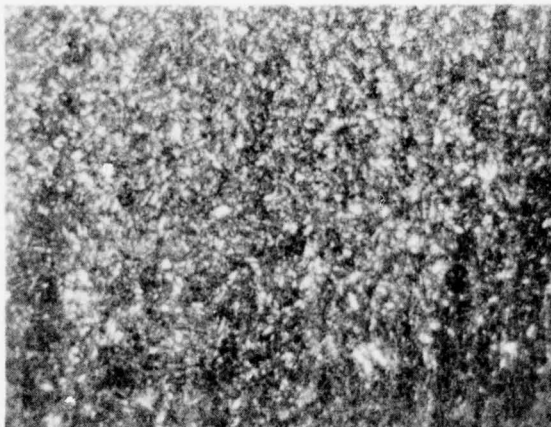
In this investigation the heat affected zone properties are representative of low-high deposition rate arc welding over a wide range of thermal conditions. As previously reported, Reference 2, several transverse tensile failures occurred immediately adjacent to the dark etching region of the heat affected zone. The tensile ductility for both the CW-GTAW and CW-PAW weld tensile specimens was



FINE GRAIN REGION
OUTBOARD OF FZ/HAZ INTER-
FACE
KHN - 550



DARK ETCHING "EYEROW"
REGION - INCREASE IN
REVERTED AUSTENITE
KHN - 510
MAGNIFICATION - 1000X



OUTBOARD OF DARK ETCHING
REGION - OVERLAVED MICRO-
STRUCTURE
KHN - 460

Figure 28 HW-GTAW Heat Affected Zone Microstructures of Unaged Base Plate

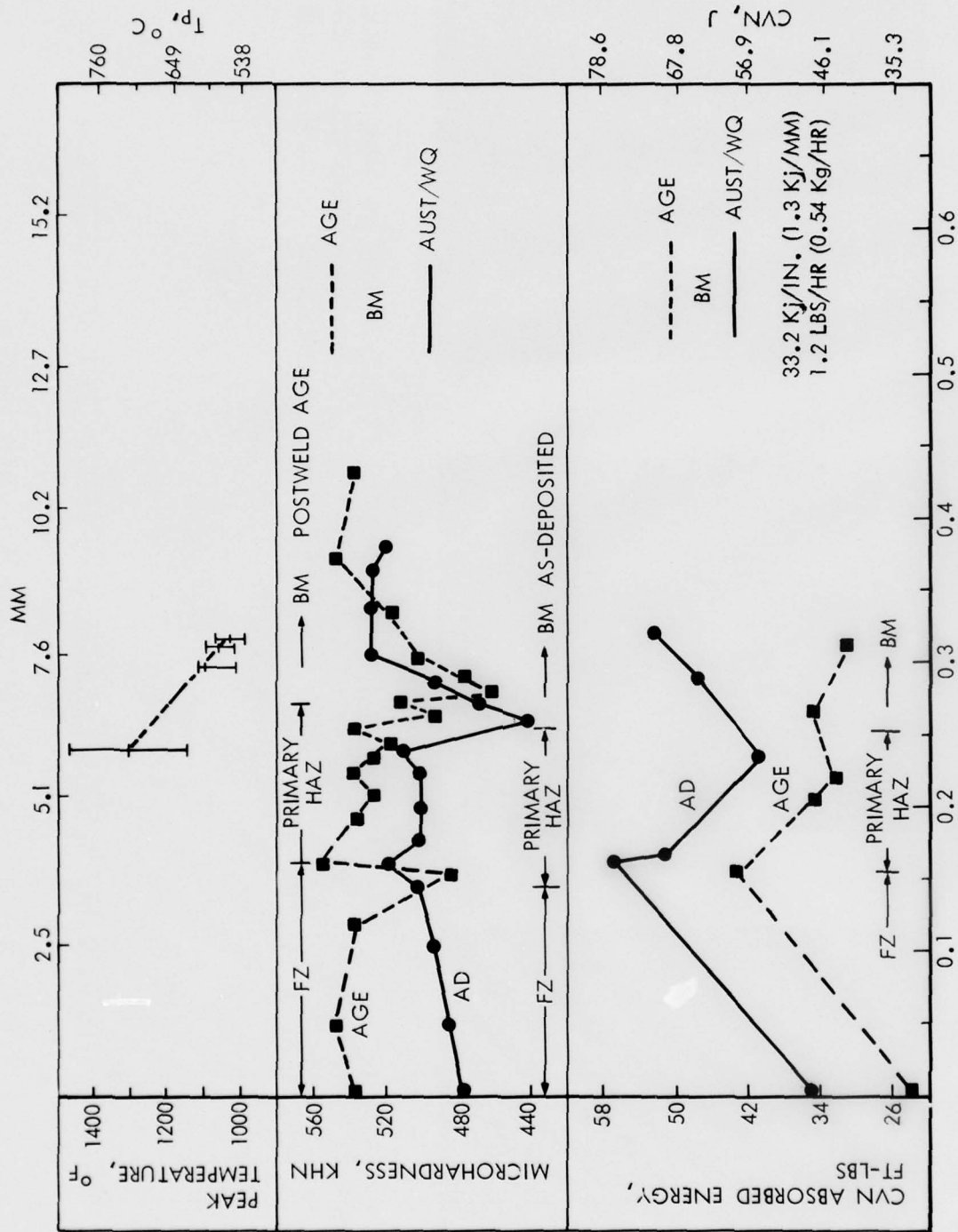


Figure 29 Cold Wire Gas Tungsten Arc Weld HAZ Properties

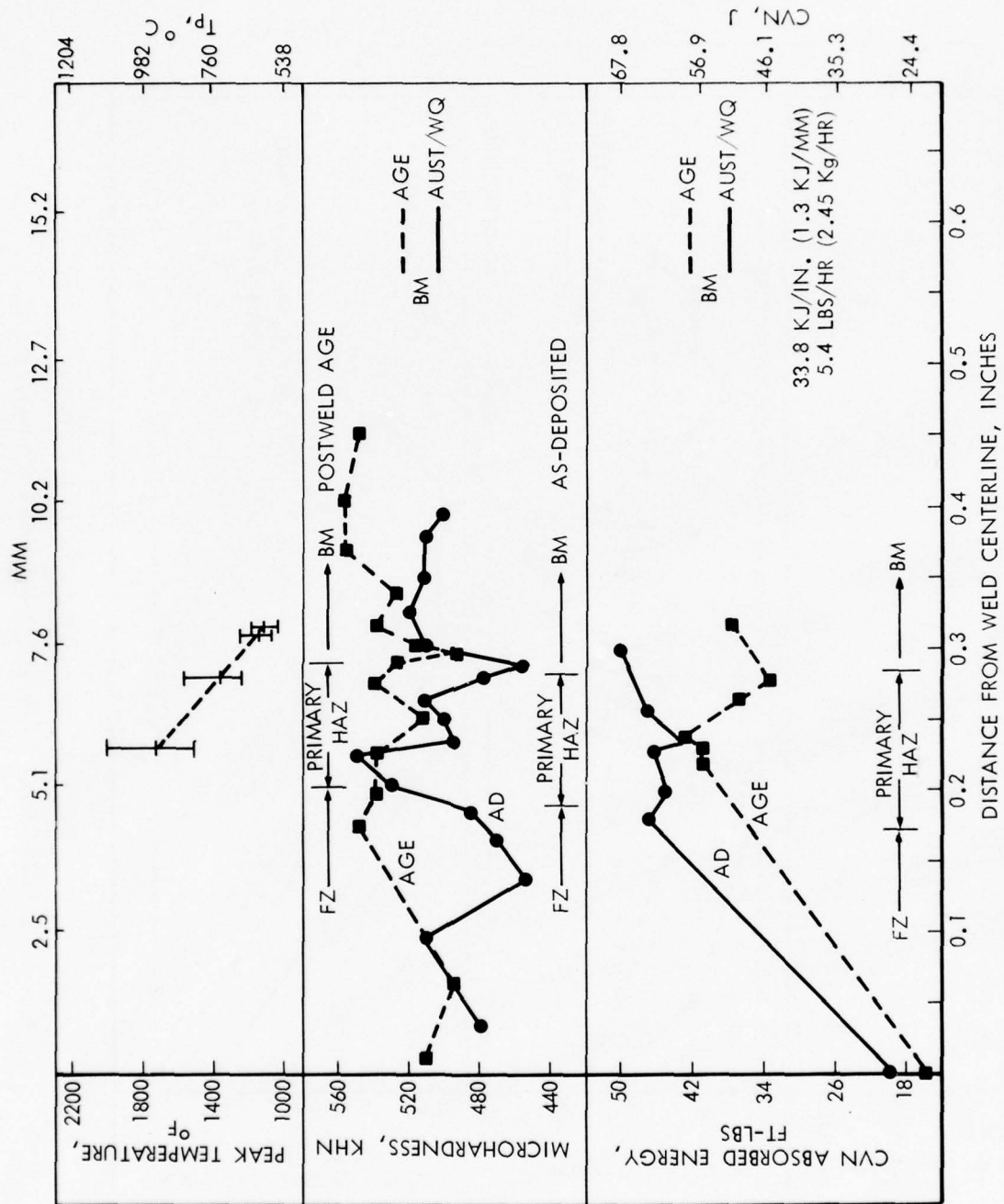


Figure 30 Hot Wire Gas Tungsten Arc Weld HAZ Properties

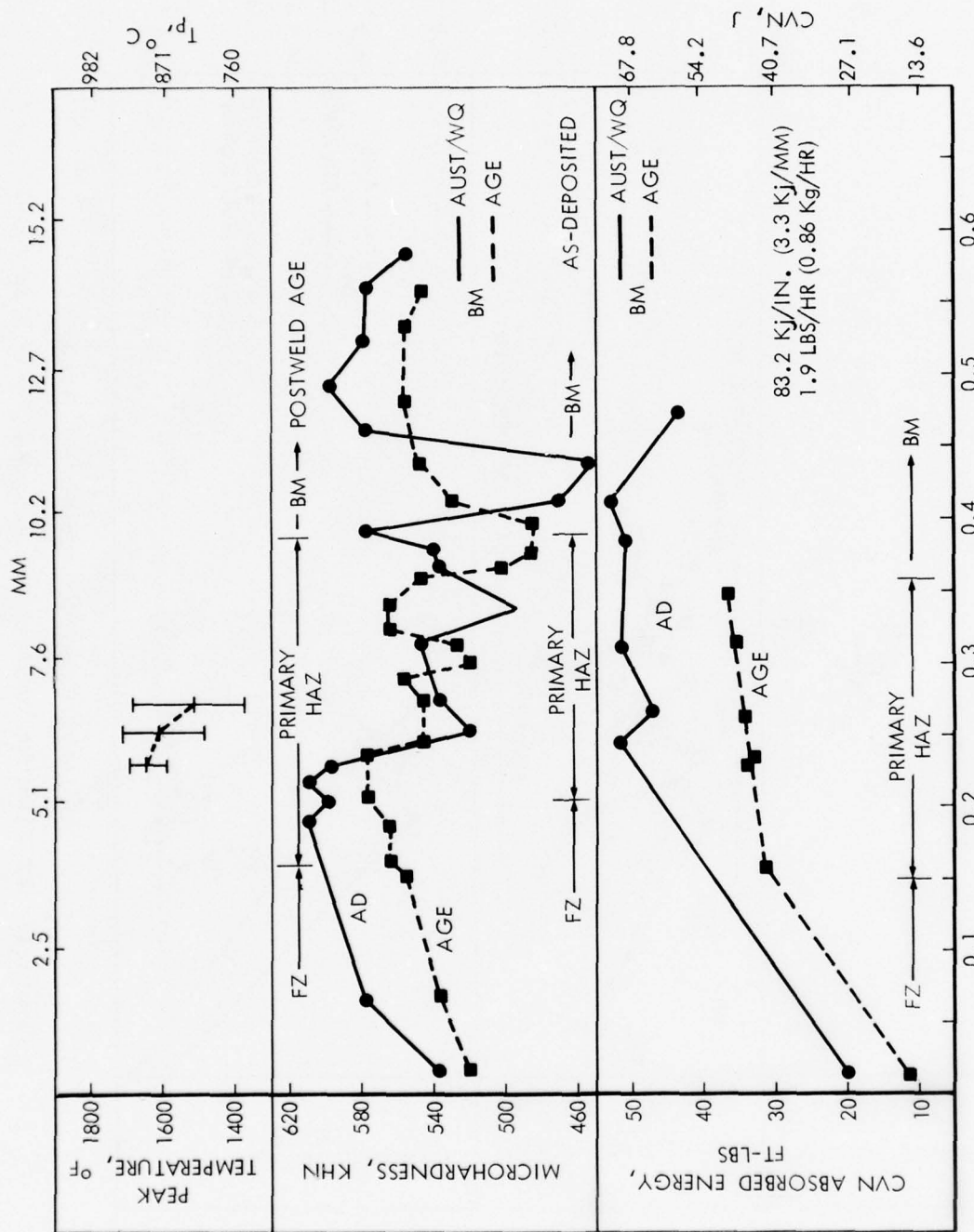


Figure 31 Cold Wire Plasma Arc Weld HAZ Properties

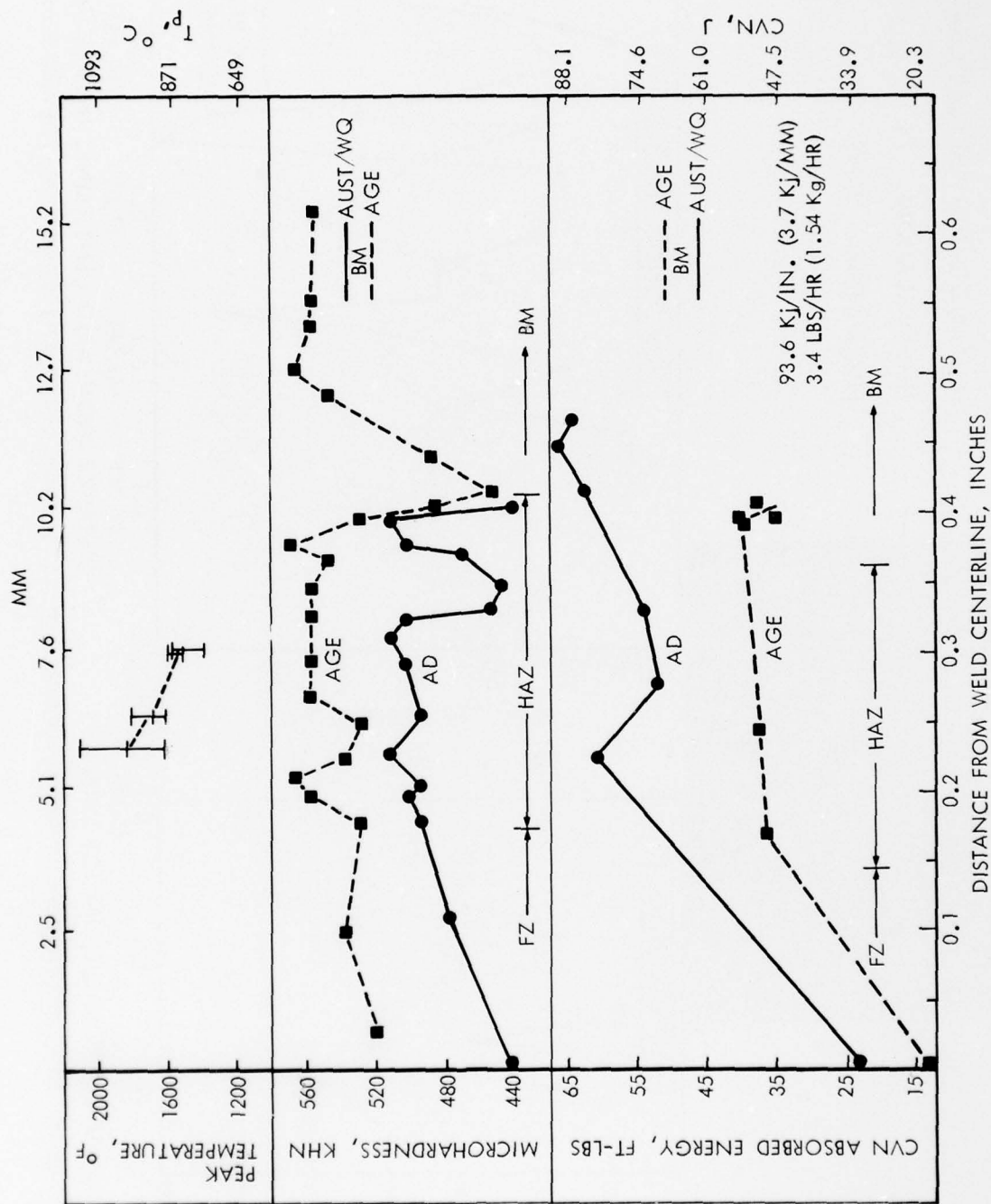


Figure 32 Cold Wire Plasma Arc Weld HAZ Properties

POSTWELD AGED: 950°F(510°C)-4 HRS

MAGNIFICATION: 2X

FILLER METAL - VE799

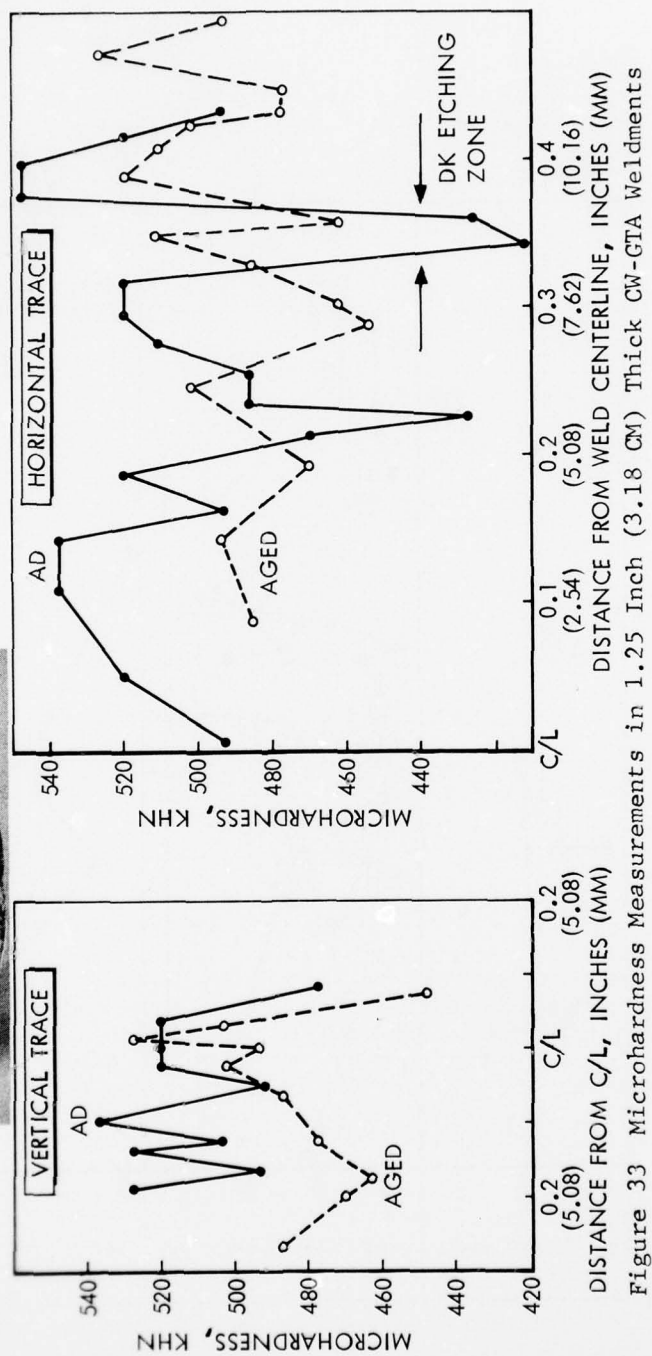


Figure 33 Microhardness Measurements in 1.25 Inch (3.18 CM) Thick CW-GTA Weldments

considerably reduced when compared to fusion zone or baseplate values, Appendix 4. Electron fractography of previous HAZ tensile fractures disclosed that (1) the shear zone of the fracture was predominantly quasicleavage-shear ridges (2) the fibrous zone revealed the presence of both void coalescence and quasicleavage, Reference 2. The fracture apparently initiates adjacent to the austenite containing dark etching region in an overaged microstructure indicative of overaging at lower temperatures. Measurement of reverted austenite on the fracture surfaces of the tensile specimens support this as the volume percent austenite was found to be 1.5% and 2.5% for the CW-GTA and CW-PAW heat affected zones. The corresponding austenite in the adjacent dark etching region of each respective HAZ was 8.1-8.5 volume percent (CW-GTAW) and 8.8-10.3 volume percent (CW-PAW) Appendix 10. Also, the reduced lattice parameter, A, of the martensite unit cell in the fracture region indicated a low level of C and/or Mo contained in solution.

Since in the initial stages of this investigation the post weld aged HAZ notch toughness, >34 ft-lbf (46.1J), was substantially greater than the FZ notch toughness, <25 ft-lbf (33.9J), of filler metal Heats VE 716 and VE 717; further HAZ investigations were curtailed, Appendix 4. It was decided the level of strength and/or toughness degradation in the 14Co-10Ni-2Cr-1Mo-0.16C steel HAZ will not impair the weldability of this alloy when compared to the fusion zone properties. Note that the HAZ notch toughness, 30 ft-lbf (40.7J), recorded in Table 12 for the CW-GTAW thick plate weldment is representative only of the low toughness base plate.

Substantial improvements in the control of impurity and/or deoxidation elements in the filler metal compositions resulted in sizeable increases in fusion zone notch toughness. The CVN absorbed energy of post weld aged CW-GTAW fusion zones varied from 38-46 ft-lbf (51.5-62.4J). Since the FZ strength and toughness now meet program goals the impetus of further investigations should be redirected toward the HAZ properties. The resistance to stress corrosion cracking, which approaches program goals in the FZ, could prove to be somewhat reduced in the HAZ. With a diversity of microstructures existing in the HAZ, there is a reduced opportunity to obtain SCC resistance microstructures. For example, thermal treatments which lead to the formation of platelet Fe_3C carbides and spherical M_xC carbides at non-optimum sites (lath/packet boundaries) will result in degraded fracture toughness and stress corrosion resistance, Reference 4.

Further investigations leading to an understanding of the effect HAZ microstructures have on mechanical properties will be required before improvements in K_{ISCC} can be suggested. The above discussion was only intended to point out a possible "weak link"

in the AF 1410 steel weldment since the mechanical properties of both the FZ and HAZ are very competitive with other high strength steel weldments.

SECTION V

CONCLUSIONS

1. Filler metal heats with a 14Co-10Ni-2Cr-1Mo-0.16C-bal Fe base composition and controlled levels of impurity/deoxidizing elements e.g., ($< 0.005\%S$, $< 0.003\%O$, $< 0.015\%Al$) can be expected to exceed minimum program strength and toughness requirements for fusion zone weld metal.
2. The mechanical properties of a high purity filler metal heat (No. VE 799) deposited by the CW-GTAW process, which was subsequently post weld aged, compared favorably with rolled plate data as follows:

	<u>AF 1410 Plate</u>	<u>Heat VE799</u>
a. TYS, Ksi (MPa)	210 (1448)	212 (1462)
b. TUS, Ksi (MPa)	230 (1586)	224 (1544)
c. CVN, ft-lbf (J)	≥ 35 (47.5)	43.5 (58.9)

The TUS will also be met when the carbon content is maintained at the nominal composition.

- d. The fusion zone weld metal failed to meet a K_{ISCC} of ≥ 100 Ksi $\sqrt{\text{in}}$ (109.9 MPa $\sqrt{\text{m}}$) which was required to achieve equivalent stress corrosion resistance with the AF 1410 steel plate. The FZ K_{ISCC} did not exceed 91 Ksi $\sqrt{\text{in}}$ (100 MPa $\sqrt{\text{m}}$).
 - e. The crack growth rate was slower in the fusion zone, in both dry air and 3.5% NaCl solution, than experienced in AF 1410 steel rolled plate in dry air.
 - f. The fusion zone S/N fatigue properties ($K_t = 1$, $R = 0.1$) did not meet the level of fatigue resistance achieved in the AF 1410 steel rolled plate.
3. The post weld aged HAZ notch toughness was greater than 34 ft-lbf (46.1 J) absorbed energy at equivalent FZ strength levels for all the arc weld processes evaluated.
4. The best balance of fusion zone strength-toughness was achieved in the CW-GTAW and CW-PAW weldments with deposition rates of 1.1 lb/hr (0.50 Kg/hr) and 1.5 lb/hr (0.68 Kg/hr), respectively.

5. The as-deposited CW-GTAW fusion zone microstructure consisted of dislocated lath martensite with minor amounts of interlath retained austenite. The intralath autotempered widmanstatten cementite platelets appear to have completely gone into solution. The alloy carbides, tentatively identified as M_2C and M_7C_3 type precipitates, form at martensite lath boundaries and intralath dislocation sites. The amount of reverted austenite nucleated at the interlath boundary and intralath sites proved to be quite extensive as compared to the as-deposited weld metal.
6. The volume percent stabilized austenite in both the fusion and heat affected zones apparently increases with decreasing cooling rate and number of thermal reversals in the as-deposited weldments.
7. The AF 1410 steel weld system is capable of achieving high toughness and high stress corrosion resistance concomitant with required strength levels in arc welds.

SECTION VI
RECOMMENDATIONS

1. Impurity and/or deoxidizing elements, e.g., S and Al could be controlled within closer limits by using master heats for filler metal melt stock.
2. Further development of welding parameters for low heat input-low deposition rate CW-PAW weldments may equal the mechanical properties obtained by the CW-GTAW process.
3. Further improvements in FZ mechanical properties, e.g., fracture toughness and stress corrosion resistance should be possible by optimizing the effect the combined weld thermal cycles and post weld treatments have on the aging transformation of as-deposited microstructures.
4. Additional studies of the cumulative effect weld thermal reversals have on HAZ microstructure and mechanical properties are required for an understanding of the reverse transformation mechanisms involved.

APPENDIX 1
CHEMICAL ANALYSIS OF MELT STOCK
VIM Heats VE 798-803

Element	Iron	Cobalt	Nickel	Chromium	Molybdenum	Ferro Vanadium	Silicon	Aluminum
Carbon	25	60	55	400	<20	2,500	-	-
Cobalt	50	Bal.	<0.2	-	<10	-	-	-
Copper	40	15	<1	-	<10	-	-	10
Iron	Bal.	40	9	2,800	<40	Bal.	6,100	-
Sulfur	25	70	2	90	-	160	-	-
Aluminum	20	-	<1	60	<20	3,100	4,100	Bal.
Manganese	20	3	<1	-	<10	80	-	-
Phosphorous	20	3	<0.2	-	-	-	-	-
Silicon	30	20	2	50	<100	6,700	Bal.	-
Chromium	20	-	-	Bal.	<10	-	-	-
Molybdenum	50	-	-	-	Bal.	-	-	-
Nickel	60	54	Bal.	-	<20	-	-	-
Tungsten	10	-	-	-	<50	-	-	-
Vanadium	30	-	-	-	<10	77.91%	-	-
Oxygen	150	-	89	390	<100	-	-	-
Hydrogen	100	-	1	-	-	-	-	-
Nitrogen	40	-	7	90	-	-	-	-

analysis of materials used to make furnace charges in ppm, unless otherwise noted.

Materials used and Supplier:

Electrolytic Iron	- Glidden & Durkee	Molybdenum	- Wah Chang
Electrolytic Cobalt	- African Metals	Ferro Vanadium	- Union Carbide
Carbonyl Nickel	- International Nickel	Silicon	- Union Carbide
VQ ElChrome	- Union Carbide	Aluminum	- Alcoa

APPENDIX 2

FUSION ZONE CHEMICAL ANALYSIS

AS-DEPOSITED CONDITION

ELEMENT	FILLER METAL HEAT NO. 717	CW-GTAW WELD E	HW-GTAW WELD G	CW-PAW WELD I	FILLER METAL HEAT NO. 716	CW-GTAW WELD F	HW-GTAW WELD H	CW-PAW WELD K	CW-PAW WELD J
C	0.15	0.15	0.12	0.13	0.15	-	-	0.12	-
Mo	0.95-1.02	1.12	1.11	1.11	0.95-1.06	-	-	1.16	-
Co	14.3-14.4	13.29	13.72	12.67	14.0-14.6	-	-	12.85	-
Cr	2.13-2.18	2.32	2.28	2.19	2.08-2.18	-	-	2.19	-
Ni	9.94-9.95	9.26	9.64	8.9	9.86-9.97	-	-	9.22	-
Si	0.12-0.13	0.21	0.20	0.22	0.12-0.14	0.23	0.21	0.19	0.20
Total Al	0.03-0.055	0.086	0.061	0.095	0.03-0.057	0.077	0.073	0.087	0.080
V	0.01-0.02	0.010	0.011	0.012	0.128	-	-	0.10	-
Mn	<0.01, <0.03	0.010	0.012	0.012	0.01, 0.03	0.012	0.013	0.014	0.012
Ti	<0.01	<0.01	<0.01	<0.01	<0.01	<0.01	<0.01	<0.01	<0.01
S	0.006-0.008	0.007	0.003	0.006	0.006-0.007	0.004	0.006	0.007	0.005
P	0.006	0.006	0.006	0.007	0.006	-	-	0.005	-
H, ppm	1	5	7	7	3	3	2	6	3
O, ppm	10	69	195	90	14-40	15	12	112	203
N, ppm	3-5	5	62	102	2-5	9	5	91	108

Notes: balance Fe
composition in weight percent
*ppm

APPENDIX 3
INGOT ALUMINUM ANALYSES

Analytical Source: Cannon-Muskegon Corporation

Method: Point to plane

Analytical Line Pairs: Al 3092.71 A°
Fe 3125.65 A°

Preburn: 5 seconds

Exposure: 10 seconds

Entrance Slit: 10 microns

Standards Used: Bowser Marner Test Lab. <0.002% Al
U.S. Steel-Heat 61557 0.009% Al
NBS 1156 0.046% Al

Analytical Source: Misco, Division of Howmet Corporation

Misco used the above standards in conducting their aluminum analysis, using a Direct Reader under air interrupted spark source and aluminum line 3092.71 A°.

Values found at both analytical sources on ladle samples are . . .

	C-M Melt No.	C-M Values	Misco Values	National Spectro- graphic Values
Heat 1	VE-798	0.011%	0.016%	0.012%
Heat 2	VE-803	0.052%	NA	NA
Heat 3	VE-802	0.049%	0.094%	0.073%
Heat 4	VE-801	0.044%	0.074%	0.071%
Heat 5	VE-800	0.044%	0.062%	0.083%
Heat 6	VE-799	0.019%	0.032%	0.018%

National Spectrographic data was a recheck.

APPENDIX 4
AF 1410 STEEL WELDMENT MECHANICAL PROPERTIES

Weld Identi- fication	Filler Metal	Post Weld Heat Treatment	Tensile Specimen Orientation	Fracture Location	Cold Wire GTA (Pulse Arc) Welds				Reduction of Area %	Charpy V-Notch Absorbed Energy RT, ft.-lbs	Comments
					Yield Strength (0.2% Offset) KSI	Tensile Strength KSI	Elongation in 1 inch %				
A	7310-8091	As-Deposited	Transverse	HAZ	203.2	239.1	11.0	44.7	56.8, 51.7, 41.2, 47.8, 50.9		
		950°F-4 hrs (510°C)	Transverse	HAZ	226.0	239.6	8.0	36.0	41.7, 35.2, 32.8, 34.9, 31.0		
		As-Deposited	Longitudinal	FZ	202.6	229.1	19.0	66.7	33.5, 37.3		
E	VE 717	950°F-4 hrs (510°C)	Longitudinal	FZ	225.0	229.9	13.0	54.7	24.9, 23.8		
F	VE 716	As-Deposited	Longitudinal	FZ	193.3	236.1	15.0	50.0	28.7, 28.8		
		950°F-4 hrs (510°C)	Longitudinal	FZ	235.5	243.9	13.0	54.7	24.5, 24.5		
Hot Wire GTA (Pulse Arc) Welds											
B	VE 717	As-Deposited	Transverse	FZ	182.1*	190.7	2.0	8.2	45.4, 47.2, 46.7 43.4, 47.0, 50.3	Surface Crack	
		950°F-4 hrs (510°C)	Transverse	FZ	223.0	232.6	7.0	28.7	43.2, 33.8, 36.9, 41.6, 41.3, 37.7		
G	VE 717	As-Deposited	Longitudinal	FZ	195.3 (a)	221.7	10.0	30.5	15.7 (b), 23.8 (b)	Minor porosity and lack of fusion	
		950°F-4 hrs (510°C)	Longitudinal	FZ	208.2	224.5	15.0	52.8	14.6 (b), 17.8 (a)		
H	VE 716	As-Deposited	Longitudinal	FZ	196.4 (a)	235.3	11.0	29.3	22.8 (a), 19.5 (a)	Minor porosity	
		950°F-4 hrs (510°C)	Longitudinal	FZ	220.0	238.0	12.0	35.2	13.3, 18.0		

APPENDIX 4 (CONTINUED)
AF 1410 STEEL WELDMENT MECHANICAL PROPERTIES

Weld Identifi- cation	Filler Metal	Post Weld Heat Treatment	Tensile Specimen Orientation	Fracture Location	Yield Strength (0.2% Offset) KSI	Tensile Strength KSI	Elongation in 1 inch %	Reduction of Area %	Charpy V-Notch Absorbed Energy RT, ft-lbf	Comments
Cold Wire Plasma Arc Welds										
C	VE 717	As-Deposited	Transverse	FZ HAZ		208.4*	4.0	7.1	58.8, 52.2, 54.0 62.7, 67.0, 64.8	Lack of fusion
		950°F-4 hrs (510°C)	Transverse	HAZ	200.4		2.0	4.0	35.2, 39.8, 40.2, 37.7, 37.3, 36.6	
D	VE 717	As-Deposited	Transverse	FZ HAZ		206.4 ^(a)	3.0	9.1	51.8, 47.3, 51.8, 53.0, 51.0, 38.5	Minor porosity
		950°F-4 hrs (510°C)	Transverse	HAZ	209.0		7.0	37.1	31.4, 34.2, 33.7, 34.5, 35.8, 36.6	
I	VE 717	As-Deposited	Longitudinal	FZ	162.5*	208.8	4.0	14.8	24.0, 22.2	Massive gas
		950°F-4 hrs (510°C)	Longitudinal	FZ	222.0	234.8	15.0	57.2	14.6, 11.9 ^(b)	
J	VE 716	As-Deposited	Longitudinal	FZ	163.7	234.3	15.0	53.7	19.8*, 19.9*	Lack of fusion in root pass
		950°F-4 hrs (510°C)	Longitudinal	FZ	235.5 ^(a)	249.7	10.0	39.5	11.9*, 16.7 ^(b)	
K	VE 716	As-Deposited	Longitudinal	FZ	174.3	237.7	14.0	43.7	21.1, 19.9	
		950°F-4 hrs (510°C)	Longitudinal	FZ	228.8	241.1	10.0	33.5	10.6, 12.2	

Notes: All CVN specimens transverse
* - Adversely affected data, gaseous contamination
a - porosity
b - lack of fusion
1 Ksi x 6.8947 = MPa
1 ft-lbf x 1.3558 = 1 Joule (J)

APPENDIX 5

LOW TEMPERATURE CVN IMPACT PROPERTIES OF CW-GTAW WELDED AF 1410 STEEL PLATE

Test Temp. °F (°C)	Plate Thickness inch (cm)	Specimen Number	CVN Absorbed Energy ft-lbf (J)
RT	0.625 (1.59) ↓	3E14	47.5 (64.4)
RT		3E15	48.0 (65.1)
0 (-17.8)		3E16	41.4 (56.1)
-50 (-45.6)		3E17	36.5 (49.5)
-100 (-73.3)		3E18	32.8 (44.5)
-150 (-101.1)		3E19	32.0 (43.4)
-200 (-128.9)		3E20	28.0 (38.0)
-320 (-195.6)		3E21	23.9 (32.4)
RT	1.25 (3.18) ↓	4A5	33.3 (45.1)
RT		4A6	34.5 (46.8)
-25 (-31.6)		4A7	28.8 (39.0)
-100 (-73.3)		4A8	24.9 (33.8)
-200 (-128.9)		4A9	16.0 (21.7)
-320 (-195.6)		4A10	13.6 (18.4)

Fusion Zone Data

Post Weld Age - 950°F (510°C) 4 hrs/WQ

Filler Metal Heat No. VE 799

APPENDIX 6

AXIAL FATIGUE PROPERTIES OF CW-GTA WELDED AF 1410 WELDMENT

$$K_t = 1, R = 0.1$$

Spec. No.	Width Inch (cm)	Thickness Inch (cm)	Max. Stress Ksi (MPa)	Cycles to Fail, KC	Location of Failure
4D1	0.500 (1.27)	0.254 (0.645)	210 (1448)	18	S-ND/FZ
4D2	0.506 (1.29)	0.256 (0.650)	210 (1448)	17	S-ND/HAZ
4D6	0.497 (1.26)	0.245 (0.622)	180 (1241)	18	S-ND/FZ
4D3	0.496 (1.26)	0.246 (0.625)	160 (1103)	87	S-ND/FZ
4D5	0.501 (1.27)	0.237 (0.602)	140 (965)	219	IC/FZ
4D4	0.501 (1.27)	0.257 (0.653)	120 (827)	1100	IC/FZ

- (1) All specimens longitudinally polished with 400 grit emery
- (2) Tested in SF-10-U at 30 Hz.
- (3) Flat specimens - 0.625 inch (1.59 cm)-t
- (4) S - surface, ND - no visible defect, FZ - fusion zone,
HAZ - heat affected zone, IC - internal crack.
- (5) Filler Metal - Heat VE 799

APPENDIX 7

DRY AIR FATIGUE CRACK GROWTH RATE DATA

Cold Wire Gas Tungsten Arc Welded
 1.0 Inch (2.54 cm) Thick Plate-Double J Groove
 Fusion Zone Data, Filler Metal Heat VE 799
 Cyclic Rate 360 cpm (6 Hertz)

Identification	dN KC	Crack Length A, Inches (cm)	P _{max} LBS (Kg)	da/dN x 10 ⁻⁶ inch/cycle (cm/cycle)	ΔK Ksi $\sqrt{\text{in}}$ (MPa $\sqrt{\text{m}}$)
4C2 inch (cm)	30	0.946 (2.403)	2300 (1043)	0.47 (1.19)	19.7 (21.6)
R = 0.1 (0.254)	40	0.955 (2.426)	2300 (1043)	0.23 (0.58)	19.9 (21.9)
B = 0.500 (1.27)	40	0.978 (2.484)	2300 (1043)	0.58 (1.47)	20.2 (22.2)
W = 2.551 (6.48)	120	0.991 (2.517)	2200 (998)	0.11 (0.28)	19.6 (21.5)
A ₀ = 0.932 (2.37)	60	1.013 (2.573)	2200 (998)	0.37 (0.94)	19.9 (21.9)
H/2W = 0.486	100	1.064 (2.703)	2100 (953)	0.51 (1.30)	19.6 (21.5)
	100	1.077 (2.736)	1900 (862)	0.13 (0.33)	18.3 (20.1)
	100	1.148 (2.916)	1900 (862)	0.71 (1.80)	19.0 (20.9)
	30	1.165 (2.960)	2100 (953)	0.57 (1.48)	21.8 (23.9)
	30	1.185 (3.010)	2100 (953)	0.67 (1.70)	22.2 (24.4)
	10	1.200 (3.048)	2300 (1043)	1.50 (3.81)	24.7 (27.1)
	10	1.211 (3.076)	2300 (1043)	1.10 (2.80)	25.0 (27.5)
	20	1.236 (3.139)	2300 (1043)	1.25 (3.18)	25.4 (27.9)
	10	1.267 (3.218)	2500 (1134)	3.10 (7.87)	28.4 (31.2)
	8	1.297 (3.294)	2700 (1225)	3.75 (9.53)	31.6 (34.7)
	8	1.343 (3.411)	2900 (1315)	5.75 (14.61)	35.2 (38.7)
	4	1.379 (3.503)	3100 (1406)	9.00 (22.86)	39.4 (43.3)
	2.94	1.410 (3.581)	3300 (1497)	10.54 (26.77)	43.5 (47.8)
	1	1.424 (3.617)	3500 (1588)	14.0 (35.56)	47.4 (52.1)
	1	1.442 (3.663)	3700 (1678)	18.0 (45.72)	51.1 (56.2)
	1	1.463 (3.716)	3900 (1769)	21.0 (53.34)	55.2 (60.7)
	1	1.488 (3.780)	4100 (1860)	25.0 (63.5)	59.8 (65.7)
	1	1.521 (3.863)	4300 (1950)	33.0 (83.82)	65.2 (71.6)
	1	1.560 (3.962)	4500 (2041)	39.0 (99.06)	71.9 (79.0)
	1	1.616 (4.105)	4700 (2132)	56.0 (142.24)	80.7 (88.7)
	0.8	1.700 (4.318)	4900 (2223)	105.0 (266.7)	94.6 (103.9)
	0.2	1.733 (4.402)	5100 (2313)	165.0 (419.1)	109.6 (120.4)
	0.15	1.780 (4.521)	5300 (2404)	313.3 (795.78)	123.2 (135.4)

AD-A043 065

GENERAL DYNAMICS/FORT WORTH TEX FORT WORTH DIV
WELDABILITY OF 10 NICKEL MODIFIED TYPE STEEL.(U)
MAY 77 P M MACHMEIER, J C COLLINS, R L JONES

F/G 11/6

F33615-75-C-5091

UNCLASSIFIED

AFML-TR-77-61

NL

2 OF 2
AD
A043 065



END
DATE
FILMED
9-77
DDC

APPENDIX 8

3.5% NaCl FATIGUE CRACK GROWTH RATE DATA

Cold Wire Gas Tungsten Arc Welded
1.0 Inch (2.54 cm) Thick Plate - Double J Groove
Fusion Zone Data, Filler Metal Heat VE 799

Identification	Cyclic Rate cpm (Hertz)	dN KC	Crack Length A, Inches (cm)	P _{max} Lbs (Kg)	da/dN x 10 ⁻⁶ inch/cycle (cm/cycle)	Ksi $\sqrt{\text{inch}}$ (MPa $\sqrt{\text{m}}$)
4C3 inch (cm)	60 (1)	40	1.038 (2.636)	2300 (1043)	1.00 (2.54)	21.2 (23.3)
R = 0.1 (0.254)	6 (0.1)	17.4	1.065 (2.705)	2300 (1043)	1.55 (3.94)	21.8 (24.0)
B = 0.500 (1.27)	60 (1)	29.5	1.106 (2.809)	2400 (1089)	1.39 (3.53)	23.4 (25.7)
W = 2.550 (6.47)	60 (1)	10	1.122 (2.850)	2500 (1134)	1.60 (4.06)	25.0 (27.5)
A = 0.998 (2.53)	60 (1)	10	1.146 (2.911)	2500 (1134)	2.40 (6.10)	25.5 (28.0)
H ⁹ 2W = 0.486	6 (0.1)	14.4	1.188 (3.018)	2500 (1134)	2.92 (7.42)	26.2 (28.8)
	60 (1)	10	1.217 (3.091)	2600 (1179)	2.90 (7.37)	28.2 (31.0)
	60 (1)	8	1.248 (3.170)	2700 (1225)	3.88 (9.86)	30.1 (33.1)
	60 (1)	6	1.273 (3.233)	2800 (1270)	4.17 (10.60)	32.1 (35.3)
	60 (1)	6	1.311 (3.330)	2900 (1315)	6.33 (16.08)	34.3 (37.7)
	6 (0.1)	6	1.375 (3.493)	2900 (1315)	10.67 (27.10)	36.2 (39.8)
	60 (1)	3	1.402 (3.561)	3000 (1361)	9.00 (22.86)	39.4 (43.3)
	60 (1)	3	1.437 (3.650)	3100 (1406)	11.67 (29.64)	42.2 (46.4)
	60 (1)	1.5	1.457 (3.700)	3200 (1451)	13.33 (33.86)	45.1 (49.6)
	60 (1)	1	1.474 (3.744)	3400 (1542)	17.00 (43.18)	49.0 (53.8)
	60 (1)	1	1.493 (3.792)	3600 (1633)	19.00 (48.26)	53.2 (58.5)
	60 (1)	1	1.515 (3.848)	3800 (1724)	22.00 (55.88)	57.7 (63.4)
	60 (1)	1	1.550 (3.937)	4000 (1814)	35.00 (88.9)	63.3 (69.6)
	60 (1)	1	1.592 (4.044)	4200 (1905)	42.00 (106.68)	70.4 (77.4)
	6 (0.1)	0.7	1.643 (4.173)	4400 (1996)	72.86 (185.06)	79.5 (87.4)
	60 (1)	.413	1.691 (4.295)	4600 (2087)	116.22 (295.20)	90.5 (99.4)
	60 (1)	.293	1.748 (4.440)	4800 (2177)	194.54 (494.13)	104.0 (114.3)
	60 (1)	.200	1.820 (4.623)	5000 (2268)	360.00 (914.4)	123.2 (135.4)
	60 (1)	.044	1.867 (4.742)	5200 (2359)		

APPENDIX 9
TRANSFORMATION TEMPERATURES

<u>Cycle</u>	<u>Heat Rate</u> <u>°F(°C)/sec</u>	<u>Cool Rate</u> <u>°F(°C)/sec</u>	<u>A_s</u> <u>°F(°C)</u>	<u>A_f</u> <u>°F(°C)</u>	<u>M_s</u> <u>°F(°C)</u>
<u>Specimen #1</u>					
1	35 (1.7)/sec	41.7 (5.4)/sec	1211 (655)	1526 (830)	599 (315)
2	35 (1.7)/sec	41.7 (5.4)/sec	1229 (665)	1508 (820)	599 (315)
3	91.4 (33)/sec	203 (95)/sec	1373 (745)	1499 (815)	590 (310)
4	212 (100)/sec	219 (104)/sec	1400 (760)	1490 (810)	590 (310)
<u>Specimen #2</u>					
1	91.4 (33)/sec	192.2 (89)/sec	1409 (765)	1499 (815)	599 (315)
2	91.4 (33)/sec	197.6 (92)/sec	1400 (760)	1490 (810)	599 (315)
3	34.8 (1.6)/sec	82.4 (28)/sec	1256 (680)	1508 (820)	608 (320)
4	93.2 (34)/sec	174.2 (79)/sec	1373 (745)	1508 (820)	608 (320)
5	34.8 (1.6)/sec	45.9 (7.7)/sec	1310 (710)	1535 (835)	608 (320)
6	34.8 (1.6)/sec	46.4 (8.0)/sec	1301 (705)	1535 (835)	608 (320)
7	91.4 (33)/sec	233.6 (112)/sec	1405 (763)	1490 (810)	608 (320)

Notes: (1) Filler metal - VE 799
 (2) Austenitize - 1800°F(982°C)-15 min.
 (3) Dilatometer specimens sectioned from CW-GTA fusion zone
 subject to 2 or more thermal reversals

APPENDIX 10

WELDMENT AUSTENITE MEASUREMENTS

Weld	Heat Treatment Condition	Volume % Austenite			
		FZ	1-2 reversals	3 or more reversals	HAZ
CW-GTA 33.2 Kj/in 1.1 lb/hr	As-deposited		1.3 +0.5	3.1 +0.5	8.5 +1.0
	Aged at: 950°F(510°C) -4 hrs		1.7 +0.3	6.5 +1.0	8.1 +1.0
HW-GTA 33.8 Kj/in 5.4 lb/hr	As-deposited		2.0 +0.5	2.3 +0.7	-
	Aged at: 950 F(510°C) -4 hrs		-1.0	3.2 +1.0	-
CW-PA 83.2 Kj/in 1.9 lb/hr	As-deposited		1.5 +0.5	3.3 +1.0	8.8 +1.0
	Aged at: 950°F(510°C) -4 hrs		1.0 +0.5	4.5 +1.7	10.3 +1.0

88

Notes: Base Plate - 14Co-10Ni-2Cr-1Mo-0.16C-bal Fe
Filler Metal - (Heat No. VE 717)

The fusion zone anisotropy and heat affected zone variations
render these values as estimates only.

Kj/in x 0.0394 - Kj/mm
lbs/hr x 0.4536 - Kg/hr

REFERENCES

1. Little, C. D. and Machmeier, P. M., "Development of A Weldable High Strength Steel", Technical Report AFML-TR-75-148, September 1975.
2. Machmeier, P. M., et. al., "Evaluation of a 10Ni-Co-Cr-Mo-C Weldment," General Dynamics' Technical Report ERR-FW-1565, December 1974.
3. Speich, G. R., et. al., "Strength and Toughness of Fe-10Ni alloys Containing C, Cr, Mo, Co, "Metallurgical Transactions, Vol. 4, pp. 303-15, January 1973.
4. Machmeier, P. M., General Dynamics, Unpublished Data.
5. Longenecker, J. B., "Investigation of Austenite Reversion During Aging of 10-Nickel Modified Steel", Technical Report GAE/MC/75-7, December 1975.
6. Konkol, P. J. and Connor, L. P., "Development and Evaluation of an Improved 10Ni-Cr-Mo-Co Filler Metal," U. S. Steel ARL Report No. 39.018-007(22), June 1968.
7. Harbuck, L. H., "High Deposition Rate HY-180 Weldments," Union Carbide Corporation Status Report, July 1970.
8. Andrews, K. W., et. al. "Constitution Diagrams for Cr-Mo-V Steels," Journal of the Iron and Steel Institute, pp. 337-50, May 1972.
9. Machmeier, P. M. and Jones, R. L., "High Temperature Stability of AF 1410 Steel", General Dynamics' Technical Report ERR-FW-1646, December 1975.
10. Machmeier, P. M., et. al., "Preliminary Evaluation of High Deposition Rate Arc Welds in AF 1410 Steel", General Dynamics' Technical Report ERR-FW-1716, December 1975.
11. Kilpatrick, J. R., et. al., "Tint-Etching Improves Resolution and Contrast of Microstructures," Metal Progress, pp. 79-81, 1971.
12. Dabkowski, D. S., et. al., "The 10Ni-Cr-Mo-Co Steel Weldment - Its Fabricability and Structural Suitability For Ultraservice Applications," U. S. ARL Report 39.018-007(41), July 1970.

REFERENCES
(Continued)

13. Cox, T. B. and Low, J. R., Jr., "Investigation of the Plastic Fracture of High Strength Steels," NASA Technical Report No. 3, May 1972.
14. Gladman, T., et. al., "Effects of Second Phase Particles on Strength, Toughness, and Ductility", Effect of Second-Phase Particles On the Mechanical Properties of Steel, the Iron and Steel Institute, pp. 68-78, 1971.
15. Goodenow, R. H. and Hehemann, R. F., "Transformation in Iron and Fe-9 Pct. Ni Alloys", Trans. of the AIME, Vol. 223, pp. 1777-86, 1965.
16. Floreen, S., "The PHysical Metallurgy of Maraging Steels", Metallurgical Reviews, Review 126, pp. 115-28, 1968.
17. Lana S. and Wayman, C. M., "Martensite to FCC Reverse Transformation in an Fe-Ni Alloy", Trans. of the Metallurgical Society of AIME, Vol. 239, pp. 1187-93, 1967.
18. Krauss, G. and Cohen, M., "Strengthening and Annealing of Austenite Formed by the Reverse Martensitic Transformation", Trans. of the Metallurgical Society of AIME, Vol. 224, pp. 1212-21, 1962.
19. Snide, J., "Some Aspects of the Physical Metallurgy and Weldability of 10 Nickel Modified Steel", Ph.D. Dissertation, Ohio State University, 1975.
20. Kenyon, N., "Effect of Austenite On The Toughness of Maraging Steel Welds", AWS, pp. 193A-198S, May 1968.
21. Habrovec, F. et. al., "Rapid Re-Austenitizing of An Fe-Ni-C Alloy", Journal of the Iron and Steel Institute, pp. 861-865, 1967.
22. Pellissier, G. E., "Microstructure in Relation to Fracture Toughness of 18Ni (250) Maraging Steel Weldments", Symposium on Weld Imperfections, September 1966.
23. Goldberg, A., "Influence of Repeated Thermal Cycling Under Various Conditions on The Hardness of A Maraging Steel," AWS Welding Research Supplement, pp. 199-S-202-S, May 1968.

REFERENCES
(Continued)

24. Goldberg, A., "Effects of Repeated Thermal Cycling On The Microstructure of 300-Grade Maraging Steel", Transactions of the ASM, Vol. 61, pp. 26-36, 1968.